SAPIENZA
UNIVERSITÀ DI ROMA

PhD School in Biology and Molecular Medicine

PhD in Human Biology and Medical Genetics (cycle XXX)

(PhD Coordinator: Prof. Antonio Pizzuti)

EXPRESSION LEVELS AND ROLE OF THE *de novo* DNA METHYLTRANSFERASES IN RHABDOMYOSARCOMA

Supervisor

Prof. Antonio Pizzuti

Co-supervisor

Dr Francesca Megiorni

PhD Student

Dr Simona Camero

Academic Year 2016-2017

Se non puoi essere un pino sul monte,
sii una saggina nella valle,
ma sii la migliore piccola saggina
sulla sponda del ruscello.
Se non puoi essere un albero,
sii un cespuglio.
Se non puoi essere una via maestra
sii un sentiero.
Se non puoi essere il sole,
sii una stella.
Sii sempre il meglio
di ciò che sei.
Cerca di scoprire il disegno
che sei chiamato ad essere,
poi mettiti a realizzarlo nella vita.

Martin Luther King

INDEX

ABSTRACT

Aberrant DNA methylation has been frequently observed in human cancers, including rhabdomyosarcoma (RMS), the most common soft tissue sarcoma in children, representing approximately 5% of malignant solid tumour in the paediatric population. However, the specific mechanisms and targets are still poorly understood. We showed the up-regulation of DNA methyltransferase (DNMT) family members in 14 RMS primary tumour biopsies and 4 RMS cell lines in comparison to normal skeletal muscle (NSM). Our study focused on DNMT3B gene, which exhibited particularly high levels in RMS samples, in order to establish its individual role in this malignancy. RNA interference-mediated DNMT3B knock-down decreased cell proliferation, by arresting cell cycle at G1 phase, as demonstrated by the reduced expression of Cyclin B1, Cyclin D1 and Cyclin E2, and by the concomitant up-regulation of the p21 and p27 checkpoint regulators. DNMT3B depleted cells also showed a decreased migratory capacity and clonogenic potential in comparison to mocked controls. Interestingly, DNMT3B silencing was able to reactivate the skeletal muscle differentiation program in embryonal RMS (ERMS) cells, as confirmed by the acquisition of a myogenic-like phenotype and by the increased expression of the myogenic markers MYOD1, Myogenin and MyHC. Inhibition of MEK/ERK signalling by U0126 resulted in a reduction of DNMT3B protein, leading to cell cycle arrest and myogenic terminal differentiation, this supporting the methyltransferase as a down-stream molecule of the MEK/ERK oncogenic pathway. Moreover, we showed that DNMT3B is a target of specific miR-29 family members in RMS cells and that the restoration of miRNA expression levels, by miRNA mimic transfection, lead to decreased cell proliferation and migration and to G1 cell cycle arrest. Finally, DNMT3B silencing radiosensitizes ERMS cells by altering DNA damage response signalling. Taken together, our data shed further light on RMS development, underlying a pivotal role of DNMT3B gene in myogenic program. Epigenetic therapy, by targeting the DNA methylation machinery, may represent a novel and promising strategy against RMS tumour able to ameliorate traditional therapies in order to improve the survival rate for patients with this soft tissue sarcoma.

INTRODUCTION

1 Rhabdomyosarcoma

1.1 Soft tissue sarcoma

Soft tissue sarcomas are a heterogeneous group of rare tumours that arise predominantly from the embryonic mesoderm and start in soft tissues of the body, including muscle, tendons, fat, lymph vessels, blood vessels, nerves, and tissue around joints (Cormier and Pollock, 2004). Tumours can be found anywhere but mainly originate in an extremity (59%), the trunk (19%), the retroperitoneum (15%), or the head and neck (9%) (DeVita et al., 2005). Currently, more than 50 subtypes of soft tissue sarcoma have been identified. However, soft tissue sarcomas share many clinical and pathologic features: widespread infiltration into surrounding tissues, local recurrence, frequent hematogenous dissemination (Hartmann and Bauer, 2006). The most common site of metastasis is the lung, whilst lymph node metastasis is rare (less than 5%), except for a few histologic subtypes such as epithelioid sarcoma, synovial sarcoma, rhabdomyosarcoma, clear-cell sarcoma, and angiosarcoma (Fong et al., 1993).

Although most of soft tissue sarcoma is sporadic, i.e. not associated with hereditary syndromes, a small proportion of cases is linked to congenital anomalies or is associated with particular genetic disorders such as Beckwith-Wiedemann, Li-Fraumeni, tuberous sclerosis, neurofibromatosis type I and Gardner syndrome (Goldblum et al., 2013; Smith et al., 2001; Trahair et al., 2007; Yang et al., 1995). Furthermore, external radiation therapy is a well-established risk factor for soft tissue sarcoma development (Brady et al., 1992; Zahm and Fraumeni, 1997).

In patients with localized high-risk soft tissue sarcoma, the five-year survival rate is less than 50%, whilst is about 10% in patients with metastatic tumour (Lawrence et al., 1987).

1.2 Rhabdomyosarcoma: epidemiology and clinical features

Rhabdomyosarcoma (RMS) is the most common soft tissue sarcoma in children (more than 60%) and is one of the 10 most common childhood malignancies, counting for about 5% of paediatric tumours (Parham and Barr, 2013)

A bimodal age distribution was observed for RMS, including a larger peak between ages 0-5 years and a smaller peak in adolescence (11-15 years) (A.I.E.O.P.). Males have a moderately higher incidence of RMS than females, with a rate ratio of 1.4:1 (M Fatih Okcu et al., 2016).

RMS can occur almost anywhere in the body, but the common primary sites are: head and neck (32%), genitourinary tract (bladder/prostate 11%), genitourinary tract non-bladder/prostate (male 12%, female 5%) and limbs (16%) (McDowell, 2003) (**Figure 1**).

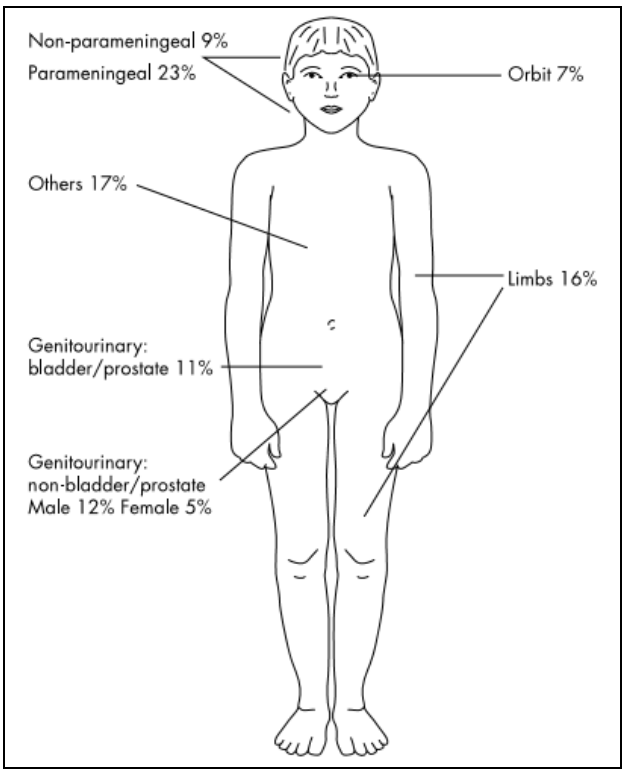

Figure 1: Distribution of rhabdomyosarcoma by primary site. (McDowell, 2003).

About 20-30% of the cases reveal metastasis already at diagnosis; the most frequently affected sites are: lung, lymph node, bones and bone marrow (Raney et al., 1988).

The role of genetic factors in the development of RMS has been confirmed by several recent epidemiological observations and in molecular genetic advances.

1.3 Histogenesis and histologic classification

RMS originates from myogenic precursors which have lost control of cell growth and differentiation (Merlino and Helman, 1999; Tiffin et al., 2003). Rubin et al. observed that rhabdomyosarcoma develops from all subpopulations of muscle cells, including muscle satellite cells and differentiating myoblasts (Rubin et al., 2011) (**Figure 2**).

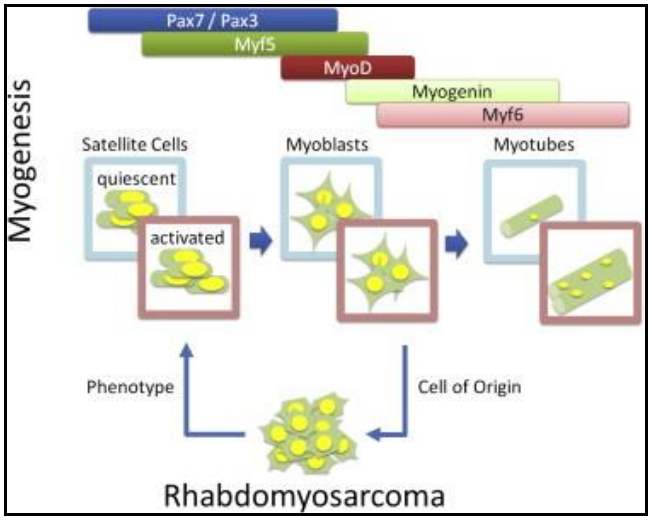

Figure 2: Rhabdomyosarcoma histogenesis. (Rubin et al., 2011).

Skeletal muscles are formed from the paraxial mesoderm surrounding the neural tube. Cells of the dermomyotome develop into skeletal muscles of the trunk and limbs. Pax3 is involved in the induction and migration of myoblast precursors, by directly modulating the levels of the c-Met tyrosine kinase receptor (Epstein et al., 1996; Relaix et al., 2003) and the expression of the muscle-specific transcription factors, MYOD, Myf-5 and Myogenin. When muscle tissues begin to differentiate, and the myogenic transcription factors are activated, Pax3 gene is down-regulated (Bailey et al., 2001; Lamey et al., 2004). In muscle tumours, Pax3 ectopic expression is observed, this resulting in a significant c-Met up-regulation (Chen et al., 2007).

Although RMS has been described for the first time in 1854, histologic subtypes have been defined many years later. In 1958, Horn and Enterline proposed that RMS could be classified into embryonal, alveolar, botryoid, and pleomorphic types (Horn & Enterline, 1958).

Embryonal rhabdomyosarcomas (ERMS), the most common subtype, comprise a range of histological features that encompass variable degrees of embryonic rhabdomyogenesis. A

common theme is a variably “loose and dense” cellularity within a myxoid matrix. ERMS arises in infants and young children and often involve head, neck, and the urogenital tract. Alveolar rhabdomyosarcomas (ARMS) resemble fetal lung alveoli with malignant cells that form aggregates interrupted by fibrovascular septa and areas of discohesion. ARMS tumour most commonly occurs in adolescents and arises in extremities and parameningeal locations. Botryoid rhabdomyosarcoma (BRMS), also called as “sarcoma botryoides,” forms grape-like polypoid masses partially lined by epithelium and shows heightened subepithelial cellularity. BRMS, by definition, occurs in hollow viscera, usually in young children.

Finally, pleomorphic rhabdomyosarcoma (PRMS) contains intersecting bundles of large, variably myogenic spindle cells with hyperchromatic, irregular nuclei and prominent nucleoli; the spindle cells are often arranged in storiform whorls resembling “malignant fibrous histiocytoma”. PRMS arises from the skeletal muscle of the extremities and mainly occurs in adults.

The classification proposed by the *Intergroup Rhabdomyosarcoma Study Group* (IRSG) subdivides the histotypes into four prognostic groups: ARMS and undifferentiated sarcoma are associated with unfavorable prognosis, BRMS is associated with favorable prognosis, ERMS with intermediate prognosis and finally RMS with rabdoid features is associated with uncertain prognosis (Newton et al., 1988).

The five-year survival rate is about 73% for patients with ERMS and 48% for patients with ARMS (Ognjanovic et al., 2009). ARMS subtype often shows metastasis already at diagnosis and is characterised by a more aggressive growth compared to the ERMS subtype, with poor response to therapy and worse prognosis (Breneman et al., 2003).

1.4 Genetic alterations in rhabdomyosarcoma

Cytogenetic and molecular analysis have identified chromosomal abnormalities in all the RMS subtypes, however, karyotypic studies revealed nonrandom chromosomal translocations that distinguish ARMS from ERMS and other solid tumours (Parham and Barr, 2013). The most common chromosomal translocation in ARMS is t(2;13)(q35;q14), which involves the long arm of chromosome 13 and the long arm of chromosome 2 (Douglass et al., 1987; Wang-Wuu et al., 1988), and more rarely is present the

translocation t(1;13)(p36;q14), which involves the long arm of chromosome 13 and the short arm of chromosome 1 (Biegel et al., 1991; Douglass et al., 1991) (**Figure 3**).

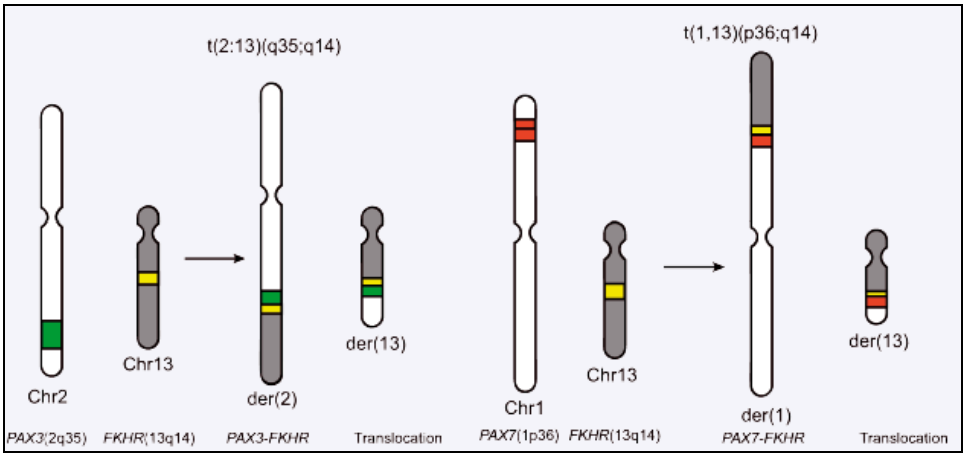

Figure 3: Schematic representation of the chromosomal translocations involving PAX3/PAX7 and FKHR. (Wang et al., 2008).

The involved genes on chromosomes 2 and 1 are PAX3 and PAX7, respectively, which encode highly related members of the *paired box* family of transcription factors (Barr et al., 1993; Lovell et al., 1994). These genes are characterised by three highly conserved domains: the *paired box* domain (PD), the octapeptide (OP) and the *homeobox* domain (HD) (**Figure 4A**). The temporal and spatial expressions of these highly conserved genes are tightly regulated during fetal development including organogenesis (Wang et al., 2008b). The fusion partner on chromosome 13 is FOXO1 (also known as FKHR), which encodes a member of the *forkhead* family of transcription factors encompassing a *forkhead* preserved domain (FH) (Galili et al., 1993; Lovell et al., 1994) (**Figure 4A**). The fusion genes generated by t(2;13)(q35;q14) and t(1;13)(p36;q14) translocations are expressed as fusion transcripts and translated into PAX3-FOXO1 and PAX7-FOXO1 fusion proteins, which respectively contain the PAX3 or PAX7 DNA-binding domain and the FOXO1 transcriptional activation domain (TAD) (Parham and Barr, 2013) (**Figure 4B**). These fusion proteins activate transcription from PAX3/PAX7-binding sites but are more potent (10-100 times) as transcriptional activators than the wild-type PAX3 and PAX7 proteins (Bennicelli et al., 1996, 1999).

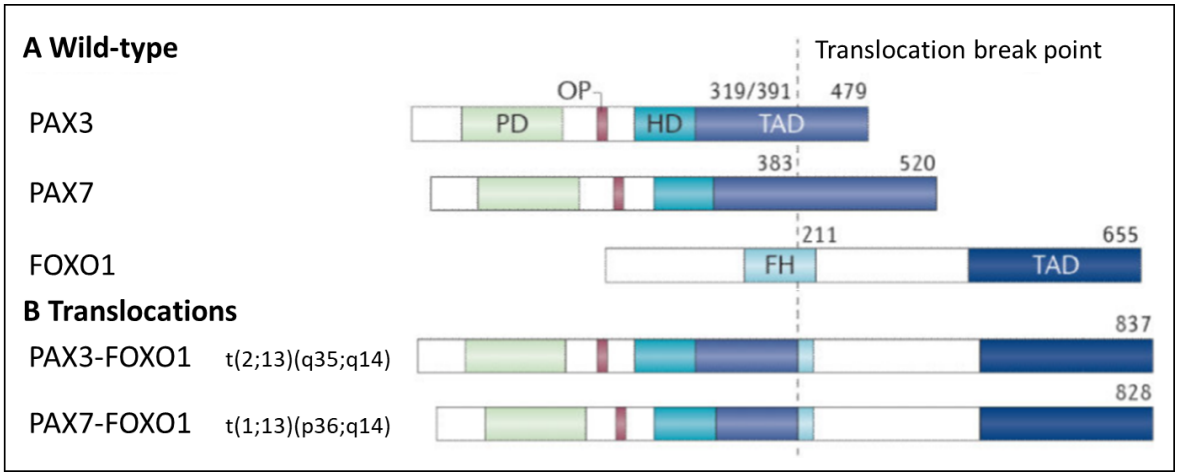

Figure 4: Gene translocations in alveolar rhabdomyosarcoma. A Wild-type proteins and the resulting **B** fusion proteins arising from chromosomal translocations occurring in ARMS. **(**Adapted from Kashi et al., 2015).

In addition to functional changes, the PAX3-FOXO1 and PAX7-FOXO1 fusion products are expressed at higher levels than the corresponding wild-type proteins (Davis and Barr, 1997). During normal development, PAX3 expression occurs in the dermomyotome and it is required for the normal migration of skeletal muscle precursors to the limb bud (Daston et al., 1996). PAX7 expression is a marker of satellite cells in adult skeletal muscle (SEALE, 2000) and it is required for normal self-renewal (Oustanina et al., 2004). These changes result in high expression of potent transcription factors that contribute to tumorigenesis by altering growth and apoptotic pathways, modulating myogenic differentiation, and stimulating motility and other metastatic pathways (Barr, 2001). Barr et al. (Barr et al., 1996) showed that PAX3-FOXO1 is a more potent oncogene than PAX7-FOXO1, since genomic amplification of PAX7-FOXO1 is required for tumorigenesis, whilst a single copy of PAX3-FOXO1 is sufficient.

Comparison between fusion-negative and fusion-positive tumours has highlighted that the *failure-free survival* is worst in ARMS patients carrying PAX3/7-FOXO1 translocations (Skapek et al., 2013).

In ERMS tumours, the most common chromosomal aberration is loss of heterozygosity (LOH) of the short arm of chromosome 11 (11p15.5) (Koufos et al., 1985; Scrable et al., 1987), this leading to over-expression of the insulin-like growth factor II (IGF-II) (Minniti et al., 1994; Xia et al., 2002). Other paediatric tumours also show loss of heterozygosity or loss of imprinting (LOI) in this region, which is associated with the Beckwith-Wiedemann

syndrome (O'Brien et al., 2012). The 11p15.5 region contains numerous tumour suppressor genes, such as H19 and p57 (CDKN1C) (Xia et al., 2002), which are specifically expressed from the maternal allele and encode for proteins or RNA products with cell growth inhibitory activity (Onyango and Feinberg, 2011; Weksberg et al., 2010). Analysis of the parental derivation of the two alleles revealed that ERMS tumours preferentially maintain the inactive paternal allele and lose the active maternal allele, leading to the inactivation of tumour suppressor genes (Scrable et al., 1989) (**Figure 5**).

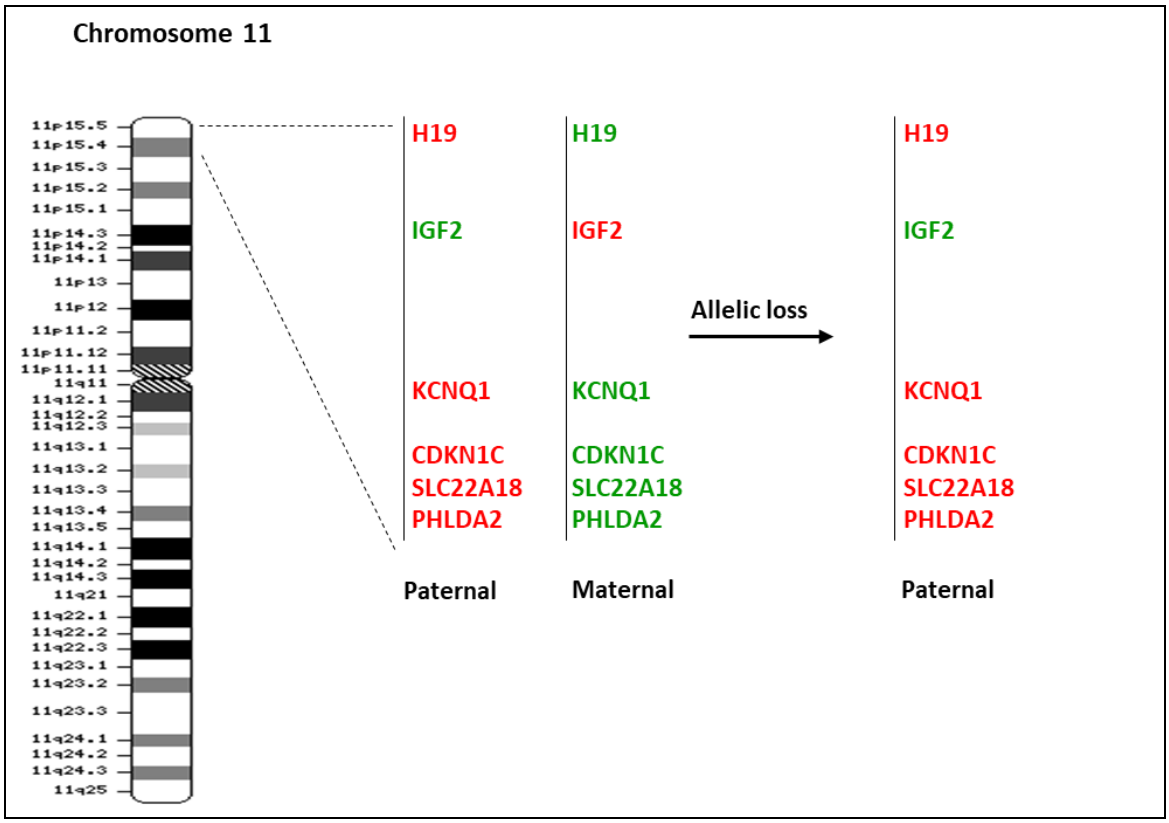

Figure 5: Allelic loss of imprinted region at 11p15.5 in ERMS. Green indicates an expressed allele and red indicates an unexpressed allele.

Several studies described the presence of point mutations in potential oncogenes and tumour suppressor genes both in ARMS and ERMS cases (Felix et al., 1992; Gao et al., 1998; Stratton et al., 1989), with point mutations being more frequent in ERMS than in ARMS tumours (Shukla et al., 2012). Mutated genes are members of the RAS family, including FGFR4, PIK3CA, CTNNB1, BRAF, p53 and PTPN11. Gene amplification

(MYCN, MDM2, GLI, SAS and CDK4) and chromosome duplication (2, 8, 12 and 13) have also been described (Anderson et al., 1999; Gordon et al., 2001).

1.5 Diagnosis and staging

The histologic patterns and cytologic features of RMS range from undifferentiated small round blue cell neoplasms to lesions with advanced cytohistologic features, reminiscent of rhabdomyomas (Kodet et al., 1991). For the RMS diagnosis, it is necessary to identify embryonic myogenesis by using diagnostic tests and biopsy that allow to measure myogenic markers such as desmin, muscle-specific actin, myosin, or myoglobin. In recent years, nuclear transcription factors that initiate myogenesis, such as MYOD or Myogenin, have become common immunohistochemical markers, because of their expression precedes later events of myogenesis such as the identification of cytoplasmic striations, myosin-ribosome complexes, and markers of terminal differentiation like myoglobin and muscle-specific actin (Cessna et al., 2001; Folpe, 2002).

As for other tumours, staging classification is necessary for RMS (1) to classify tumour and its severity in order to make the best choice from the different modalities of treatment and (2) to compare the results of treatment in different countries. Two systems of staging have been used throughout the world. The pre-surgical and post-surgical staging system, known as TNM/pTNM, which describes the size of the primary tumour (T), the involvement of the regional limph nodes (N) and the presence of distant metastasis (M) before any treatment administration (**Table 1A, 1B**). The post-surgical staging system, known as the Intergroup Rhabdomyosarcoma Study (IRS) Grouping System, is based on surgery (**Table 2**) (Panda et al., 2017). In Europe, the most used system is the European Paediatric Soft Tissue Sarcoma Study Group (EpSSG) Risk Classification, which considers histology (alveolar vs. non-alveolar), post-surgical stage (according to IRS grouping), tumour site and size, limph node involvement and patient age (**Table 3**).

Table 1A: TNM classification

Tumour:	
T0: No evidence of tumour	
T1: Tumour confined to organ or tissue of origin	T1a: Tumour ≤ 5 cm in greatest dimension T1b: Tumour > 5 cm in greatest dimension
T2: Tumour not confined to organ or tissue of origin	T2a: Tumour ≤ 5 cm in greatest dimension T2b: Tumour > 5 cm in greatest dimension
TX: No information on size and tumour invasiveness	
Lymph nodes:	
N0: No evidence of lymph node involvement	
N1: Evidence of regional lymph node involvement	
NX: No information on lymph node involvement	
Metastasis:	
M0: No evidence of metastases or non-regional lymph nodes	
M1: Evidence of distant metastasis or involvement of non-regional lymph nodes	
MX: No information on metastasis	

Table 1B: pTNM classification

pT
pT0: No evidence of tumour found on histological examination of specimen.
pT1: Tumour limited to organ or tissue of origin. Excision complete and margins histologically free
pT2: Tumour with invasion beyond the organ or tissue of origin. Excision complete and margins histologically free
pT3: Tumour with or without invasion beyond the organ or tissue of origin Excision incomplete pT3a: Evidence of microscopic residual tumour pT3b: Evidence of macroscopic residual tumour pT3c: Adjacent malignant effusion regardless of size
pTX: Tumour status may not be assessed
pN
pN0: No evidence of tumour found on histological examination of regional lymph nodes
pN1: Evidence of invasion of regional lymph nodes pN1a: Evidence of invasion of regional lymph nodes Involved nodes considered to be completely resected pN1b: Evidence of invasion of regional lymph nodes Involved nodes considered not to be completely resected
pNX: N status may not be assessed due to lack of pathological examination or inadequate information on pathological findings
pM
pM0: No evidence of metastasis found on histological examination of non-regional lymph nodes
pM1: Evidence of metastasis on histological examination
pMX: M status may not be assessed due to lack of pathological examination or inadequate information on pathological findings

Table 2: IRS Grouping System

IRS Group	Definition
I	Tumour macroscopically and microscopically removed
(IA)	Tumour confined to organ or tissue of origin
(IB)	Tumour not confined to organ or tissue of origin
II IIA IIB	Macroscopic complete resection but microscopic residuals Lymph nodes not affected Lymph nodes affected but removed
III	Macroscopic complete resection but microscopic residuals and lymph nodes affected and not removed
	Macroscopic residuals after resection or biopsy with malignant effusion
IV	Metastasis present or non-regional lymph nodes involved

Table 3: EpSSG Risk Classification

Risk Group	Subgroups	Pathology	Post-surgical Stage (IRS Group)	Site	Node Stage	Size & Age
Low Risk	A	Favourable	I	Any	N0	Favourable
Standard Risk	B	Favourable	I	Any	N0	Unfavourable
	C	Favourable	II, III	Favourable	N0	Any
	D	Favourable	II, III	Unfavourable	N0	Favourable
High Risk	E	Favourable	II, III	Unfavourable	N0	Unfavourable
	F	Favourable	I, II, III	Any	N1	Any
	G	Unfavourable	I, II, III	Any	N0	Any
Very High Risk	H	Unfavourable	I, II, III	Any	N1	Any

1.6 Treatment of rhabdomyosarcoma

Because local progression and relapses are the main causes of failure, treatment for RMS involves a multimodality approach that includes local surgery, radiotherapy and systemic chemotherapy (Panda et al., 2017). Surgery should be considered if the tumour can be completely excised with histologically clear margins and no anatomical or functional impairment (Sultan and Ferrari, 2010). Radiotherapy is a fundamental part in the strategy for treating RMS, it is use both pre- and post- surgery (Michalski et al., 2004; Schuck et al., 2004). Dosage, timing and method of radiotherapy must be planned in relation to the patients' risk stratification and the late effects of treatment (Stevens, 2005). Moreover, it should be considered, that radiotherapy has been implicated in the development of secondary malignancies (Heyn et al., 1993; Paulino, 2004). Because RMS patients are assumed to have micrometastatic disease already at diagnosis, chemotherapy represents the *gold standard* for all the patients (Ferrari and Casanova, 2005; Meyer and Spunt, 2004; Parham, 2001; Raney et al., 2001; Ruymann and Grovas, 2000). To date, there are two protocols of chemotherapy. In North America the *standard* is vincristine, actinomycin D, and cyclophosphamide (VAC) (Maurer et al., 1988), whilst in Europe the *standard* is represented by ifosfamide, vincristine and actinomycin D (IVA) (Casanova and Ferrari, 2011; Crist et al., 2001).

For 30% of RMS cases these approach is still not effective, or not effective enough to achieve a definitive cure (Casanova and Ferrari, 2011). In the recent years, *targeted therapy* has been developed as novel and promising molecular strategy that specifically target crucial genes of the tumour biology without affecting normal cells (Sultan and Ferrari, 2010; Wachtel and Schäfer, 2010). Potential therapeutic targets have been identified in RMS. Receptor tyrosine kinases (RTKs) such as IGF1R (Cao et al., 2008; Kalebic et al., 1998; Maloney et al., 2003; Tsokos and Helman, 1994), c-MET (Taulli et al., 2006), PDGFR (Maris et al., 2008a; Taniguchi et al., 2008) and c-KIT (Maris et al., 2008a). Intracellular signalling molecules such as mTOR (Hosoi et al., 1999; Houghton et al., 2008a; Wan et al., 2006) and MEK/ERK (Ciccarelli et al., 2005; Marampon et al., 2006). Cell cycle or apoptosis regulators such as CDK4/CDK6 (Saab et al., 2006), p53 (Ganjavi et al., 2005; Shetty et al., 2002), BCL-2 (Lock et al., 2008), and TRAIL (Clayer et al., 2001; Izeradjene et al., 2004; Komdeur et al., 2004; Petak et al., 2000; Tomek et al., 2003). Moreover, proteasome (Bersani et al., 2008; Houghton et al., 2008b), histone deacetylases

(Jaboin et al., 2002; Kutko et al., 2003), regulators of angiogenesis such as VEGF (Gee et al., 2005) and VEGFR (Maris et al., 2008b) and finally the cancer specific fusion proteins PAX3-FOXO1 and PAX7-FOXO1 (Amstutz et al., 2008; Van Den Broeke et al., 2006; Dagher et al., 2002; Gardner and Montminy, 2005; Mackall et al., 2008) (**Figure 6**).

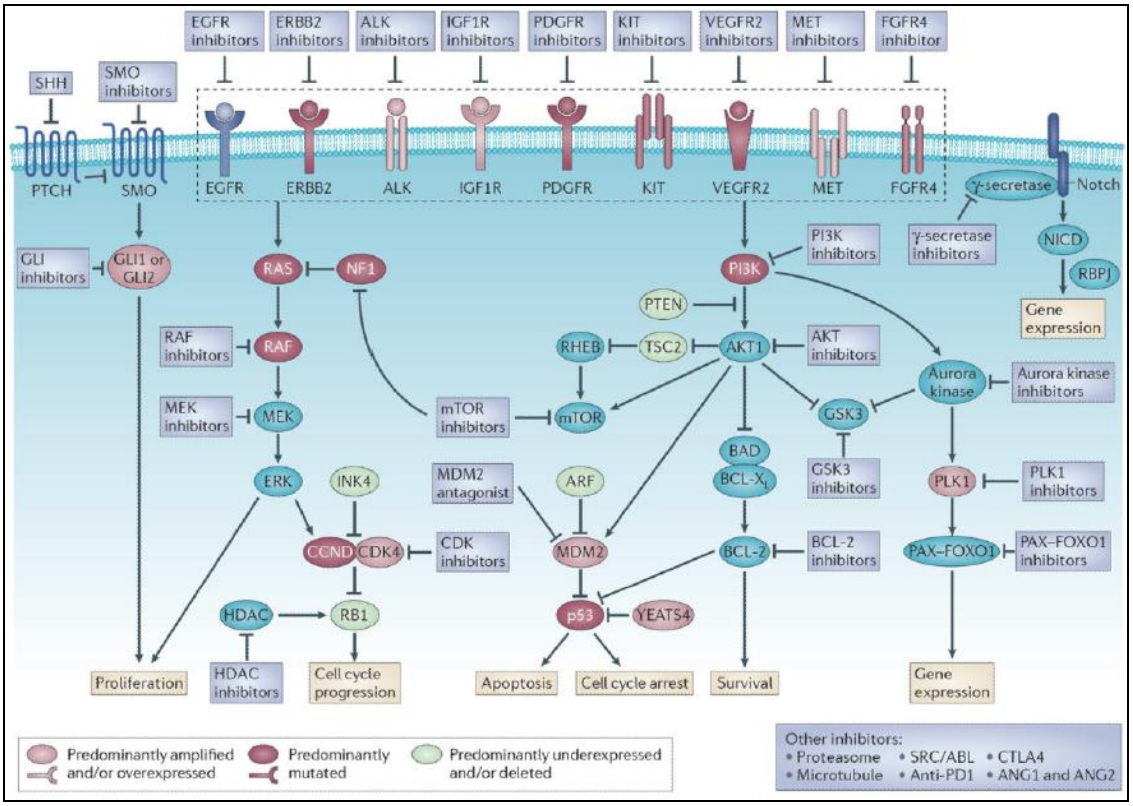

Figure 6: Rhabdomyosarcoma pathways for *targeted therapy*. (Kashi et al., 2015).

2 Epigenetics

The term "epigenetics" literally means "above genetics", indeed, the Greek prefix *epi-* (ἐπι- "over, outside of, around") in *epigenetics* implies features that are "on top of" or "in addition to" the traditional genetic basis for inheritance (Laker and Ryall, 2016). Conrad Waddington introduced the term "epigenetics" in the early 1940s. He defined epigenetics as "the branch of biology which studies the causal interactions between genes and their products which bring the phenotype into being" (Waddington, 1942, 1968). The meaning of the word has gradually narrowed. Today, epigenetics is defined as "the study of changes in gene function that are mitotically and/or meiotically heritable and that do not entail a change in DNA sequence" (Wu Ct and Morris, 2001). The most frequent epigenetic modifications are histone and/or DNA methylation, generally associated with gene silencing, and histone acetylation, related to transcriptional activation (Allfrey et al., 1964; Bogdanović and Veenstra, 2009; Esteller, 2008).

2.1 DNA methylation

DNA methylation plays a key role in the regulation of gene expression, genomic imprinting, X chromosome inactivation, and tumorigenesis (Jones and Baylin, 2007; Smith and Meissner, 2013). In mammals, the addition of a methyl group at the carbon fifth position of a cytosine in the context of the cytosine-guanosine (CpG) dinucleotide (**Figure 7**) is catalysed by a group of enzymes called DNA methyltransferases (DNMTs) (Hamidi et al., 2015).

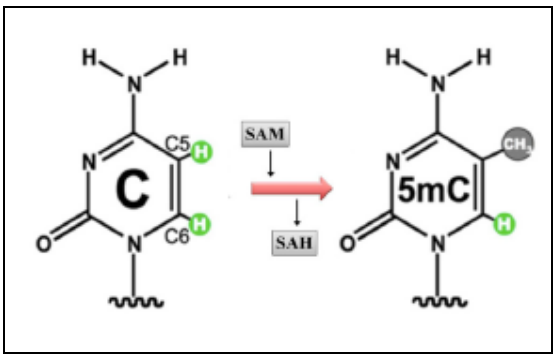

Figure 7: DNA methylation. DNMTs transfer a methyl group at the DNA cytosine ring carbon C5 by using S-adenosyl methionine (SAM) as methyl donor. S-adenosyl homocysteine (SAH) is the cofactor product. (Adapted from Maresca et al., 2015).

In the human genome there are 56 million of CG sites, 60–80% of which are methylated, corresponding to 4–6% of all cytosines (Laurent et al., 2010). Around 70% of human gene promoter regions present CpG islands. Methylation levels and patterns are cell and tissue specific.

The mammalian DNMT family includes four members: DNMT1, DNMT3A, DNMT3B, and DNMT3L (Kim et al., 2009; Mohan and Chaillet, 2013). These enzymes share conserved motifs in their C-terminal catalytic domains, but have different N-terminal regulatory regions (**Figure 8**) (Jurkowska et al., 2011). N-terminal region is involved in the interaction with DNA, chromatin, and other proteins and furthermore contains 621 amino acids required for discriminating between hemimethylated and unmethylated DNA (Maresca et al., 2015). DNMT1 contains multiple functional domains in the N-terminal region:

- DNA methyltransferase associated protein 1 ($DMAP_1$) involved in the interaction of DNMT1 with the transcriptional repressor DMAP1 as well as in the stability of the enzyme and in its binding to DNA CpG sites (Ding and Chaillet, 2002; Rountree et al., 2000),
- a nuclear localization signal (NSL), a replication foci-targeting sequence (RFTS) that localizes DNMT1 at the centromeric chromatin and to the DNA replication fork (Easwaran et al., 2004; Fellinger et al., 2009),
- a zing finger CXXC domain that specifically recognizes unmethylated CpG-containing DNA (Pradhan et al., 2008),
- a pair of bromo-adyacent homology (BAH1, BAH2) domains,
- a glycine-lysine (GK) repeat that link N-terminal regulatory region to the C-terminal catalytic domain.

The N-terminal region of DNMT3A and DNMT3B have two functional domains: a proline-tryptophan-tryptophan-proline (PWWP) domain, which is required for heterochromatin localization (Chen et al., 2004; Cheng and Blumenthal, 2008; Qiu et al., 2002) but not for CpG methylating activity (Qiu et al., 2002), and an ATRX-DNMT3A/3B-DNMT3L (ADD) domain that binds to H3K4-unmethylated histone H3 and constitutes a platform for various protein–protein interactions (Otani et al., 2009). DNMT3L lacks a PWWP domain but has an ADD domain, which interacts with histone H3 when K4 is unmethylated (Ooi et al., 2007).

The C-terminal catalytic domain is composed by 500 amino acids and harbors the active center of the enzyme, which contains amino acid motifs, called the “AdoMet-dependent MTase fold", that are typical of the cytosine-C5 methyltransferases (Jurkowska et al., 2011). Motifs I and X of this domain are involved in cofactor binding whereas motifs IV, VI, and VIII have a catalytic function. The non-conserved region between motifs VIII and IX is the target recognition domain (TRD), which is crucial for DNA recognition and specificity (Cheng, 1995; Cheng and Blumenthal, 2008; Jeltsch, 2002). DNMT3L lacks the DNMTs motifs IX and X and all the important catalytic residues in its C-terminal portion (Maresca et al., 2015).

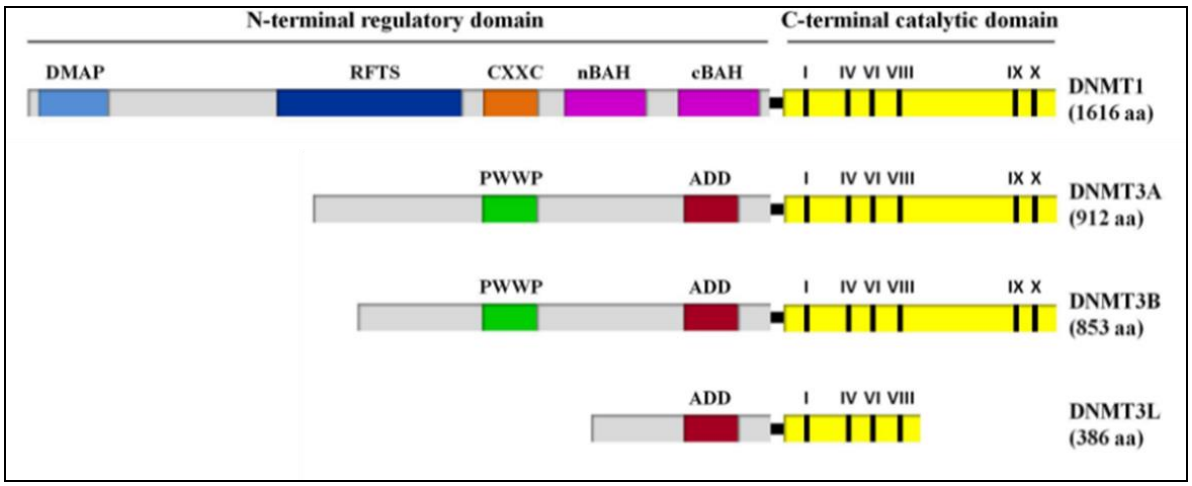

Figure 8: A schematic representation of the domain structure in the human DNMT isoforms. (Adapted from Maresca et al., 2015).

DNMT1, DNMT3A and DNMT3B have different functions in the methylation process. DNMT1 is required for the maintenance of all methylation in the genome. During DNA replication, DNMT1 methylates hemimethylated DNA and restores the specific methylation pattern from the parental strand on the newly synthesized daughter strand. Mice deficient in Dnmt1 exhibit embryonic lethality (Li et al., 1992). Conversely, DNMT3A and DNMT3B function as *de novo* methyltransferases, which establish DNA methylation patterns during gametogenesis and early embryogenesis, and set up genomic imprints during germ cell development (Chen and Li, 2006; Li and Zhang, 2014). Although they are highly expressed in early mammalian embryos, DNMT3A and DNMT3B levels decrease during cell differentiation. These two proteins have distinct

functions throughout embryonic development, showing both spatial and temporal differences. DNMT3A primarily methylates a set of genes and sequences at the late stage of embryonic development (mainly after birth), whilst DNMT3B modifies a broader region of genomic sequences in early embryos (Li and Zhang, 2014; Smith and Meissner, 2013). Knockout of DNMT3A or DNMT3B is lethal, being both essential for embryonic development in mice. Mouse embryos with dnmt3b knockout die in utero, whilst animals with dnmt3a knockout exhibit postnatal growth retardation and dysplasia, and die shortly after birth (Okano et al., 1999). A classical model of DNA methylation is schematized in **Figure 9**.

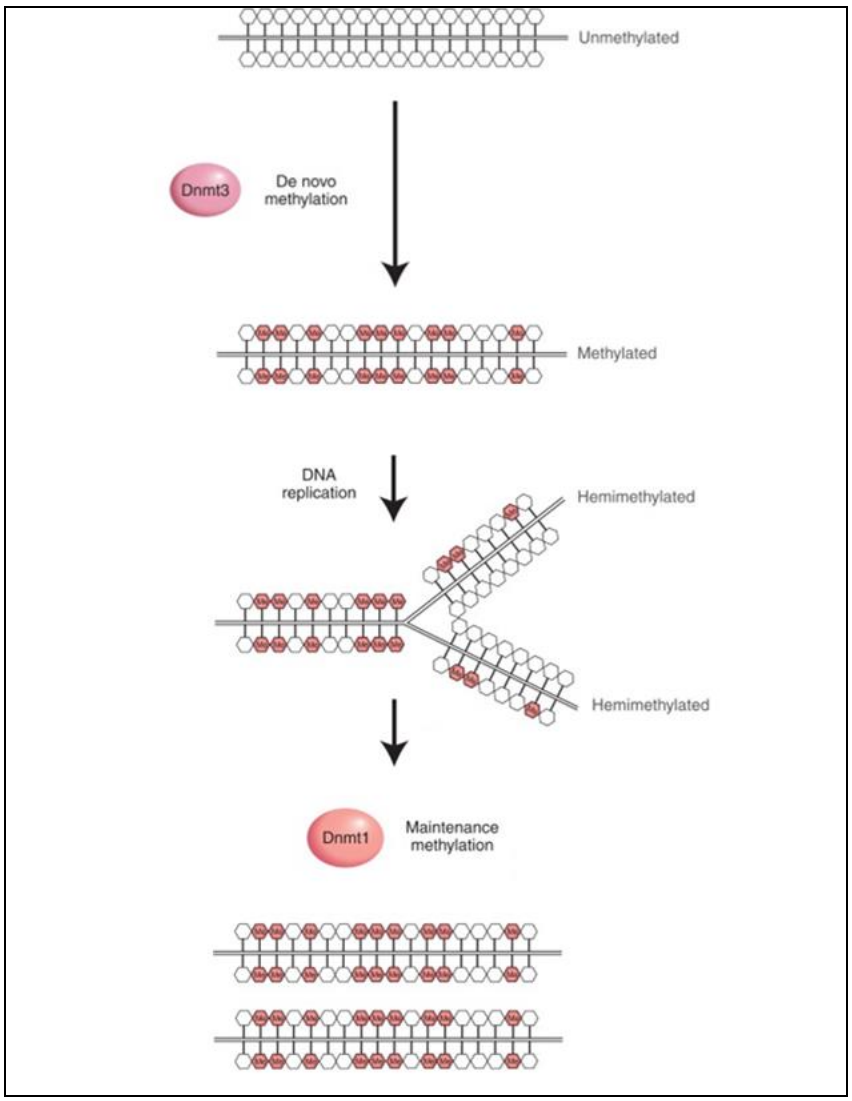

Figure 9: DNA methylation model. *De novo* and maintenance methylation. (Adapted from Li and Zhang, 2014).

DNMT3L, an important regulator without catalytic activity, is a co-factor of DNMT3A (Chen and Li, 2004; Li and Zhang, 2014; Smith and Meissner, 2013) and is essential for the establishment of genomic imprinting in germ cells (Bourc'his et al., 2001). Mice with dnmt3l knockout are viable, but male are sterile (Hata et al., 2002).

The DNMT family also includes DNMT2, which methylates small transfer RNAs (tRNAs) (Goll et al., 2006) and is not currently considered to be a DNA methylase. Thus, DNMT2 seems to have intermediate properties, sharing structural/catalytic features of a DNMT and nuclear-cytoplasmic localization of a RNA methyltransferase (Schaefer et al., 2008).

Moreover, a recent study identified a new *de novo* DNA methyltransferase, called DNMT3C, in murine germ cells. DNMT3C exhibits high identity with DNMT3B, and is specialized in methylating the young retrotransposons. Male mice without Dnmt3c are sterile (Barau et al., 2016).

2.2 DNMTs and tumorigenesis

An altered pattern of epigenetic modifications is central to many common human diseases, including cancer. Deregulation of DNA methylation induces imbalances in DNA modification, resulting in chromatin remodelling, genomic instability and gene inactivation (Zhang and Xu, 2017). Unlike normal tissue genomes, tumour cell genomes generally display global hypomethylation throughout, with localized hypermethylation in particular regions (**Figure 10**) (Dawson and Kouzarides, 2012).

Low level of DNA methylation was one of the first epigenetic alterations found in human cancers in comparison to normal tissues (Feinberg and Vogelstein, 1983). During the development of a neoplasm, the degree of DNA hypomethylation increases as the lesion progresses, from a benign proliferation of cells to an invasive cancer (Fraga et al., 2004).

The global DNA hypomethylation in tumour cells results in a reduction of 5-methylcytosine, generally at gene-coding regions and satellite repeats. These changes cause mitotic recombination, leading to deletions and translocations (Eden et al., 2003) and even loss of imprinting and reactivation of transposable elements (Esteller, 2008; Zhang and Xu, 2017). Two examples of the hypomethylation mechanisms are the activation of PAX2 gene, which encodes a transcription factor involved in cell proliferation, as well as

the expression of let-7a-3 miRNA gene, which is implicated in colon cancer (Brueckner et al., 2007; Wu et al., 2005).

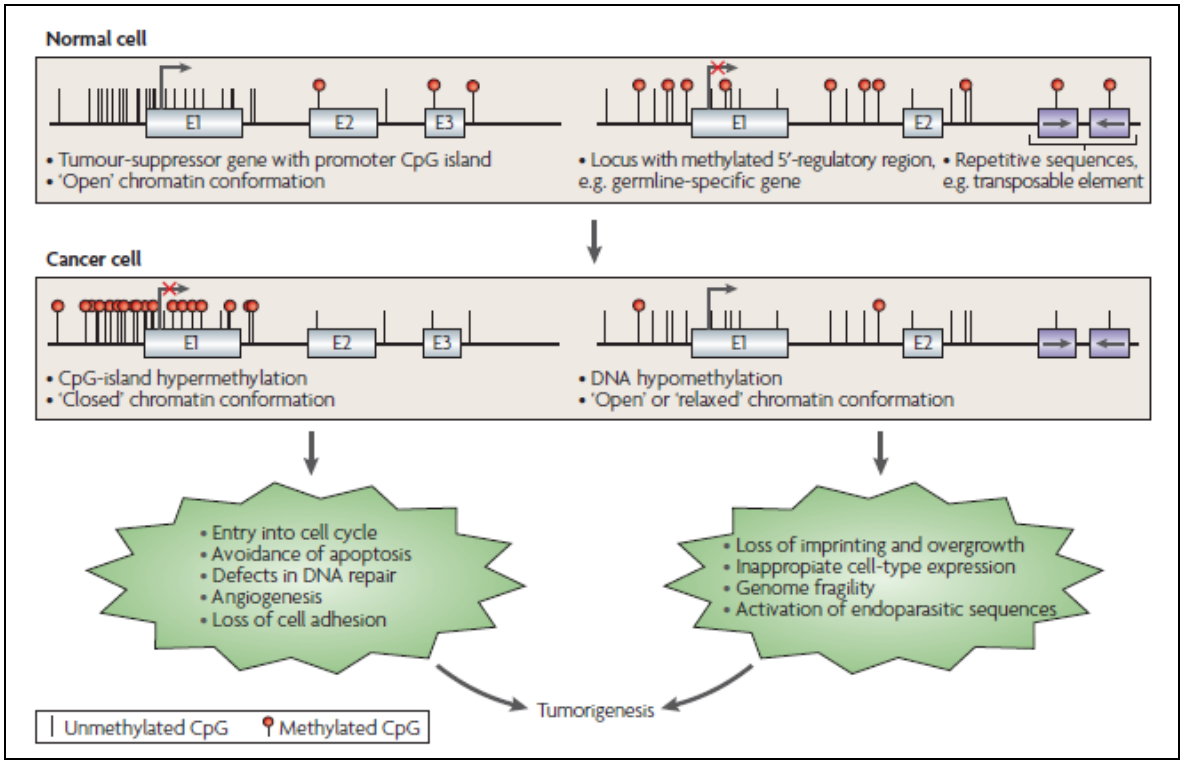

Figure 10: Aberrant DNA methylation in tumorigenesis. (Esteller, 2007).

Throughout malignant transformation, localized hypermethylation of several CpG-island promoters induces the transcriptional silencing of tumour suppressor genes (TSGs) (Baylin and Jones, 2014; Feinberg et al., 2016; Hanahan and Weinberg, 2000). Profiles of hypermethylation of the CpG islands in tumour-suppressor genes are specific to cancer type (Costello et al., 2000; Esteller et al., 2001a). A defining DNA "hypermethylome" can be assigned to each tumour type. These alterations can affect genes involved in the cell cycle, DNA repair, carcinogen metabolism, cell-to-cell interaction, apoptosis, and angiogenesis, all of which are involved in the development of cancer (Esteller, 2007; Herman and Baylin, 2003). Indeed, transcriptional repression of different TSGs, such as Rb (Greger et al., 1989; Sakai et al., 1991), p16/CDKN2A (Gonzalez-Zulueta et al., 1995; Herman et al., 1995; Merlo et al., 1995), RASSF1, MLH1 (Herman and Baylin, 2003), BRCA1 (Butcher and Rodenhiser, 2007; Esteller et al., 2000a; Herman and Baylin, 2003) *etc*., has been extensively described in several malignancies (Shafiei et al., 2008; Zhao et

al., 2010). Silencing of the DNA-repair gene blocks the repair of genetic mistakes, thereby opening the way to neoplastic transformation of the cell (Esteller, 2008).

Although deregulation of DNA methylation pattern is attributed to different mechanisms, alteration of DNMT1, 3A and 3B is a primary causative factor (Herman et al., 1996; Laird, 2003). Aberrant quantity/activity of DNMT3 family enzymes may depends on deletion, over-expression and mutation, however, the over-expression of DNMTs is the most described alteration in several human tumour types, including lymphomas, liver, prostate, colorectal, breast, lung, pancreatic and endometrial cancer (Eads et al., 1999; Gao et al., 2011; Girault et al., 2003; Jin et al., 2005; Patra et al., 2002; Saito et al., 2003), and is generally associated with a more aggressive phenotype, indicating that DNMT1, 3A and 3B likely act as oncogenes (Fernandez et al., 2012).

2.3 Epigenetics in clinical use

The DNA-methylation and histone-modification patterns have potential clinical use. DNA hypermethylation markers are under study as complementary diagnostic tools, prognostic factors, and predictors of treatment responses (**Figure 11**) (Esteller, 2008).

For instance, the glutathione S-transferase gene (GSTP1) is hypermethylated in 80 to 90% of patients with prostate cancer (Cairns et al., 2001; Esteller et al., 1998; Lee et al., 1994), but it is not hypermethylated in benign hyperplastic prostate tissue (Jerónimo et al., 2001). Moreover, because hypermethylation of the CpG island is an early event in the development of cancer, identification of DNA hypermethylation in a breast-biopsy specimen from a carrier of a BRCA1 mutation could be useful when the pathological diagnosis is uncertain (Esteller et al., 2001b), considering that for breast cancer, as for other cancers types, early detection is the most efficient strategy to decrease mortality (Lo and Sukumar, 2008). The application of DNA hypermethylation as cancer cell markers in clinical practice will require rapid, accurate, quantitative and cost-effective techniques as well as objective criteria for the selection of genes having a pivotal role in different tumour types (Esteller, 2008).

Epigenomic profiles might be used as biomarkers for tumour prognosis. For example, hypermethylation of the death-associated protein kinase (DAPK), p16, and epithelial membrane protein 3 (EMP3) has been linked to poor outcomes in lung, colorectal, and

brain cancer, respectively (Esteller, 2007). Muller et al. studied 39 genes in serum circulant DNA from normal control patients and patients with primary or metastatic breast cancer and identified two genes, RASSF1A and APC, whose methylation has a statistically significant association with poor outcome (Muller et al., 2003). Prognostic dendograms have also been developed. These epigenomic profiles have the advantage that they can be assayed using DNA that has been extracted from archived material (Esteller, 2005, 2007; Laird, 2003).

Finally, the hypermethylation of specific genes can potentially be used as a predictor to evaluate the chemotherapy response in affected patients. Two studies have shown that the hypermethylation of MGMT is an independent predictor of a favourable response of gliomas to carmustine (BCNU) (Esteller et al., 2000b) or Temozolomide (Rimel et al., 2009). Widschwendter et al. showed that the methylation status analysis of the oestrogen receptor (ERα) represents an alternative parameter to determine whether endocrine therapy will be effective in breast cancer patients (Widschwendter et al., 2004), since 30% of breast tumours show promoter hypermethylation of ERα gene (Lapidus et al., 1998; Ottaviano et al., 1994) and are resistant to endocrine therapy.

Because epigenetic alterations are potentially reversible, DNMTs also represent attractive therapeutic targets since their inhibition might have the ability to overturn tumour cell phenotype (Aldawsari et al., 2015; Erdmann et al., 2015; Subramaniam et al., 2014). DNA-demethylating drugs in low doses have shown a significant antitumoral activity and US Food and Drug Administration (FDA) has approved the use of two such agents, 5-azacytidine (Vidaza) and 5-aza-2-deoxycytidine (decitabine), as elective treatments for myelodisplastic syndrome and leukemia (Mack, 2006; Müller et al., 2006; Oki et al., 2007).

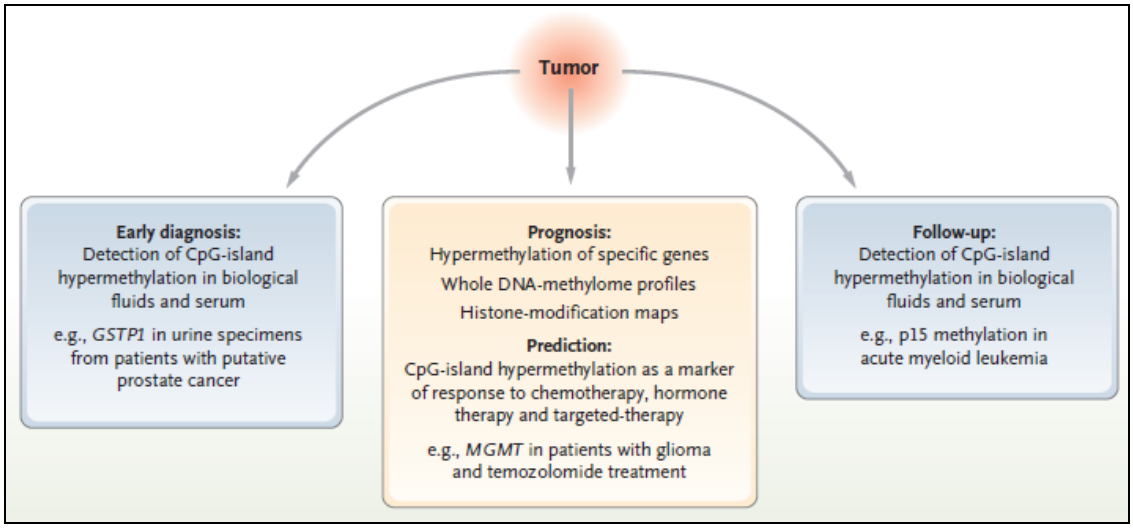

Figure 11: Epigenetics in Cancer Management. (Esteller 2008).

2.4 Epigenetics and RMS

In a previous work Chen et al. have analysed the expression of DNMT1 in 32 RMS and 12 normal muscle samples showing an increased expression of this gene with a statistically significant difference in ARMS and ERMS cases (Chen et al., 1999). Moreover, DNA methylation signatures have been recently described in ARMS and ERMS patients, suggesting that aberrant DNA methylation may contribute to the development of RMS. Furthermore, cluster analysis revealed that embryonal and alveolar subtypes have distinct DNA methylation patterns, with ARMSs being enriched in DNA hypermethylation of polycomb target genes (Mahoney et al., 2012). Indeed, hypermethylated CpG islands have been identified in several genes involved in oncogenesis, skeletal muscle development and differentiation in both RMS cell lines and primary tumour samples (Chen et al., 1998; Gastaldi et al., 2006; Mahoney et al., 2012). Consistently, treatment with 5-aza-2'-deoxycytidine (5-aza-dC), a general DNA demethylating agent, is able to suppress tumorigenicity and partially reactivate myogenic program in different RMS cell lines (Gastaldi et al., 2006; Megiorni et al., 2014).

AIM

The aim of the present research project was to analyse the expression levels and the specific role of the *de novo* DNA methyltransferase DNMT3A and DNMT3B in RMS tumorigenesis.

In this regard, we examined the transcript levels of these DNMTs in RMS primary tumour cases and cell lines and the biological consequences of their inhibition in RMS *in vitro* models. Indeed, we performed RNA-interference experiments to evaluate the effects of DNMT3A or DNMT3B silencing on phenotype, cell cycle, apoptosis, migration and ability to form colonies of RMS cells. We also investigated the ability of cells depleted of the two specific DNMTs to properly reactivate the myogenic differentiation program by morphologic analysis, as well as the expression of specific muscle markers. Finally, we analysed whether DNMT silencing can potentiate the antitumour effects in RMS of standard radiotherapy.

The results of our project represent a further step towards the comprehension on RMS development, which might lead to more efficient and less toxic treatments for RMS patients.

MATERIALS AND METHODS

Patient clinical features

Fourteen RMS primary tumour samples, 7 ARMSs and 7 ERMSs, were obtained at diagnosis before any treatment from children admitted to the Department of Paediatrics and Infantile Neuropsychiatry at "Sapienza" University, and the Department of Oncology at the Alder Hey Children's NHS Foundation Trust, Liverpool. Histopathological diagnosis was confirmed using immunohistochemistry. All 7 ARMS cases were investigated for t(2;13)(q35;q14) or t(1;13)(p36;q14) translocations that involve PAX3/7 genes (mapped on chromosome 2 and 1, respectively) and FOXO1 gene (mapped on chromosome 13) by using standard FISH (Fluorescent In Situ Hybridization), analysis: 5 tumours were PAX3-FOXO1-positive, 1 was PAX7-FOXO1-positive and 1 was fusion-negative. Patients were grouped according to the IRS post-surgical Grouping System. Details of the patients are described in **Table 5.**

Samples were immediately frozen in liquid nitrogen after surgery and stored at -80°C. Normal skeletal muscle (NSM), obtained from eight children undergoing surgery for non-oncological conditions, was used as negative control. Institutional written informed consent was obtained from the patient's parents or legal guardians. The study underwent ethical review and approval according to the local institutional guidelines (Alder Hey Children's NHS Foundation Trust Ethics Committee, approval number 09/H1002/88).

Table 5: Clinicopathological features of the analysed tumour cases. Fusion status - **PAX3**: PAX3-FOXO1-positive; **PAX7**: PAX7-FOXO1-positive; **n. a.**: not applicable.

Case	Age at diagnosis (month)	Sex	Histology	Fusion status	Primary site	Clinical stage (IRS)
ARMS1	108	F	alveolar	PAX3	trunk	III
ARMS2	82	F	alveolar	PAX3	extremity	III
ARMS3	59	M	alveolar	negative	trunk	II
ARMS4	5	F	alveolar	PAX7	uterus-vagina	III
ARMS7	131	M	alveolar	PAX3	extremity	IV
ARMS36	7	F	alveolar	PAX3	trunk	III
ARMS37	90	F	alveolar	PAX3	uterus-vagina	II
ERMS1	63	M	embryonal	n. a.	retroperitoneum	III
ERMS2	122	M	embryonal	n. a.	bladder-prostate	III
ERMS3	61	M	embryonal	n. a.	bladder-prostate	III
ERMS4	45	M	embryonal	n. a.	trunk	III
ERMS12	18	M	embryonal	n. a.	bladder-prostate	III
ERMS21	3	M	embryonal	n. a.	retroperitoneum	III
ERMS23	37	F	embryonal	n. a.	uterus-vagina	II

Cell lines and cultures

Human alveolar (RH4 and RH30) and embryonal (RD and TE671) cell lines were maintained in high-glucose Dulbecco's modified Eagle's medium (DMEM-HG) supplemented with 10% foetal bovine serum (FBS), 1% v/v L-glutamine, 100 µg/ml streptomycin and 100 U/ml penicillin, and grown at 37°C in a humidified atmosphere of 5% CO_2. To minimize the risk of working with misidentified and/or contaminated cell lines, we later stocked the cells used in this report at very low passages and used at <20 subcultures. DNA profiling using the GenePrint 10 System (Promega Corporation, Madison, WI) was carried out to authenticate cell cultures, comparing the DNA profile of our cell cultures with those found in GenBank. Human foetal myoblast (HFM) cells were maintained in DMEM-HG supplemented with 20% FBS, 1% v/v L-glutamine, 100 µg/ml streptomycin and 100 U/ml penicillin, and grown at 37°C in a humidified atmosphere of 5% CO_2.

Transient transfection and RNA interference

RD and TE671 cells were seeded at 2×10^5 cells/well in 12-well plates. Just a few hours before transfection, the DMEM-HG was removed, and after PBS (Calcium and Magnesium-Free Phosphate-Buffered Saline) wash, antibiotic free DMEM-HG medium was replaced. Small interfering RNA (siRNA) against human DNMT3A (si-DNMT3A, sc-37757 by Santa Cruz Biotechnology, Dallas, TX), DNMT3B (si-DNMT3B, sc-37759 by Santa Cruz Biotechnology) or siRNA negative control (si-NC, sc-37007 by Santa Cruz Biotechnology) were combined with RNAiMAX (Invitrogen) and used at 60 nM final concentration; si-DNMT3B is a pool of 3 target specific 19-25 nt siRNAs designed to specifically knock-down DNMT3B gene and this product was previously validated in other publication (Galli et al., 2013; Gravina et al., 2011). miRNA mimics (miR-29a-3p, MC12499 or miR-29c-3p, MC10518, Dharmacon Research) or negative control (miR-Ctr, Dharmacon Research) were transfected using Lipofectamine 2000 reagent (Life Technologies) at 50 nM final concentration, following the manufacturer's protocol. The day after transfection, DMEM-HG was replaced, and cells were incubated at 37°C in 5% CO_2 for different times. Cells were collected for cell cycle analysis, Q-PCR, western blot, immunofluorescence, migration, etc. at different times after transfection.

Radiation exposure

RD cells transfected with DNMT3A, DNMT3B or NC siRNAs were cultured for 48 h before radiation exposure. Radiation was delivered at room temperature using an x-6 MV photon linear accelerator. The total single dose of 4 Gy was delivered with a dose rate of 2 Gy/min using a source-to-surface distance of 100 cm. Doses of 200 kV X-rays (Yxlon Y.TU 320; Yxlon, Copenhagen, Denmark) filtered with 0.5 mm Cu. The absorbed dose was measured using a Duplex dosimeter (PTW, Freiburg, Germany). The dose-rate was approximately 1.3 Gy/min and applied doses ranged from 0 to 600 cGy. At 72h post transfection and 24 h after radiation exposure, cells were collected for cell proliferation assay, colony formation assay, cell cycle analysis and western blot experiments.

RNA isolation

Total RNA was extracted from samples and cell lines. Tumour tissues and NSM were disrupted and homogenised using TissueLyser II (QIAGEN) through the beating and grinding effect of beads on the sample material in an appropriate volume of TRIzol (Invitrogen, Carlsbad, CA). For RNA isolation from cell lines, 1 ml of TRIzol was added directly on the cell pellet. From this point the protocol was the same for both tumour samples and cell lines. Briefly, the samples were incubated 5 minutes (min) at room temperature (RT) to allow the complete dissociation of nucleoprotein complexes. After adding of chloroform, samples were vortexed, incubated for 2-3 min at RT and centrifugated at 14000 rpm (rotation per minute) for 15 min at +4°C. The upper aqueous phase was recovered, and RNA was collected by alcohol precipitation using isopropanol. After incubation of 10 min at RT the samples were centrifugated at 14000 rpm for 10 min at +4°C. The supernatant was removed, and the pellet was washed twice in 75% ice-cold ethanol, then, after a further centrifugation step the ethanol was removed, and the nucleic acid pellet was allowed to dry before being resuspended in adequate volume of RNAse free water. RNA purity, integrity and quantity were checked using NanoDrop 2000 (Thermo Scientific, Waltham, MA).

Reverse Transcription and Quantitative real time PCR (Q-PCR)

Total RNA (2 μg) was subjected to reverse transcription with High Capacity cDNA Reverse Transcription kit (Applied Biosystems, Foster City, CA). Master mix 2x was prepared as reported in **Table 6A** and then dispensed into the tubes containing RNA. Tubes were added on the 2720 Thermal Cycler (Applied Biosystem) machine and the program reported in **Table 6B** has run.

Quantitative Real Time PCR (Q-PCR) for human DNMT1 (Hs00154749_m1), DNMT3A (Hs01027166_m1), DNMT3B (Hs00171876_m1) and MyHC (Hs00428600_ m1) mRNAs was performed using specific TaqMan RealTime Gene Expression Assays (Applied Biosystems) (**Table 7A and 7B**).

Table 6A

Reagent	µl/sample
dNTPs 100 mM	0.8
10X RT Buffer	2.0
10X RT Random Primers	2.0
Reverse Transcriptase, 50 U/µL	1.0
nuclease-free water	4.2

Table 6B

Step	Time	Temperature
Hold	10 min	25 °C
Hold	120 min	37 °C
Hold	5 min	85 °C
Hold	∞	4 °C

Table 7A

Reagent	µl/sample
TaqMan® Small RNA Assay (20x)	0.5
Product from RT reaction (50ng/µl)	1
TaqMan® Universal PCR Master Mix II (2x)	5
nuclease-free water	3.5

Table 7B

	Temp.	Time	cycles
Polymerase activation	95°C	10 min	1
Denaturation Annealing/Extension	95°C 60°C	15 sec 1 min	40

Q-PCRs for human MYOD and Myogenin transcripts was carried out with the SensiFAST SYBR Hi-ROX Kit (Bioline, London, UK) (**Table 8A and 8B**). All Q-PCR assays were performed on a StepOne Real Time System (Applied Biosystems) machine. Samples were normalized according to the glyceraldehyde-3-phosphate dehydrogenase (GAPDH) mRNA levels.

Table 8A

Reagent	µl/sample
SensiFast™ SYBR Hi-ROX Mix 2x	5
Product from RT reaction (10ng/µl)	1
Primer Fw 20uM	0.2
Primer Rev 20uM	0.2
nuclease-free water	3.6

Table 8B

	Temp.	Time	cycles
Polymerase activation	95°C	2 min	1
Denaturation Annealing/Extension	95°C 60°C	5 sec 30 sec	40

Reverse transcription for human miR-133a (000458), miR206 (000510), miR-29a-3p, miR-29c-3p was carried out with TaqMan MicroRNA Assay kit (Applied Biosystems) using 20 ng of total RNA sample and the specific stem-loop primer as reported in the following tables (**Table 9A, 9B, 9C and 9D**):

Table 9A

Reagent	µl/sample
dNTPs 10 mM	0.75
10X RT Buffer	0.75
RNase Inhibitor	0.095
Reverse Transcriptase, 50 U/µL	0.5
Specific primer 5x	1.5
nuclease-free water	1.405

Table 9B

Step	Time	Temperature
Hold	30 min	16 °C
Hold	30 min	42 °C
Hold	5 min	85 °C
Hold	∞	4 °C

Table 9C

Reagent	µl/sample
TaqMan® Small RNA Assay (20x)	0.5
Product from RT reaction	0.665
TaqMan® Universal PCR Master Mix II (2x)	5
nuclease-free water	3.835

Table 9D

	Temp.	Time	cycles
Polymerase activation	95°C	10 min	1
Denaturation	95°C	15 sec	40
Annealing/Extension	60°C	1 min	

Data were normalized to U6 small nuclear RNA (RNU6, 001093) levels. The amount of each mRNA/miRNA was calculated by the comparative Ct method and expressed as fold change using the StepOne v2.3 software (Applied Biosystems). Each sample was run in triplicate in at least three independent experiments, unless specified differently in the figures.

Cell proliferation assays

Direct counting of RH4, RH30, RD and TE671 living cells was performed with trypan blue exclusion dye (Sigma-Aldrich, Saint Louis, MO) using the Countess II Automated Cell Counter (Thermo Fisher) at 72 h after si-DNMT3A, si-DNMT3B or si-NC transfection and after radiation exposure of RD cells or at 72 h post miRNA mimic transfection. Experiments were repeated at least three times, unless specified differently in the figures. Cell viability of the siRNA-transfected cells was determined by using MTT [3-(4,5-dimethylthiazol2-yl)-2,5-diphenyltetrazolium] assay. RD cells (10^4) were plated onto 96-well plates in sextuplicates and, after 24 h, transfected with synthetic DNMT3B siRNA; mocked control cells (transfected with si-NC) and blank cell-free wells were also included.

At designated times after transfection (0-24-48-72 h), 10 µl of MTT (5 mg/ ml, Sigma-Aldrich) were added to each well and plates were incubated at 37°C for 3 h. Media were removed and 100 µl of DMSO was added into each well to dissolve the dark blue formazan crystals. Absorbance was read at wavelength of 550 nm, with reference at 630 nm, using a microtitre plate reader (SelectScience, Corston, UK). The percentage cellular viability was calculated with the appropriate controls taken into account. The results were plotted as means ± SD of two separate experiments having six determinations per assay for each experimental condition.

Morphological assessment of siRNA-transfected cells

An Axio Vert.A1 microscope (Carl Zeiss Microscopy, Thornwood, NY), furnished with an AxioCam MRc5 camera (Carl Zeiss Microscopy) was used to observe the morphological changes of the cells transfected with si-DNMT3A, si-DNMT3B or si-NC siRNAs. Cells were photographed at 72 and 144 h post-transfection using a 20x magnification. Images were analysed by using the ImageJ software (NIH ImageJ 1.47).

Cell cycle analysis

In order to study cell cycle distribution, RH4, RH30, RD and TE671 cells, transfected with DNMT3A, DNMT3B or NC siRNAs for 48 h, RD cells, transfected with miR-29a-3p, miR-29c-3p or miR-Ctr for 48 h, and RD cells 24 h after radiation exposure, were trypsinised, centrifugated at 1500 rpm for 5 min at + 4 °C and washed twice in ice-cold PBS. Cells were counted and at least 10^6 cells were fixed in 70% ice-cold ethanol overnight at +4°C. The day after, cells pellets were washed twice in ice-cold PBS, treated with RNase A (50 µg/ml) for 30 min at 37°C and then stained with propidium iodide (10 µg/ml) solution. DNA content was measured by BD FACSCalibur Flow Cytometer (BD Biosciences, San Jose, CA). Data were analysed using ModFit 3.1 software (BD Biosciences). Experiments were carried out three times, unless specified differently in the figures.

Apoptosis analysis

Apoptosis was analysed by flow cytometry using PE Annexin V Apoptosis Detection Kit I (BD Biosciences). Briefly, floating and attached RD cells transfected with DNMT3B or NC siRNAs were collected at 72 h after transfection, washed twice in ice-cold PBS and resuspended in fresh 1x Annexin V Binding Buffer at a concentration of 10^6 cells/ml. Approximately $2x10^5$ cells were stained with Annexin V and 7-Amino-Actinomycin (7-AAD) for 15 min at RT in the dark according to the manufacturer's instructions. Annexin V and 7-AAD fluorescence intensities of control or treated samples were analysed using a BD FACSCalibur (BD Biosciences). Data were collected and analysed using Cell Quest Pro software (BD Biosciences). Experiments were performed three times.

Trans-well migration assay

For cell migration assay, BD FalconTM Cell Culture Inserts with 8 μm pore polycarbonate filters were placed into a 24-well culture plate. Briefly, serum-free cell suspension, containing 10^5 si-DNMT3B, si-NC, miR-29a-3p, miR-29c-3p or miR-Ctr RD cells, was added to the upper compartment of the chamber at 48 h post-transfection. The lower compartment contained DMEM-HG with 10% FBS, used as chemoattractant. After incubation at 37°C for additional 24 h, the inserts were washed twice in PBS and migrated cells at the base of the inserts were fixed in 100% methanol for 20 min at -20°C. After two washing in PBS, cells were stained with 0.1% crystal violet dye in 25% methanol for 5 min at RT. Non-migrating cells on the upper surface of the membrane were removed with cotton swabs and then the inserts were washed in water and allowed to dry. Cells were photographed under a light microscope at 10x. The area occupied by migrated cells in si-DNMT3B and si-NC samples was measured by using the ImageJ software (http://imagej.nih.gov/ij/). Experiments were carried out three times, unless specified differently in the figures.

Colony formation assay

For anchorage-dependent colony formation assays, RD cells after DNMT3A, DNMT3B or NC-siRNA transfection, irradiated or not with 4 Gy and miR-29a-3p, miR-29c-3p or miR-

Ctr RD cells were plated in 6-well plates at 4×10^3 cells/well and cultured for 11 days. Colonies were washed twice in PBS and fixed in 100% methanol for 20 min at -20°C. After two washing in PBS, cells were stained with 0.1% crystal violet dye in 25% methanol for 10 min at RT. Colonies were washed in water, allowed to dry and finally photographed. To quantify colonies, crystal violet was solubilized in 30% acetic acid in water for 15 min at RT and absorbance was measured using the Biochrom Libra S22 UV/VIS spectrophotometer (Biochrom, Berlin, DE) at wavelength of 595 nm; 30% acetic acid in water was used as the blank. Assays were carried out three times, unless specified differently in the figures.

U0126 treatment

RD and TE671 cells were seeded at $4x10^5$ cells/well in 6-well plates. After 24 h, the MEK/ERK inhibitor U0126 (Santa Cruz Biotechnology) was added to a final concentration of 10 μM. Following different times of treatment, cells were collected for western blot and Q-PCR experiments. Mocked control cells were treated with DMSO.

Protein extracts and western blot analysis

RH4, RH30, RD and TE671 cells, transfected with siRNAs/miRNA mimics, treated with U0126 or after radiation exposure, were lysed in RIPA buffer (150 mM NaCl, 1% NP-40, 50 mM tris-HCl pH 8, 0.5% deoxycholic acid, 0.1% SDS, 1 mM PMSF, 1 μg/ml leupeptin, 1 μg/ml aprotinin, 1x protease inhibitor, 1 mM Na_3VO_4 and 50 mM NaF) for 20 min on ice. Samples were centrifugated at 14000 rpm for 10 min at +4°C, and the supernatant, containing total protein, was recovered. Protein extracts were quantified using the Biorad Protein Assay Kit (Biorad, Berkeley, CA) by measuring the absorbance of samples and BSA (bovine serum albumin) standard curve at wavelength of 595 nm. Total protein extracts (30 μg) were separated on 6-15 % sodium dodecyl sulfate (SDS) polyacrylamide gel (100 V for about 2 h) and transferred (250 mA for about 1 h 30 min) onto polyvinylidene fluoride (PVDF) membranes (EMD Millipore Corporation, Billerica, MA). Filters were stained in Ponceau S solution (Sigma-Aldrich), washed in 1x PBS with 0.1% Tween (PBS-T) and then blocked in 5 % not-fat milk or 3% BSA and incubated over-night

at +4 °C or 2 h at RT with the following primary antibodies: Bcl-xL, Cyclin B1, Cyclin E2, DNMT3B, E2F1, p21, p27, Caveolin 1, DNA-PK_{cs}, ATM, and RAD51 by Santa Cruz Biotechnology; cleaved PARP, MYOD1, Myogenin and MyHC by EMD Millipore Corporation; DNMT1 and DNMT3A by GeneTex, Irvine, CA; Cyclin D1 by MBL International, Woburn, MA; phospho-pRB at Ser807/811 (p-RB), total RB, phospho-p38 at Thr180/Tyr182, total p38 and phospho-H2AX by Cell Signalling Technology, Danvers, MA. Filters were washed three times in PBS-T and were incubated with appropriate horseradish peroxidase (HRP)-conjugated secondary antibodies (Santa Cruz Biotechnology) for 1 h at RT. After three washing in PBS-T protein signals were detected using WesternBright ECL kit (Advansta, Menlo Park, CA), according to the manufacturer's instructions, and visualized by ChemiDoc XRS+ (Bio-Rad). Tubulin (Sigma-Aldrich) was used as a normalization control for equal loading. Densitometry was performed to quantify changes in protein expression using the Image Lab 5.1 software (Bio-Rad). Briefly, signal intensity for each band was calculated by the local subtraction method. DNMT3B protein levels in si-DNMT3B samples were then normalized and reported as relative expression with respect to si-NC cells. All experiments were carried out at least three times, unless specified differently in the figures.

Immunofluorescence

RD and TE671 cells transfected with DNMT3B or NC siRNAs were cultured for 48 h before plating 10^5 cells per well in 24-well plates with 2% gelatine-coated glasses. After one additional day, cells were washed twice in PBS and fixed in 4% paraformaldehyde (PFA) in PBS for 30 min at RT, followed by treatment with 0.1 M glycine in PBS for 20 min at RT and with 0.1 % Triton X-100 in PBS for additional 5 min at RT to allow permeabilization. Cells were incubated for 1 h at RT with the following primary antibodies: Cyclin B1, DNMT3B, E2F1 and p21 (Santa Cruz Biotechnology); MYOD1 and MyHC (EMD Millipore Corporation); Cyclin D1 (MBL International); p-RB (Cell Signalling Technology). After washing in PBS, cells were incubated with appropriate Texas Red-coniugated secondary antibodies (Jackson ImmunoResearch, West Grove, PA,) for 30 min at RT in the dark. Nuclei were counter-stained with 1 μg/ml 4', 6-diamido-2phenylindole dihydrochloride (DAPI, Sigma-Aldrich). Labelled cover-slips mounted in Moviol were

acquired with Zeiss ApoTome and Axiovision software (Carl Zeiss) using a 40x magnification. Experiments were replicated twice.

Statistical analysis

Data were expressed as mean ± standard deviation (SD) of each condition. Statistical significance between groups was assessed by Student's t-test and probability (p) values of less than 0.05 were accepted as significant.

RESULTS

Expression of DNMT1, DNMT3A and DNMT3B in RMS tumours and cell lines

To explore the association between DNA methylation and RMS, transcript levels of DNMT1, DNMT3A and DNMT3B genes were assessed in 14 RMS primary tumours, 7 ARMSs and 7 ERMSs, by using Real Time PCR. DNMTs levels were significantly up-regulated in all tumour samples in comparison to NSM, used as normal tissue, with an average increase of 30.5±9.0, in accordance with previously published data (Chen et al., 1999), 22.0±3.3 and 81.2±9.4, respectively (**Figure 12** and **13**). Therefore, we focused on DNMT3B enzyme, whose over-expression was also confirmed in ARMS (RH4 and RH30) and ERMS (RD and TE671) cell lines both at mRNA and protein levels (**Figure 14A** and **14B**).

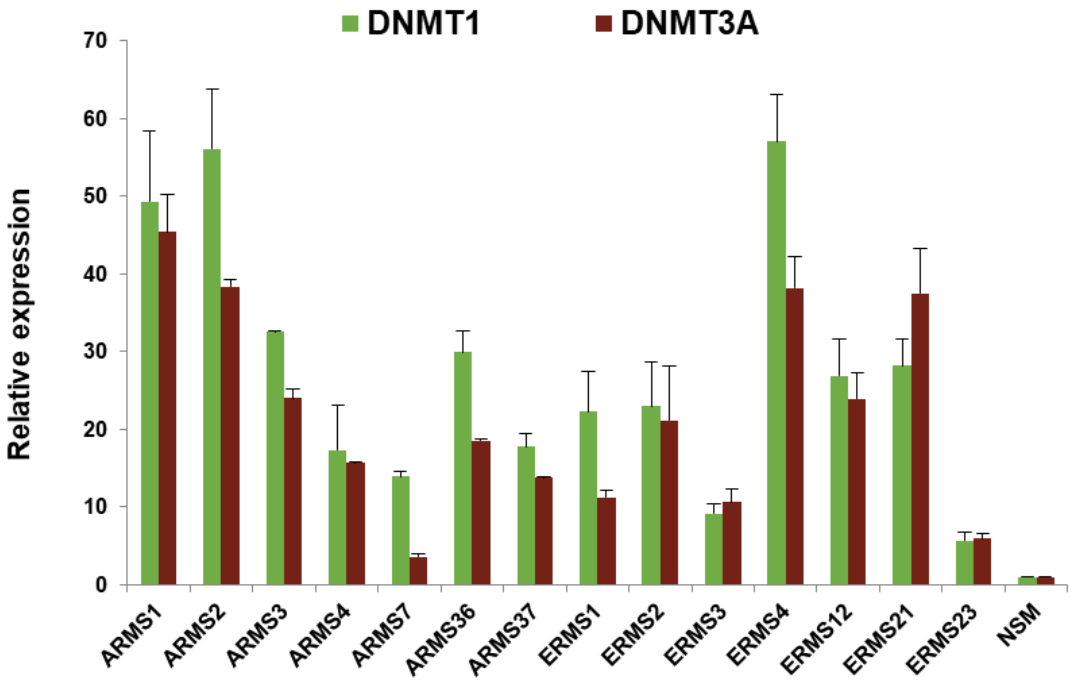

Figure 12: DNMT1 and DNMT3A expression in RMS tumours. Q-PCR analysis of DNMT1 and DNMT3A mRNA levels in 7 ARMSs and 7 ERMSs, expressed as fold increase over NSM,

arbitrarily set at 1. Transcript levels were normalized to GAPDH mRNA and error bars represent standard deviation (SD) of two independent Q-PCR reactions, each performed in triplicate.

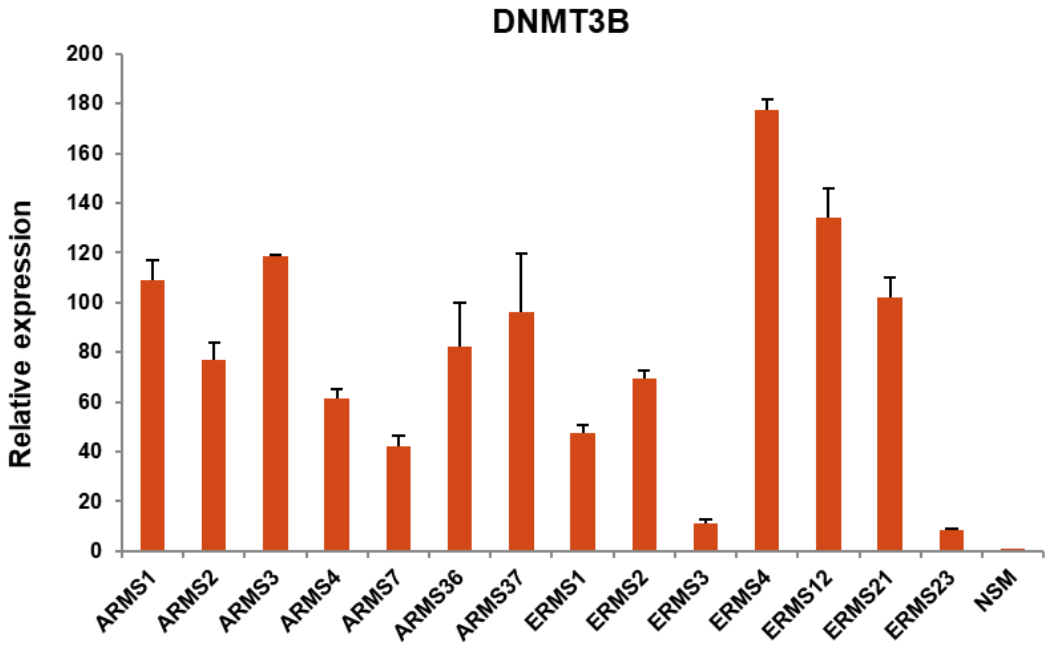

Figure 13: DNMT3B expression in RMS tumours. Q-PCR analysis of DNMT3B mRNA levels in 7 ARMSs and 7 ERMSs, expressed as fold increase over NSM, arbitrarily set at 1. Transcript levels were normalized to GAPDH mRNA and error bars represent standard deviation (SD) of two independent Q-PCR reactions, each performed in triplicate.

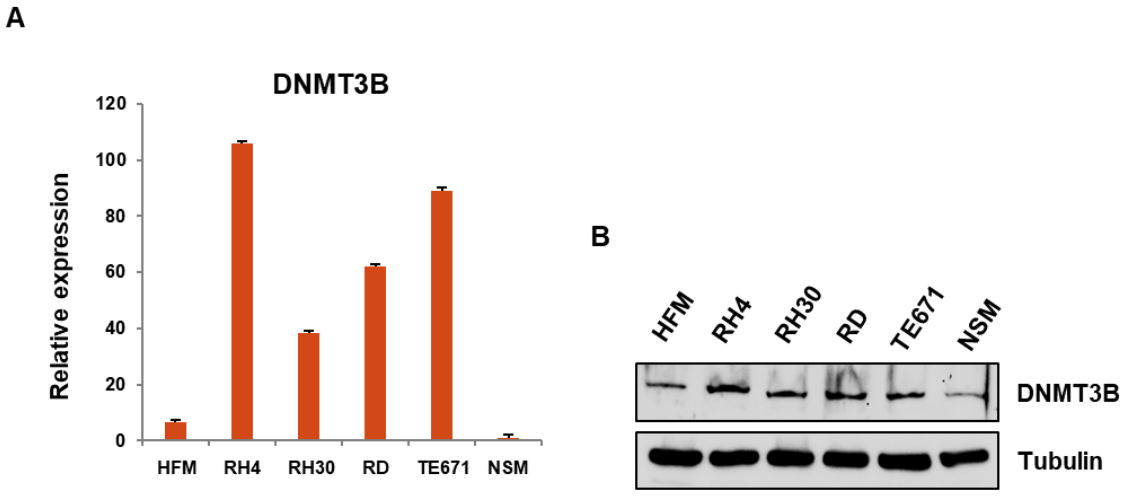

Figure 14: DNMT3B expression in RMS cell lines. A) Q-PCR of DNMT3B mRNA levels in ARMS (RH4 and RH30) and ERMS (RD and TE671) cell lines, expressed as fold increase over NSM, arbitrarily set at 1. GAPDH was used as endogenous control. Bars represent mean values of

three independent experiments, each performed in triplicate. HFM, human foetal myoblats. **B)** Western blot showing the expression of DNMT3B protein in RH4, RH30, RD and TE671 cell lines. Tubulin was used as loading control. Representative of three different experiments.

siRNA transfection down-regulates DNMT3B expression and inhibits RMS cell proliferation

To evaluate the effect of DNMT3B enzyme on the phenotype of RMS cells, we used a specific small interfering RNA (siRNA) against DNMT3B mRNA in RD cell line, an *in vitro* model of ERMS. siRNA transfections were performed in RD cells cultured in growth medium, i.e. supplemented with 10% serum. DNMT3B knock-down efficiency was assessed by using Q-PCR and western blot analysis at 72 h after transfection. A significant reduction of DNMT3B at both mRNA (0.5-fold) and protein (0.5- fold) levels (**Figure 15A** and **15B**) was observed in si-DNMT3B cells compared to those transfected with the negative control siRNA (si-NC). DNMT1 and DNMT3A expression was not significantly perturbed by transient si-DNMT3B transfection, this assessing a specific silencing (**Figure 15A** and **15B**). Immnunoflurescence experiments showed a strong nuclear distribution of DNMT3B protein in mocked control RD cells, whit a remarkable decline in its expression upon si-DNMT3B transfection (**Figure 15C**). At 72 h after transfection, direct counting for living cells using trypan blue dye exclusion test confirmed that DNMT3B depletion drastically inhibited the proliferation potential of RD cells compared to si-NC cells (**Figure 16A**). Similar results were obtained by MTT assay, which showed a significant decrease of cellular viability/proliferation rate in si-DNMT3B compared to si-NC transfected cultures, with a peak of about 50% at 72 h post transfection (**Figure 16B**). DNMT3B siRNA transfection carried out in a second ERMS cell line (TE671) gave overlapping results, showing a marked reduction in DNMT3B protein levels and a down-regulation of the enzyme in the nuclear compartment (**Figure 17A** and **17B**). DNMT3B knocked-down TE671 cells also exhibited a minor cell growth rate (**Figure 17C**).

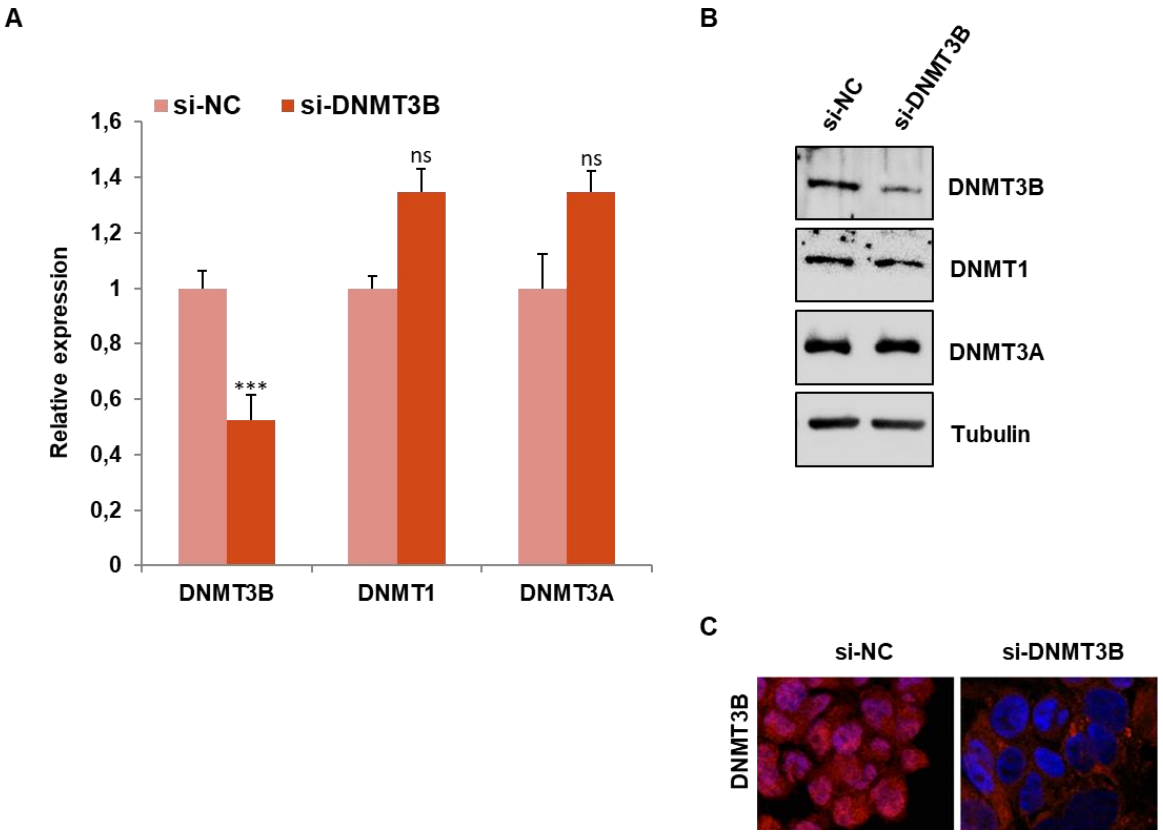

Figure 15: DNMT3B knock-down by RNA interfering in RD cells. A) DNMT transcript levels measured by Q-PCR at 72 h in RD cells after transfection with si-DNMT3B in comparison to samples transfected with si-NC, arbitrarily set at 1. GAPDH was used as a control. Shown are the means of four independent experiments. Error bars represent SD of the means. Asterisks represent the statistical significance (***, $p<0.001$; ns, not significant). **B)** Western blots showing the expression of DNMT3B protein at 72 h after si-DNMT3B transfection compared to si-NC cells. Tubulin was used as loading control. DNMT1 and DNMT3A protein levels were not perturbed by si-DNMT3B delivery. Representative of three independent experiments. **C)** Representative immunofluorescence showing the down-regulation of DNMT3B protein levels in nuclear compartment at 72 h after si-DNMT3B transfection. High levels of DNMT3B were evident in the nuclei of si-NC cells.

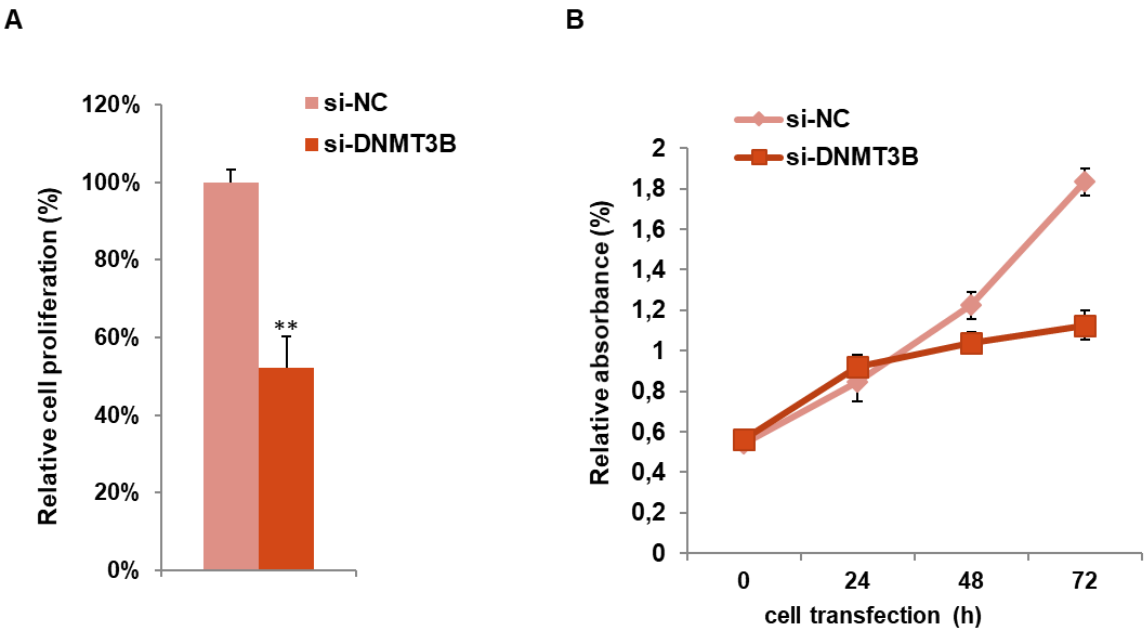

Figure 16: Depletion of DNMT3B inhibits RD cell proliferation. A) Viability of RD cells 72 h post-transfection with DNMT3B siRNA calculated with respect to control si-NC cells, assessed by trypan blue exclusion staining. Results represent the mean value of four independent experiments ± SD. Statistical significance: **, $p<0.01$. **B)** MTT assay performed to assess relative RD cell numbers at different point after si-DNMT3B or si-NC transfection (0-24-48-72 h). Each point is the mean of three replicate wells ± SD and is representative of three independent experiments.

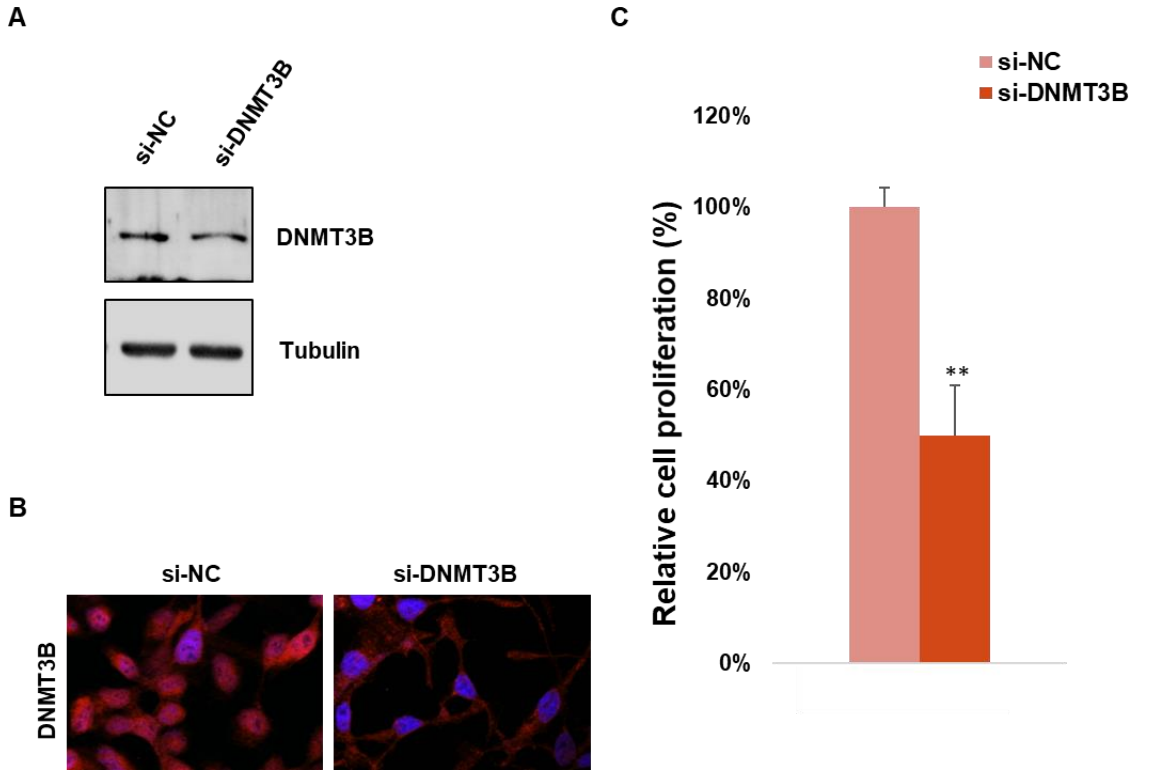

Figure 17: RNA interfering-mediated DNMT3B knock-down affects TE671 cell viability. A) Western blot showing the expression of DNMT3B protein in TE671 cells at 72 h after si-DNMT3B transfection compared to si-NC sample. Tubulin was used as loading control. **B)** Representative immunofluorescence showing the down-regulation of DNMT3B protein levels in nuclear compartment at 72 h after si-DNMT3B transfection. High levels of DNMT3B were evident in the nuclei of si-NC cells. **C)** Viability of TE671 cells 72 h post-transfection with DNMT3B siRNA calculated with respect to control si-NC cells, assessed by trypan blue exclusion staining. Results represent the mean value of four independent experiments ± SD. Statistical significance: **, $p<0.01$.

Decreased DNMT3B expression induces G1 cell cycle arrest

To further determine whether the reduced RD cell growth was due to alterations in cell cycle progression, flow cytometry analysis was performed. Based on propidium iodide staining of cellular DNA content, DNMT3B down-regulation resulted in a significant increase of cell percentage in G1 phase ($p<0.005$) with a concomitant decrease of cell percentage in S and G2 phases (G1: 78.0±2.8%, S: 15.1±2.5%, G2: 6.9±0.27%), whilst si-NC transfected cells rapidly divided and progressed through the cell cycle at high rates (G1: 43.5±0.7%, S: 44.9±2.0%, G2: 11.6±1.3%) (**Figure 18**).

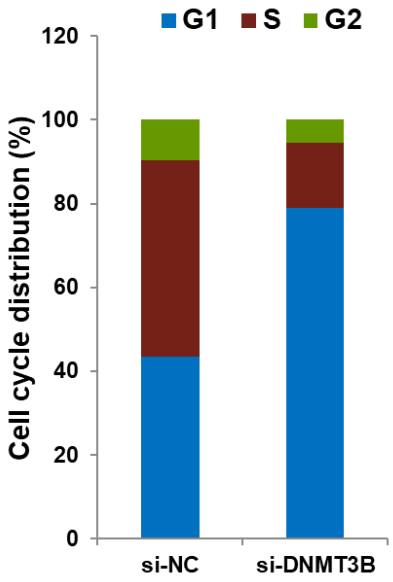

Figure 18: Cell cycle distribution. Flow cytometry data showing percentages of cells in G1, S and G2 phases in si-DNMT3B and si-NC RD cells at 48 h after transfection. Data are average values of three independent experiments.

Consistent with G1 arrest, the expression of different cell cycle regulators was modulated with a marked decrease of Cyclin B1, Cyclin D1 and Cyclin E2 expression (**Figure 19A**) and a simultaneous up-regulation of p21 and p27 levels in DNMT3B depleted cells (**Figure 19A**). Moreover, DNMT3B knock-down also efficiently abolished the phosphorylation status of retinoblastoma (RB) tumour suppressor (p-RB) and induced a parallel slight reduction in E2F1 levels (0.2-fold), this confirming the cell cycle block at G1 phase (**Figure 19A**). In accordance with western blotting expression results, immunofluorescence experiments also showed that si-DNMT3B transfection caused a strong reduction of Cyclin D1 nuclear staining with a dramatic up-regulation and relocalization of p21 in the nuclear compartment (**Figure 19B**). Consistent with the RB activity in its underphosphorylated state, nuclear shuttling of the E2F1 transcriptional factor was not evident in si-DNMT3B cells compared to si-NC samples (**Figure 19B**).

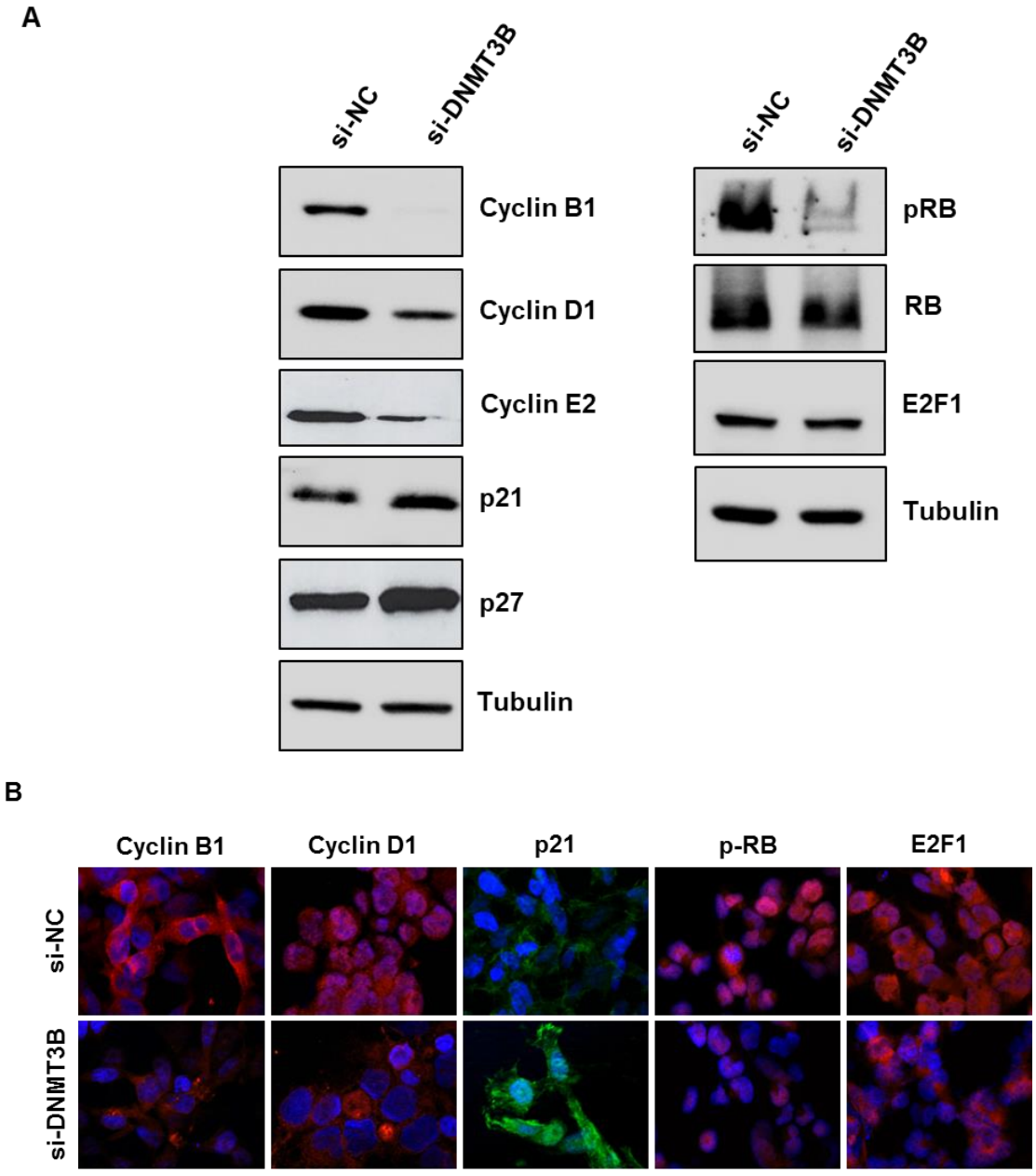

Figure 19: DNMT3B knock-down alters the expression of specific cell cycle regulators in RD cells. A) Western blot analyses of a panel of cell cycle regulatory proteins in RD cells at 72 h after si-NC or si-DNMT3B transfection. Tubulin expression was used as the internal control. Representative blots of three independent experiments. **B)** Immunofluorescence experiments showing the expression and localization of Cyclin B1, Cyclin D1, p21, p-RB and E2F1 proteins in RD cells at 72 h after DNMT3B or NC siRNA transfection. DAPI was used for nuclear staining. Images captured under ApoTome microscope at 40x magnification.

DNMT3B involvement in apoptosis and migration of RMS cells

To evaluate whether the reduced number of cells was due, not only to cell cycle arrest, but also to apoptosis, flow cytometry experiments were performed. FACS analysis showed that programmed cell death was not affected by DNMT3B knock-down since no significant changes in early or late apoptosis rates were observed in si-DNMT3B compared to si-NC transfected cells (**Figure 20A**). Furthermore, the expression levels of some specific apoptosis markers, such as cleaved PARP and Bcl-xL, resulted similar in DNMT3B-depleted cells and in negative control samples (**Figure 20B).**

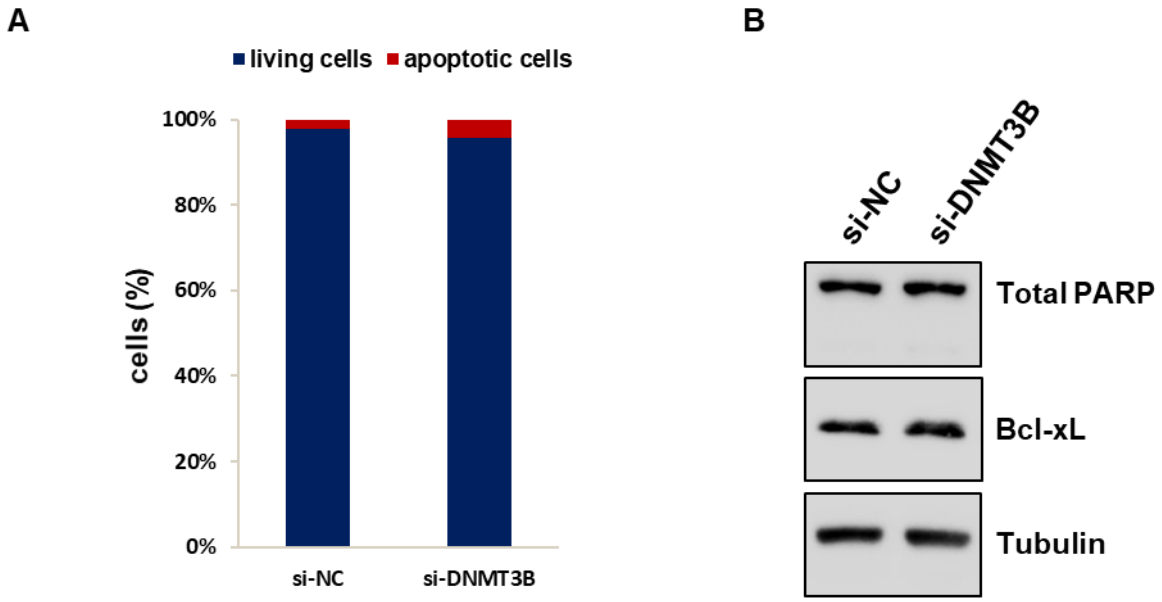

Figure 20: Decreased DNMT3B does not affect apoptosis. A) Histogram showing the rate of apoptosis in RD si-NC (2.23%) and si-DNMT3B (4.3%) cells at 72 h after transfection. Cells were stained with Annexin V and 7-AAD followed by FACS analysis. **B)** Western blots showing the expression of PARP and Bcl-xL proteins in si-DNMT3B and si-NC RD cells. Tubulin was used as loading control.

DNMT3B silencing significantly impaired the ability of RD cells to migrate through the non-matrigel-coated membranes towards serum-containing medium with respect to si-NC controls (0.5-fold) (**Figure 21A**). Furthermore, when allowed to grow at low density, si-DNMT3B cells showed a lower ability to form colonies in anchorage-dependent experiments compared to control cells, with a 0.6-fold of crystal violet absorbance (**Figure**

21B). Taken together, these results indicated that the *in vitro* under-expression of DNMT3B is able to inhibit RMS progression by reducing cell proliferation and migration.

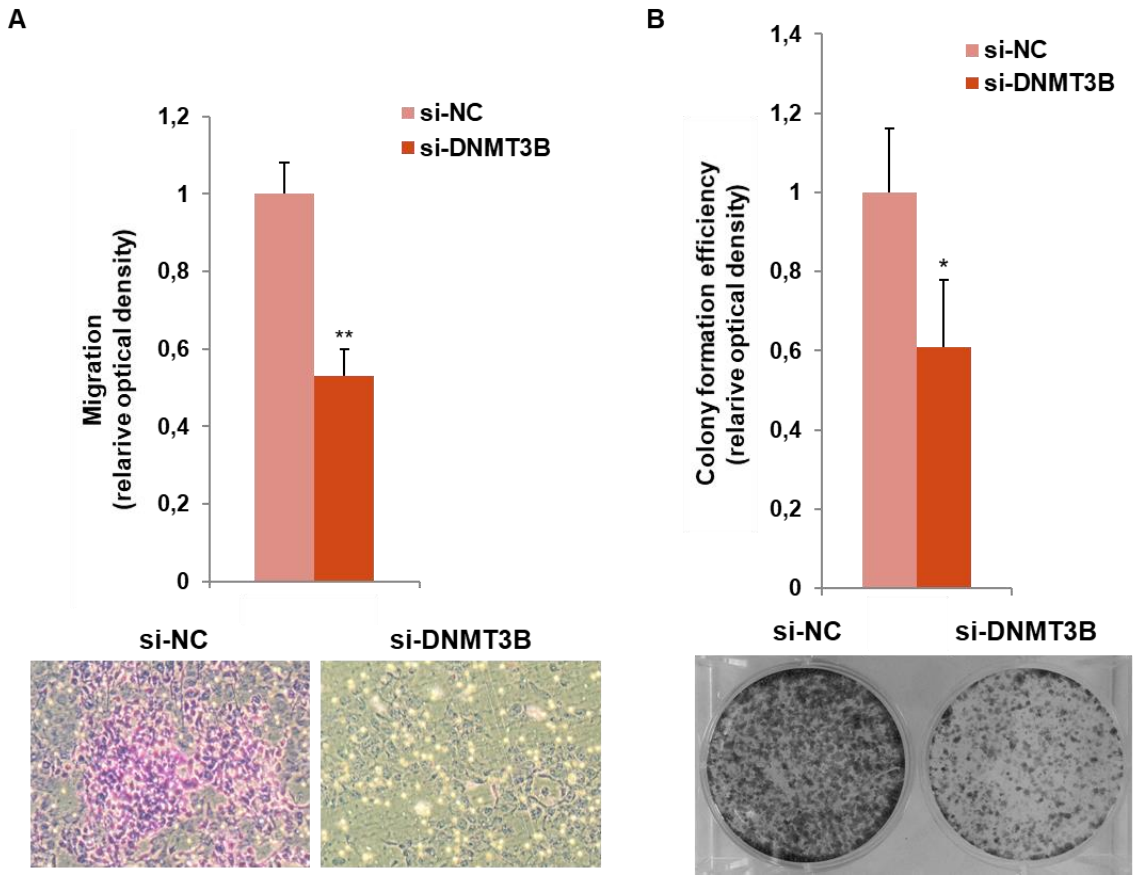

Figure 21: DNMT3B reduction correlates with altered migration and clonogenic ability of RD cells. A) Representative images of migrated cells using the transwell migration assay (magnification of 10x). Data in the histograms are expressed as the means ± SD from three separate experiments, each performed in triplicate (**, $p<0.01$). **B)** Colony forming efficiency was calculated by crystal violet absorbance from three independent experiments, each performed in triplicate (*, $p<0.05$).

DNMT3B knock-down promotes myogenic differentiation in RMS cells

DNMT3B silenced RD cells exhibited a substantial change in their morphology with more elongated cellular bodies already after 72 h post-siRNA transfection and with an increased number of multinucleated myotube-like structures at 144 h after transfection (**Figure 22A**), whilst si-NC showed the typical round proliferative shape (**Figure 22A**). The expression of specific muscle skeletal markers was thus evaluated. A sustained increase of MYOD1, Myogenin and MyHC at mRNA and protein levels was observed in both Q-PCR and immunoblotting assays, performed 72 h after DNMT3B silencing respect to si-NC transfection (**Figure 22B** and **22C**). In immunofluorescence experiments, MYOD1 factor exhibited a more evident granular staining in nuclear envelope in si-DNMT3B transfected RD cells in comparison to si-NC samples (**Figure 22D**); furthermore, elongated myotube-like si-DNMT3B cells displayed a strong fluorescence of MyHC, a marker of committed muscle cells (**Figure 22D**), indicating that the proper myogenic differentiation was triggered by the reduction of the DNMT3B levels. Notably, the phenotypic effect of DNMT3B knock-down in RD cells was also observed at 144 h post-transfection, with even lower levels of DNMT3B itself and higher levels of MyHC protein (**Figure 22E**), confirming that the commitment to terminal myogenic differentiation was preserved. Finally, we investigated whether DNMT3B was also involved in the regulation of specific miRNA levels. Indeed, we demonstrated that DNMT3B depletion was able to significantly up-regulate the expression of miR-133a and miR-206, two well-established myomiRs essential in promoting muscle cell differentiation (**Figure 22F**). DNMT3B knocked-down TE671 cells also exhibited a more elongated morphology than mocked control cells at both 72 and 144 h post-transfection (**Figure 23A**), and showed up-regulation of myogenic differentiation markers MYOD1, Myogenin and MyHC at 72 h post-siRNA injection (**Figure 23B**). Moreover, immunofluorescence experiments confirmed that DNMT3B silencing caused over-expression and nuclear staining of MYOD1 and a stronger signal intensity of MyHC in si-DNMT3B cells than in control cells (**Figure 23C**).

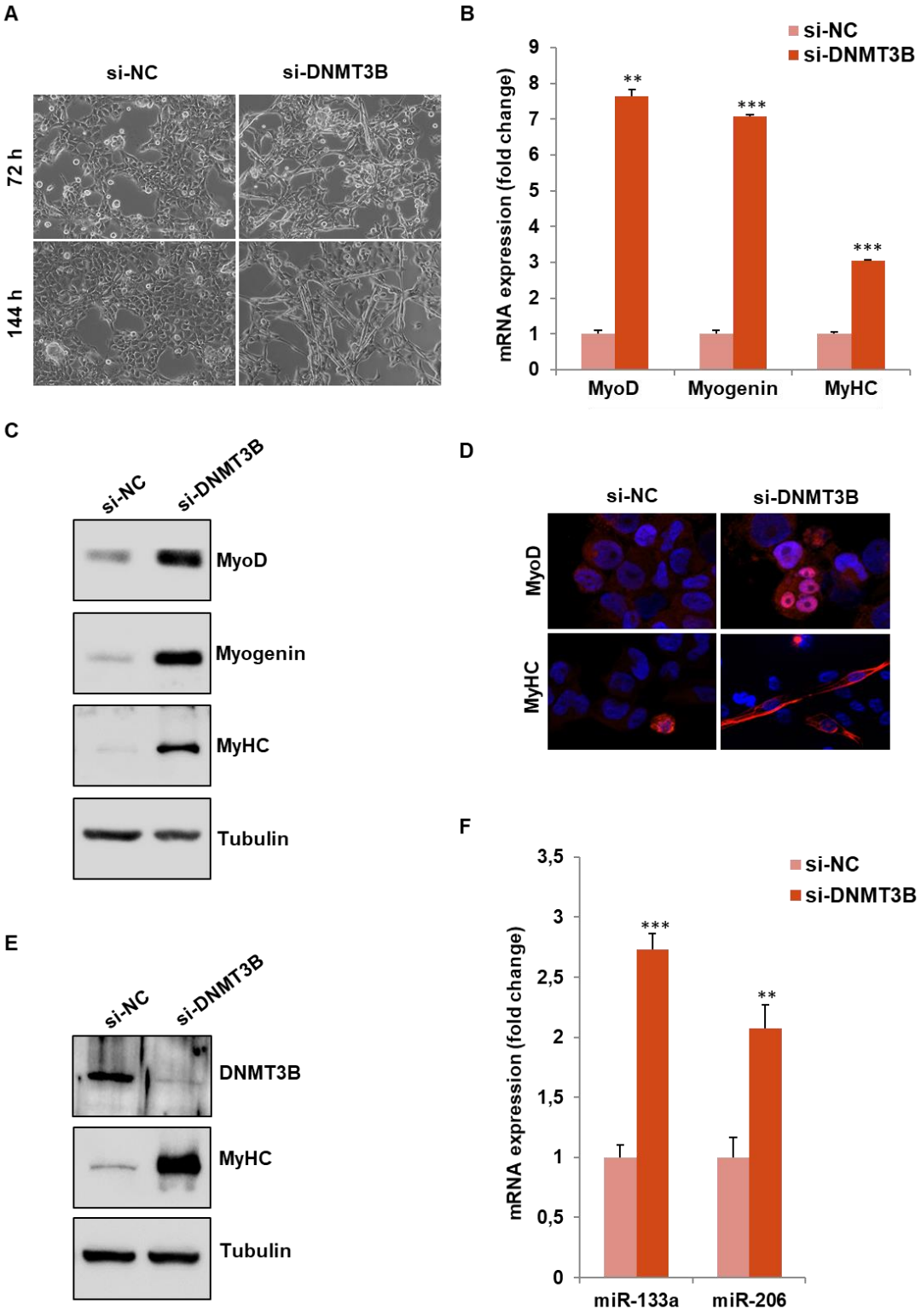

Figure 22: DNMT3B silencing by RNA-interference triggers myogenic differentiation in RD cells. A) Cellular morphology of si-NC and si-DNMT3B RD cells was analysed under light microscope at 20x magnification at 72 and 144 h after siRNA transfection. In si-DNMT3B cultures, more elongated cellular bodies were evident, many of which formed multinucleated myotube-like

structures. **B)** Expression of myogenic genes, MYOD1, Myogenin and MyHC, by Q-PCR assays in RD cells transfected with DNMT3B or NC siRNAs for 72 h. Expression of each mRNA was normalized to GADPH levels and plotted as fold change relative to si-NC samples. Histograms are means ± SD. Asterisks represent the statistical significance (**, $p<0.01$; ***, $p<0.001$). **C)** Western blots showing the expression of MYOD1, Myogenin and MyHC proteins in si-DNMT3B and si-NC RD cells at 72 h post-transfection. Tubulin was used as loading control. Representative of three different experiments. **D)** Immunofluorescence experiments showing the expression and localization of MYOD1 and MyHC at 72 h after DNMT3B or NC siRNA transfection. DAPI was used for nuclear staining. Images captured under ApoTome microscope at 40x magnification. **E)** Western blots showing the expression of DNMT3B and MyHC proteins in si-DNMT3B and si-NC RD cells at 144 h post-transfection. Tubulin was used as loading control. **F)** Expression of myogenic miRNAs, miR-133a and miR-206, by Q-PCR experiments in RD cells transfected with DNMT3B or NC siRNAs for 72 h. Expression of each miRNA was normalized to U6 levels and plotted as fold change relative to si-NC samples. Histograms are means ± SD. Asterisks represent the statistical significance (**, $p<0.01$; ***, $p<0.001$).

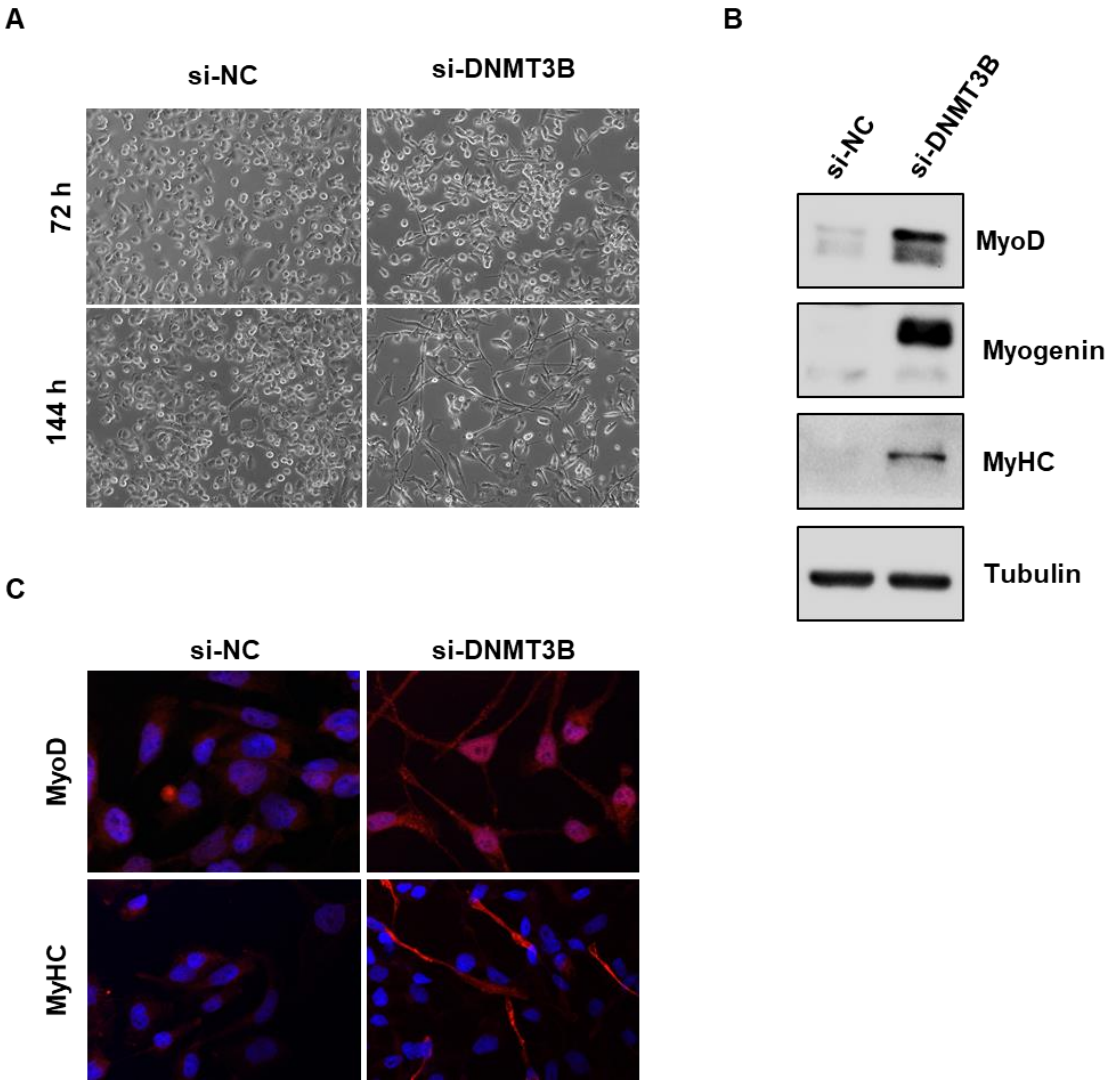

Figure 23: DNMT3B knock-down induces terminal myogenic differentiation in TE671 cells. **A)** Cellular morphology of si-NC and siDNMT3B TE671 cells was analysed under light microscope at 20x magnification at 72 and 144 h after siRNA transfection. In si-DNMT3B cultures, more elongated cellular bodies were evident, many of which formed multinucleated myotube-like structures. **B)** Western blots showing the expression of MYOD1, Myogenin and MyHC proteins in si-DNMT3B and si-NC TE671 cells at 72 h post-transfection. Tubulin was used as loading control. Representative of three different experiments. **C)** Immunofluorescence experiments showing the expression and localization of MYOD1 and MyHC at 72 h after DNMT3B or NC siRNA transfection. DAPI was used for nuclear staining. Images captured under ApoTome microscope at 40x magnification.

MEK/ERK inhibitor U0126 down-regulates DNMT3B protein expression

Since the MEK/ERK cascade is aberrantly activated in RMS and its inhibition has been shown to affect tumour growth and to rescue skeletal muscle differentiation in ERMS cells (Marampon et al., 2006), as occurred in si-DNMT3B transfected cells, we studied if DNMT3B expression could be linked to the MEK/ERK signalling pathway. RD cells treated with the MEK/ERK inhibitor U0126 (10 μM) for 96 h were able to fully differentiate, as assessed by the up-regulation of MYOD1, Myogenin, MyHC, miR-133a and miR-206 levels, but also showed a decreased expression of DNMT3B protein (**Figure 24A and 24B**). Interestingly, a drastic reduction of DNMT3B enzyme was observed at early points of U0126 treatment (12-24 h) in RD cells, subsequently to the down-regulation of ERK phosphorylation status, evident at 6 h post-exposure (**Figure 24C**). TE671 cells treated with U0126 showed matched results (**Figure 24C**).

Considering the evidence that U0126 treatment is able to activate p38 kinase for promoting myosin expression in RMS cells (Marampon et al., 2006; Mauro et al., 2002), p38 phosphorylated levels were analysed in DNMT3B depleted cells. A long-lasting increase of p38 phosphorylation (p-p38) was observed in si-DNMT3B transfected cells in comparison to si-NC samples both at 72 and 144 h in RD and TE671 cell lines (**Figure 25**). Altogether, these data indicate that DNMT3B is a down-stream component of the MEK/ERK signalling pathway and that abrogation of this enzyme is an essential step in the U0126-mediated capacity of ERMS cells to rescue myogenic differentiation program.

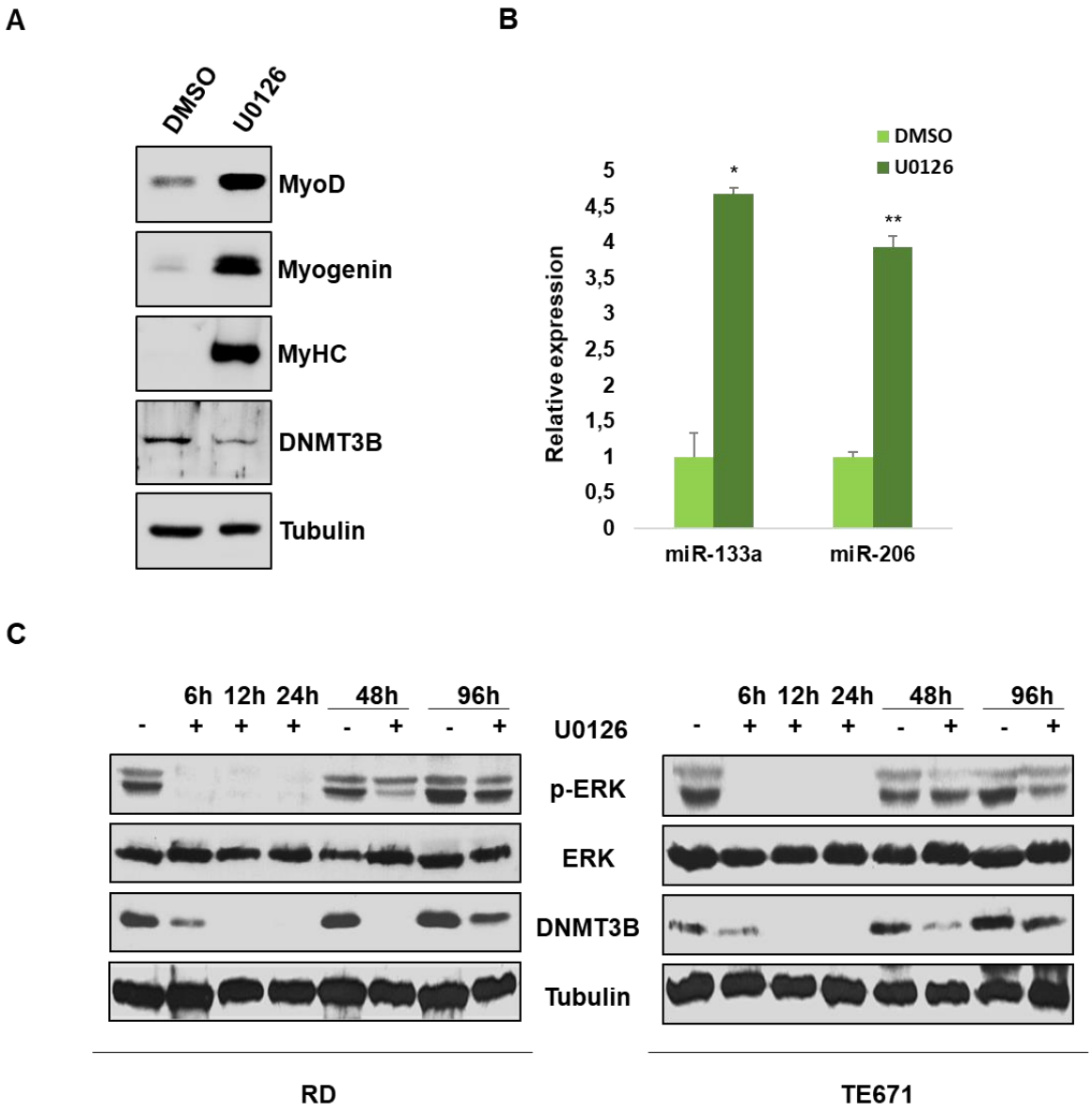

Figure 24: Inhibition of MEK/ERK pathway by U0126 down-regulates DNMT3B. A) Western blots showing the down-regulation of DNMT3B and the up-regulation of MYOD1, Myogenin and MyHC in RD cells treated with U0126 for 96 h. Mocked control cells were treated with DMSO. Tubulin was used as loading control. Representative of three different assays. **B)** Expression of myogenic miRNAs, miR-133a and miR-206, by Q-PCR experiments in RD cells treated with DMSO or U0126 for 96 h. Expression of each miRNA was normalized to U6 levels and plotted as fold change relative to control samples. Histograms are means ± SD. Asterisks represent the statistical significance (*, $p<0.05$; **, $p<0.01$). **C)** Time-course experiments showing the early decreased phosphorylation status of ERK and the down-stream reduced expression of DNMT3B protein in RD and TE671 cells upon U0126 treatment for 0-6-12-24-48-96 h. Tubulin was used as loading control. Representative of two different assays.

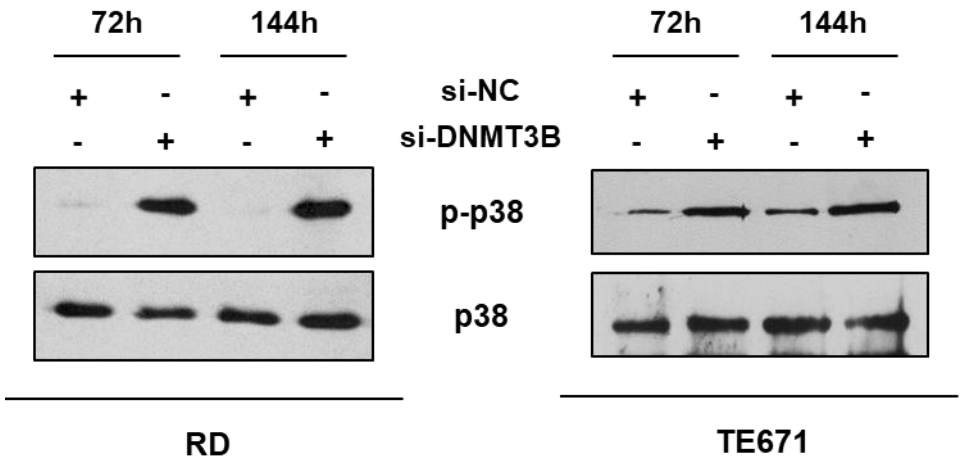

Figure 25: DNMT3B knock-down activates p38 kinase in ERMS cells. Western blots showing phosphorylated and total p38 levels in si-DNMT3B and si-NC RD and TE671 RMS cells at 72 and 144 h post-transfection. Tubulin was used as loading control. Representative of two different assays.

Down-regulation of miR-29a/c contributes to altered expression of DNMT3B in RMS cells

Since the importance of microRNAs in physiological processes and tumorigenesis and the implication of miR-29 family in skeletal muscle differentiation (Wang et al., 2008a), we analysed if DNMT3B expression could be linked to these miRNAs. Based on deep-sequencing of miRNA profile in RMS biopsies, previously carried out in our laboratory (Megiorni et al., 2014), we focused on miR-29a-3p and miR-29c-3p expression levels. The down-regulation of both miRNAs was confirmed in 14 RMS tumour tissues, 7 ARMSs and 7 ERMSs, by Q-PCR experiments. In agreement with deep-sequencing findings, a strong down-regulation of both miR-29a-3p and miR-29c-3p was observed in all tumour samples in comparison to NSM (**Figure 26**), with an average decrease of 0.1±0.19 and 0.02±0.04, respectively. To predict whether DNMT3B was a target of miR-29a-3p and miR-29c-3p, TargetScan Human (Release 7.1) and DIANA-microT algorithms were interrogated, showing a perfect complementary between DNMT3B mRNA and the seed-sequence of both miR-29a-3p and miR-29c-3p (**Figure 27**).

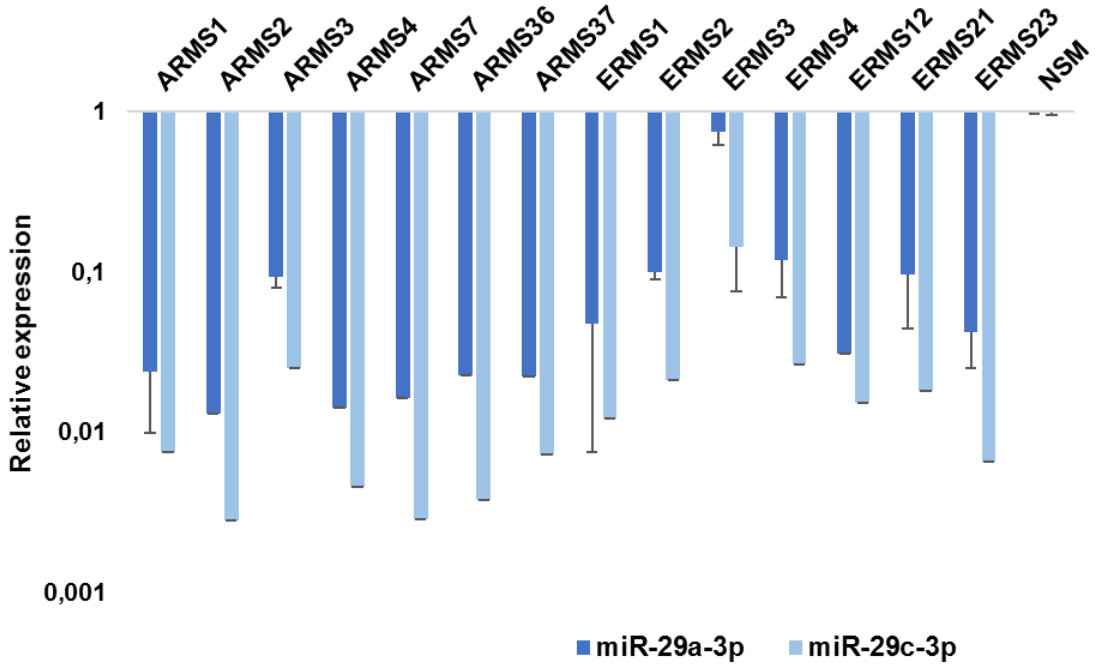

Figure 26: miR-29 expression in RMS tumours. Q-PCR showing the expression levels of miR-29a-3p and miR-29c-3p in 7 ARMSs and 7 ERMSs, expressed as fold increase over NSM, arbitrarily set at 1. Transcript levels were normalized to U6 small nuclear RNA levels and error bars represent SD of two independent Q-PCR reactions, each performed in triplicate.

	Predicted consequential pairing of target region (top) and miRNA (bottom)	Site type
Position 1202-1209 of DNMT3B 3' UTR hsa-miR-29c-3p	5' ...UUUUACUCUUCUUACUGGUGCUA... 3' AUUGGCUAAAGUUUACCACGAU	8mer
Position 1202-1209 of DNMT3B 3' UTR hsa-miR-29a-3p	5' ...UUUUACUCUUCUUACUGGUGCUA... 3' AUUGGCUAAAGUCUACCACGAU	8mer

Figure 27: Seed sequence of miR-29a-3p and miR-29c-3p on DNMT3B transcript. Sequence alignment of miR-29a-3p and miR-29c-3p seed sequences at miRNA 5'-end (bottom) and DNMT3B 3'-UTR binding sites (top). Data from TargetScanHuman 7.1 interrogation.

To validate the *in silico* analysis, transient transfections, in RD cells, were carried out. A miRNA duplex from *C. elegans* was used as a negative miRNA-Control (miR-Ctr). By using stem-loop real-time PCR, specific expression increase of miR-29a-3p (226-fold) and miR-29c-3p (115-fold) after transfection with the respective mimic was demonstrated (**Figure 28A**). A significant down-regulation of the endogenous DNMT3B at both mRNA and protein levels was observed in miR-29a-3p/miR-29c-3p RD cells at 72 h after

transfection compared to those transfected with miR-Ctr (**Figure 28B** and **28C**), consistent with the conserved binding sites for these miRNAs in the 3'-untranslated region of the DNMT3B transcript, identified by computational tools for miRNA target prediction.

In order to determine whether the restoration of normal miR-29a-3p and miR-29c-3p expression levels induced similar effects on RD cells, to those observed after si-DNMT3B transfection, a series of *in vitro* gain of function experiments were performed. Direct counting for living cells using trypan blue dye exclusion test showed a decrease of cell proliferation at 72 h after to transfection with both miRNA mimics (0.6-fold) (**Figure 29A**). Furthermore, the reduced RD cell growth was due to alterations in cell cycle progression, as shown from flow cytometry analysis. Propidium iodide staining highlighted an increase of cell percentage in G1 phase with a concomitant decrease of cell percentage in S and G2 phases (**Figure 29B**) in both miR-29a-3p and miR-29c-3p cells in comparison to miR-Ctr cells, as well as observed in si-DNMT3B RD cells.

Ectopic expression of miR-29a-3p and miR-29c-3p decreased the ability of RD cells to migrate through non-matrigel-coated membranes towards serum-containing medium when compared with a mimic negative control (**Figure 30A**). Finally, when allowed to grow at low density, miR-29a-3p and miR-29c-3p cells showed a lower ability to form colonies in anchorage-dependent experiments compared to control cells (**Figure 30B**). Altogether, these data suggest that miR-29a/c down-regulation observed in RMS contributes to abnormal expression of DNMT3B, thus promoting its oncogenic activity.

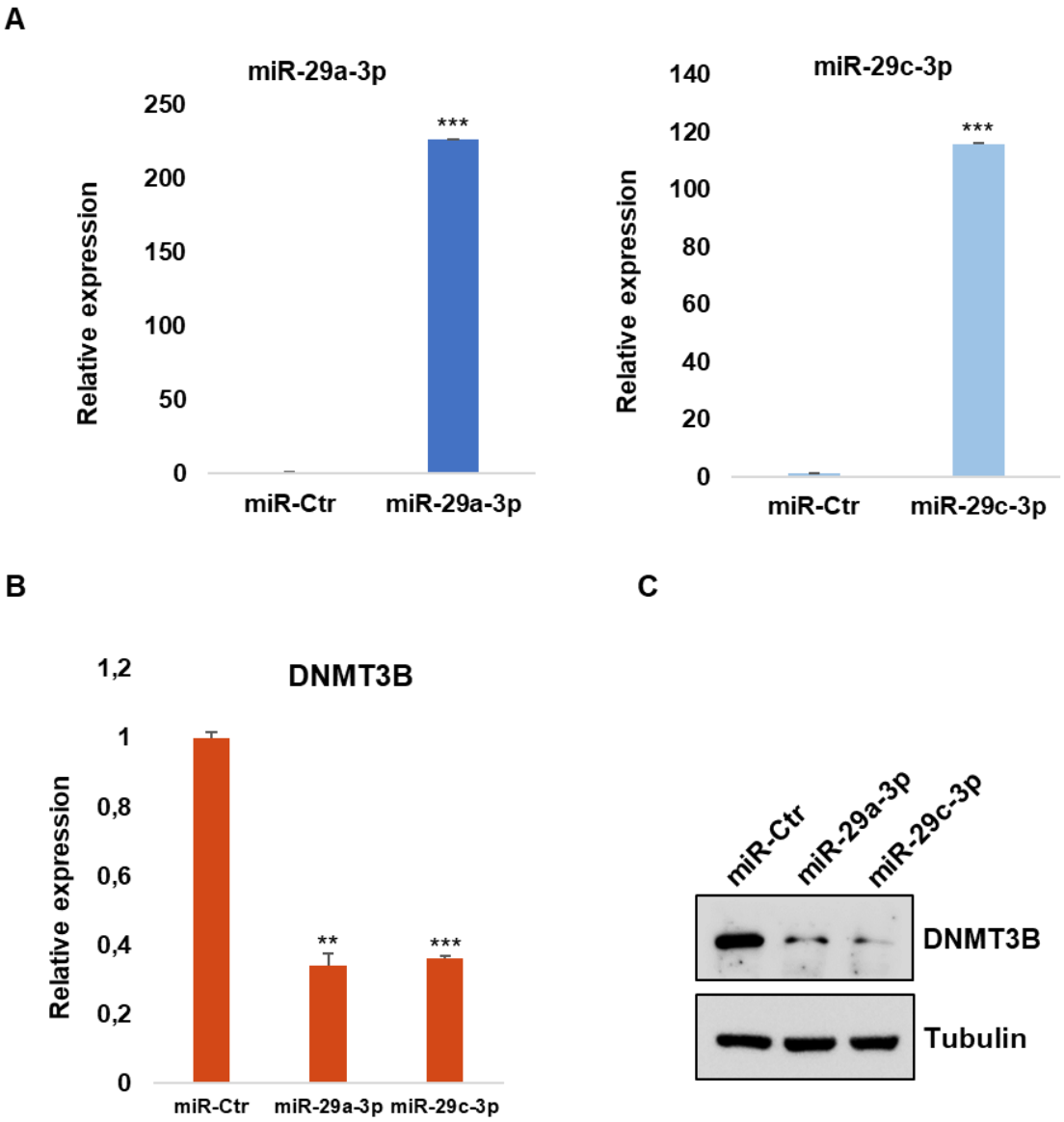

Figure 28: DNMT3B is a target of miR-29 in RMS cells. A) Relative expression of miR-29a-3p and miR-29c-3p measured by Q-PCR at 72 h in RD cells after transfection with the respective miRNA mimics in comparison to samples transfected with miR-Ctr, arbitrarily set at 1. U6 was used as a control. Error bars represent SD of the means of two independent experiments, each performed in triplicate, (***, $p<0.001$). **B)** Q-PCR showing the expression of DNMT3B mRNA, expressed as fold increase in respect to miR-Ctr cells, after miRNA mimics transfection. Bars represent mean values of two independent experiments, each performed in triplicate. Statistical significance: ***, $p<0.001$; **, $p<0.01$. **C)** western blot showing the down-regulation of DNMT3B protein levels in RD cells at 72 h after transfection with miR-29a-3p and miR-29c-3p in comparison to miR-Ctr. Tubulin was used as loading control.

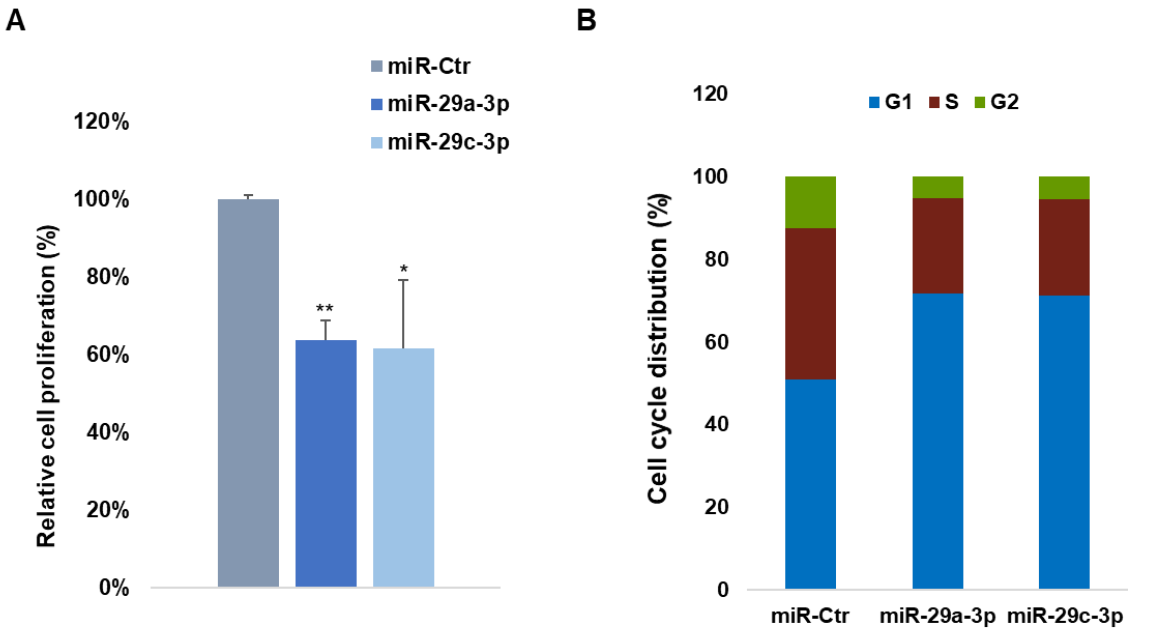

	G1 (%)	S (%)	G2 (%)
miR-Ctr	50,98	36,58	12,44
miR-29a-3p	71,85	22,97	5,18
miR-29c-3p	71,26	23,33	5,41

Figure 29: miR-29a-3p and miR-29c-3p impair RMS cell growth. A) Viability of RD cells 72 h post-transfection with miR-29a-3p and miR-29c-3p in comparison to control miR-Ctr cells, as assessed by trypan blue exclusion staining. Results represent the mean value of two independent experiments ± SD. Statistical significance: **, $p<0.01$; *, $p<0.05$. **B)** Flow cytometry data showing percentages of cells in G1, S and G2 phases in miR-29a-3p and miR-29c-3p or miR-Ctr RD cells at 48 h after transfection. Data are representative of two independent experiments.

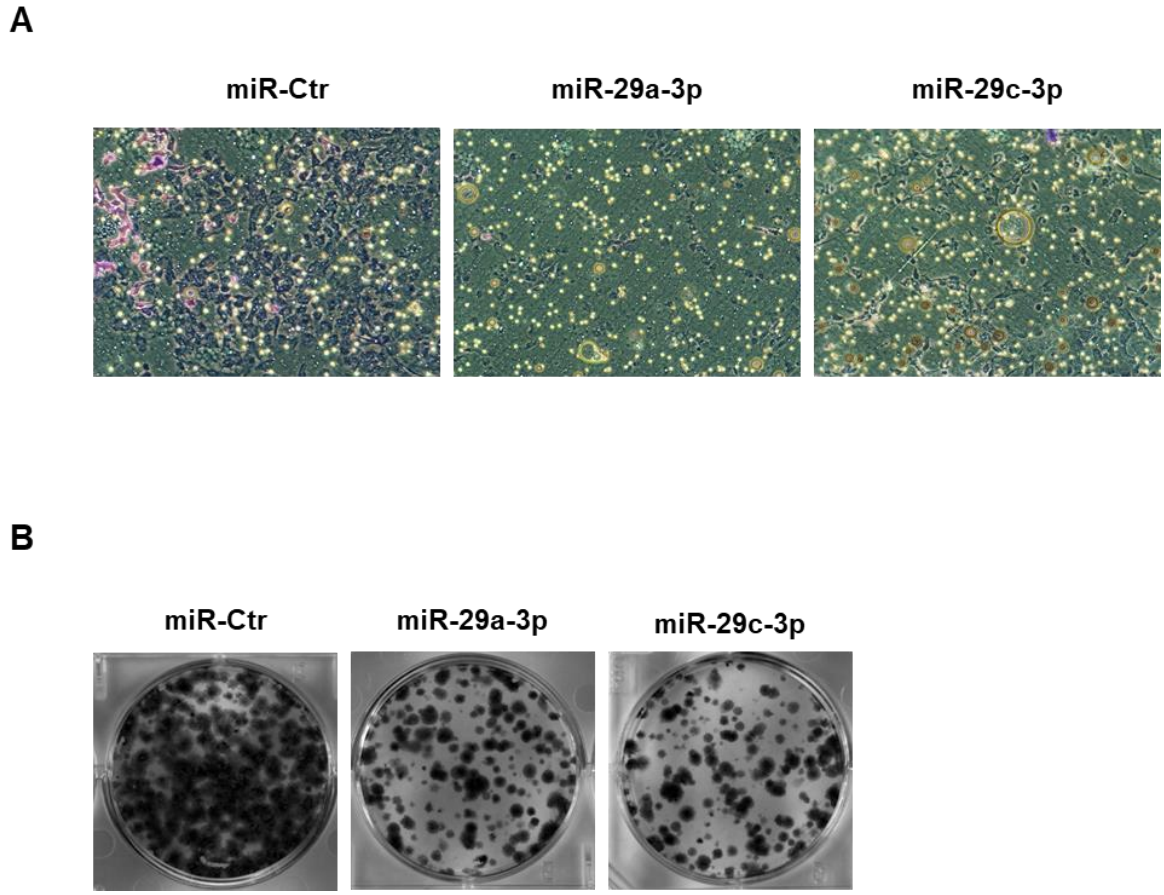

Figure 30: miR-29a-3p and miR-29c-3p decrease migration and clonogenic abilitiy of RD cells. **A)** Representative images of migrated cells using the transwell migration assay from two separate experiments, each performed in triplicate (magnification of 10x). **B)** Representative images of clonogenic ability of miR-29a-3p and miR-29c-3p cells in anchorage-dependent experiments compared to negative control cells.

Depletion of DNMT3B in alveolar RMS cell line does not have effects on proliferation and differentiation

Based on the up-regulation of DNMT3B in alveolar RMS tumour sample and the expression at both mRNA and protein levels in ARMS cell line in comparison to NSM, showed previously by Q-PCR and western blot, different experiments were performed on RH4 and RH30 cells to evaluate the possible effects of DNMT3B silencing in alveolar subtype. Direct counting for living cells using trypan blue dye exclusion test carried out at 72 h after transfection showed that DNMT3B knock-down did not affect the proliferation of RH4 and RH30 cells respect to si-NC cells (**Figure 31**).

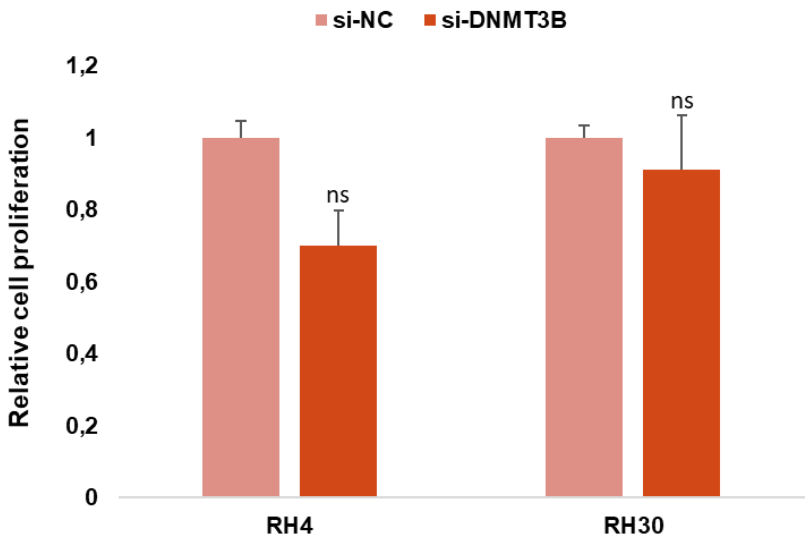

Figure 31: DNMT3B knock-down by RNA interference does not affect cell viability of ARMS cells. A) Viability of RH4 and RH30 cells 72 h post-transfection with DNMT3B siRNA calculated with respect to control si-NC cells, assessed by trypan blue exclusion staining. Results represent the mean value of three independent experiments ± SD (ns, not significant).

Furthermore, flow cytometry analysis performed on RH4 and RH30 transfected with si-DNMT3B for 48 h did not highlight alterations in cell cycle progression in comparison to those transfected with si-NC (**Figure 32**).

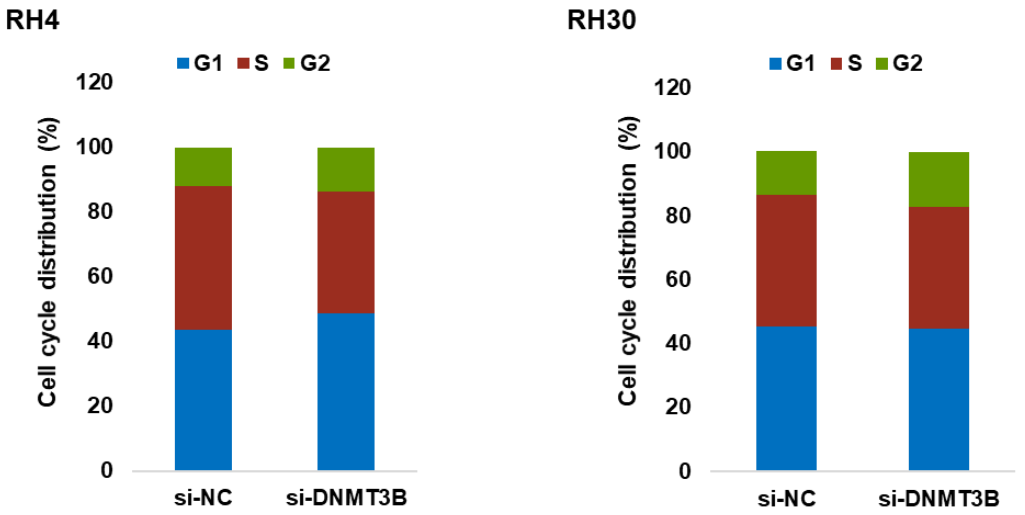

	G1 (%)	S (%)	G2 (%)
Si-NC	43,58	44,46	11,96
Si-DNMT3B	48,76	37,63	13,61

	G1 (%)	S (%)	G2 (%)
Si-NC	45,44	40,99	13,57
Si-DNMT3B	44,64	37,89	17,47

Figure 32: Cell cycle distribution of RH4 and RH30 cells. Flow cytometry data showing percentages of cells in G1, S and G2 phases in si-DNMT3B and si-NC ARMS cells at 48 h after transfection. Data are average values of two independent experiments.

Finally, unlike the RD cells, silencing of DNMT3B did not reactivate myogenic differentiation in RH4 and RH30 cells, as shown by the specific muscle markers protein levels analysed by western blot at 72 h post transfection (**Figure 33**). Indeed, the expression levels of MYOD1 and Myogenin did not increase in DNMT3B depleted ARMS cells respect to si-NC cells and the terminal differentiation marker, MyHC, was not detected (**Figure 33**).

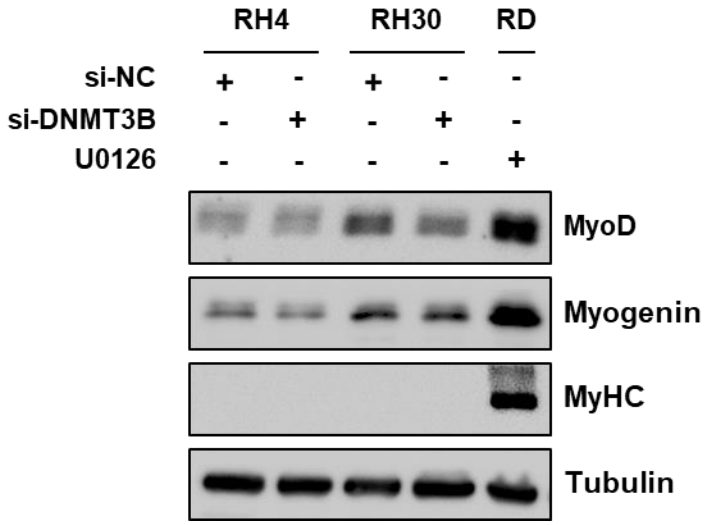

Figure 33: **DNMT3B silencing by RNA-interference does not induces myogenic differentiation in alveolar RMS cells.** Western blots showing the expression levels of MYOD1, Myogenin and MyHC in RH4 and RH30 cells transfected with si-DNMT3B or si-NC for 72 h. RD cells treated with U0126 ware used as positive control, whilst tubulin was used as loading control. Representative of two different assays.

Loss of DNMT3A expression does not alter RMS cells phenotype

Since the up-regulation of DNMT3A in all tumour samples showed by Q-PCR in comparison to NSM, we evaluated whether the knock-down of this *de novo* DNA methyltransferase had the same effects of DNMT3B knock-down on the phenotype of RMS cells. Using a specific siRNA against DNMT3A mRNA in RD cell line, at 72 h after transfection, direct counting for living cells using trypan blue dye exclusion test showed that DNMT3A depletion did not affect the proliferation of RD cells respect to si-NC cells (**Figure 34A**). In addition, unlike si-DNMT3B transfected RD cells, propidium iodide staining of cellular DNA content, showed the same cell percentage in G1 phase in si-DNMT3A (62.49%) compared with si-NC (59.88%) transfected cells and a mild increase of cell number in G2 phase (si-NC, 5.4%, si-DNMT3A, 12.86%), with a concomitant slight decrease of cell percentage in S phase (si-NC, 34.72%, si-DNMT3A, 24.65%) (**Figure 34B**). The study of specific cell cycle markers, detected by western blot experiments, confirmed the flow cytometry analysis. As shown in **Figure 34C**, cyclin B protein level was increased in si-DNMT3A RD cells, whilst cyclin D1 was down-regulated in comparison to control cells.

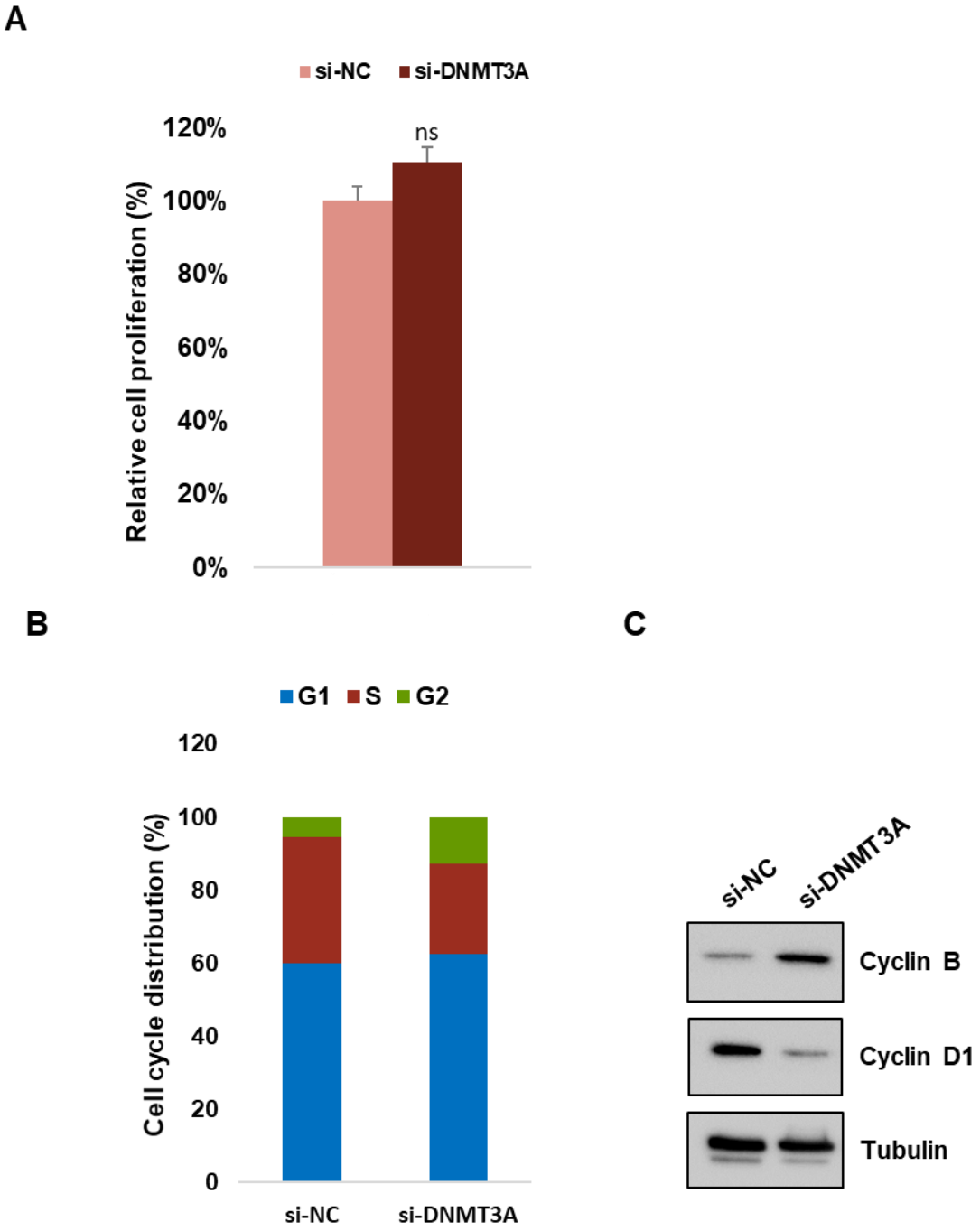

Figure 34: DNMT3A knock-down does not affect cell viability in RD cells. A) Viability of RD cells 72 h post-transfection with DNMT3A siRNA in comparison to control si-NC cells, as assessed by trypan blue exclusion staining. Results represent the mean value of two independent experiments ± SD (ns, not significant). **B)** Flow cytometry data showing percentages of cells in G1, S and G2 phases in si-DNMT3A and si-NC RD cells at 48 h after transfection. Data are average values of two independent experiments. **C)** Western blots showing the expression levels of cyclin B,

and cyclin D1 in cells transfected with si-DNMT3A or si-NC for 48 h. Tubulin was used as loading control. Representative of two different assays.

Furthermore, DNMT3A silenced RD cells did not exhibit a change in their morphology, on the contrary, they showed the typical round shape, as well as si-NC cells (**Figure 35A**). However, the expression of specific muscle markers was evaluated by western blot experiments. As expected, MYOD1, Myogenin and MyHC protein levels did not increase in si-DNMT3A transfected RD cells in comparison to si-NC samples, both at 72 h and 144 h after transfection (**Figure 35B**), whilst low levels of DNMT3A protein has been observed. Altogether, these data suggest that, despite the up-regulation of both the enzymes in RMS tumour samples, DNMT3B has a specific role in the tumorigenesis of this malignancy and acts as an oncogene, whilst the functional importance of DNMT3A is to be clarified.

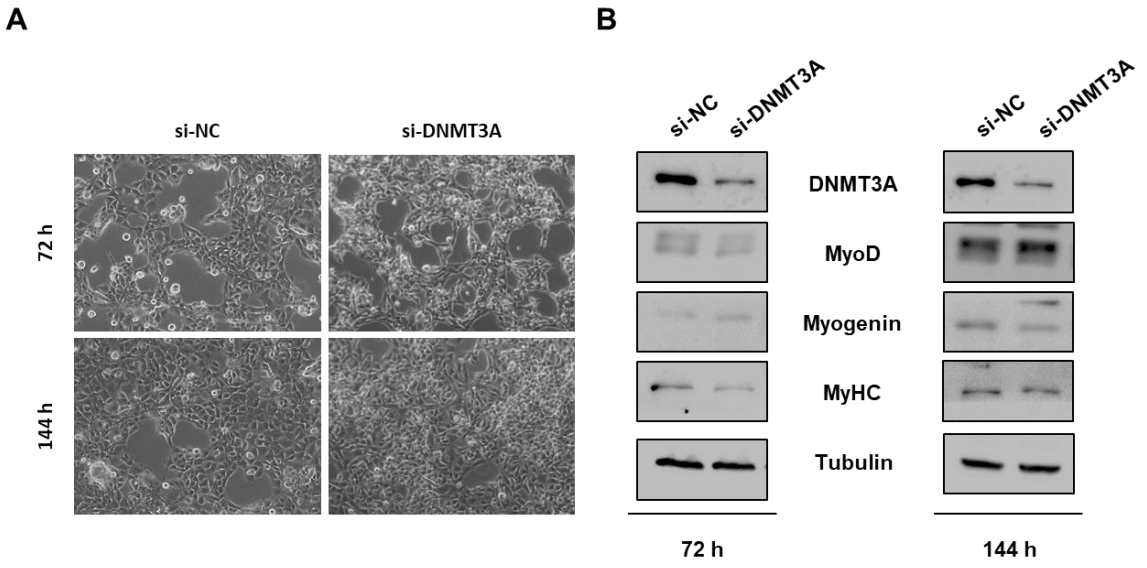

Figure 35: **DNMT3A depletion does not reactivate myogenic differentiation in RD cells. A)** Cellular morphology of si-NC and siDNMT3A RD cells was analysed under light microscope at 20x magnification at 72 and 144 h after siRNA transfection. **B)** Western blots showing the down-regulation of DNMT3A and the expression levels of MYOD1, Myogenin and MyHC in RD cells transfected with si-DNMT3A or si-NC. Tubulin was used as loading control. Representative of two different assays.

DNMT3B knock-down sensitizes ERMS cell line to radiation

We assessed whether dysfunction of DNMT3B might sensitize ERMS cells to ionizing radiation. For this purpose, RD cells were transfected with si-DNMT3A, si-DNMT3B or si-NC for 48 h and then irradiated with a single dose of 4 Gy. Twenty-four h after irradiation (IR) we analysed the survival rates of si-DNMT3A and si-DNMT3B cells compared to si-NC cells, by using trypan blue dye exclusion test. As shown in **Figure 36A** IR alone was able to slow down cell proliferation and, interestingly, DNMT3B depletion increased growth arrest (0.6-fold), suggesting that DNMT3B knock-down enhanced cellular radiosensitivity. On the contrary, cells growth was not perturbed by DNMT3A silencing in combination with IR, this assessing a specific role of DNMT3B in the DNA damage response. To further determine whether DNMT3B knock-down alters cell cycle distribution after IR, flow cytometry analysis was performed. Twenty-four h after irradiation an increase in the G2 population occurred in all the sample (G2: si-NC, 30.57% *vs.* 9.61%; si-DNMT3A, 27.51% *vs.* 8.42%, si-DNMT3B, 14.36% *vs.* 3.9%) rather than in si-DNMT3B cells, which exhibited an increased G1 phase in respect to both control and si-DNMT3A transfected samples (G1: si-NC, 60.58%; si-DNMT3A, 58.07%; si-DNMT3B, 79.04%) (**Figure 36B**). This result is line with the G1 cell cycle arrest reported above. Immunoblotting assay performed after irradiation, revealed a strong decrease of cyclin D1 protein levels in both si-DNMT3A and si-DNMT3B compared with si-NC cells and an increase of cyclin B in comparison to not irradiated cells (**Figure 36C**). In agreement with the cytofluorimetric analysis, si-DNMT3B irradiated cells exhibited lower levels of cyclin B than si-NC and si-DNMT3A irradiated cells.

Furthermore, when allowed to grow at low density for 11 days at 24 h after irradiation, the ability to form colonies decreased in all the samples compared to the respective not irradiated cells (si-NC, 0.12-fold; si-DNMT3A, 0.13-fold; si-DNMT3B, 0.10-fold). Notably, irradiated si-DNMT3B cells showed a very lower ability in anchorage-dependent experiments, with a 0.05-fold of crystal violet absorbance compared to si-NC cells (**Figure 37**).

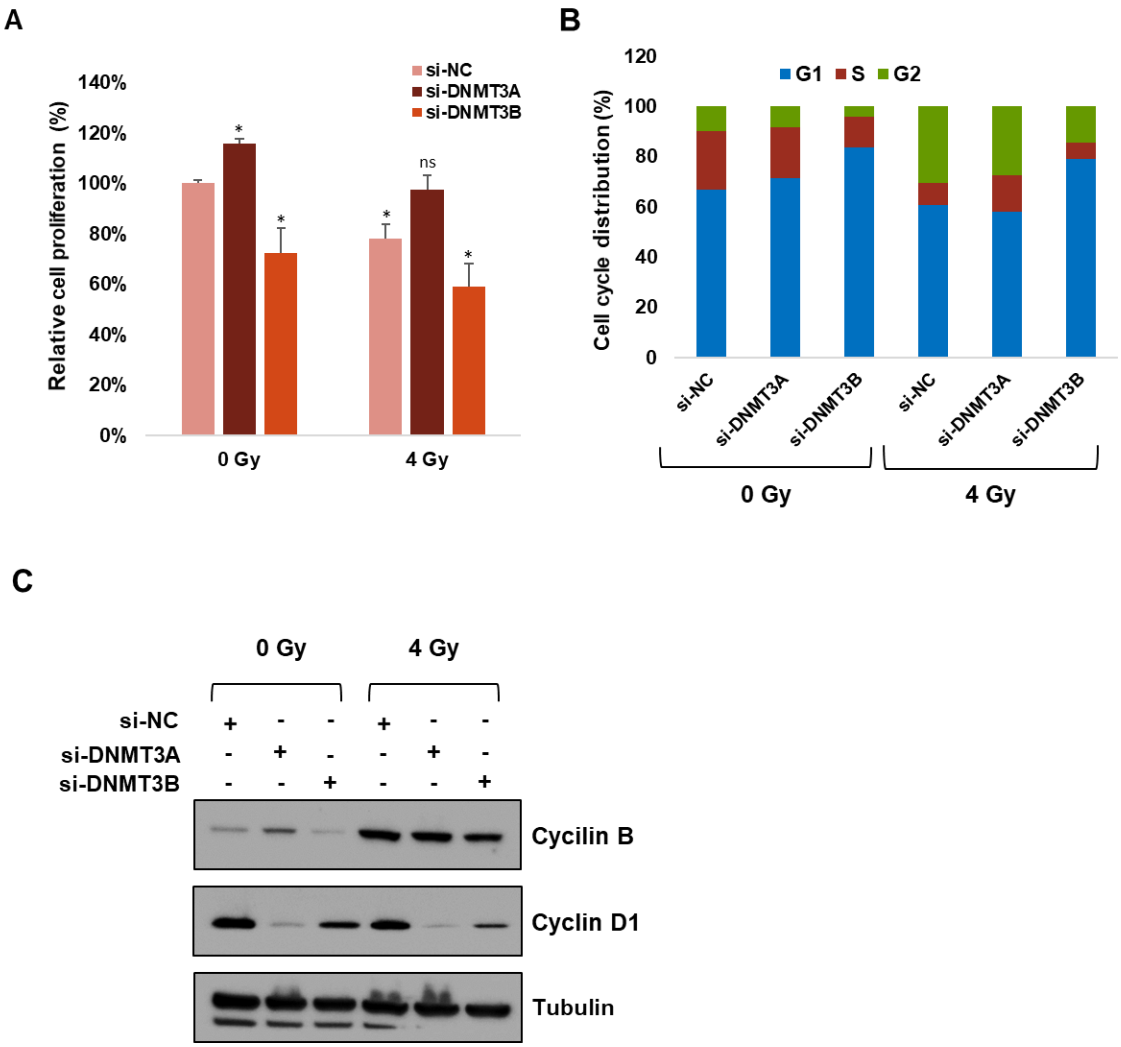

Figure 36: DNMT3B knock-down radiosensitizes RD cells. RD cells 48 h post-transfection with si-DNMT3A, si-DNMT3B or si-NC were exposed or not to 4 Gy irradiation. **A)** Viability was assessed 24 h after IR by trypan blue exclusion staining. Results represent the mean value of two independent experiments ± SD (*, $p<0.05$; ns, not significant). **B)** Flow cytometry data showing percentages of cells in G1, S and G2 phases in si-DNMT3A, si-DNMT3B or si-NC RD cells at 72h after transfection and 24 h after IR. Data are average values of two independent experiments. **C)** Western blot showing the expression levels of cyclin B and cyclin D1 in cells transfected with si-DNMT3A, si-DNMT3B or si-NC irradiated or not with 4 Gy. Tubulin was used as loading control.

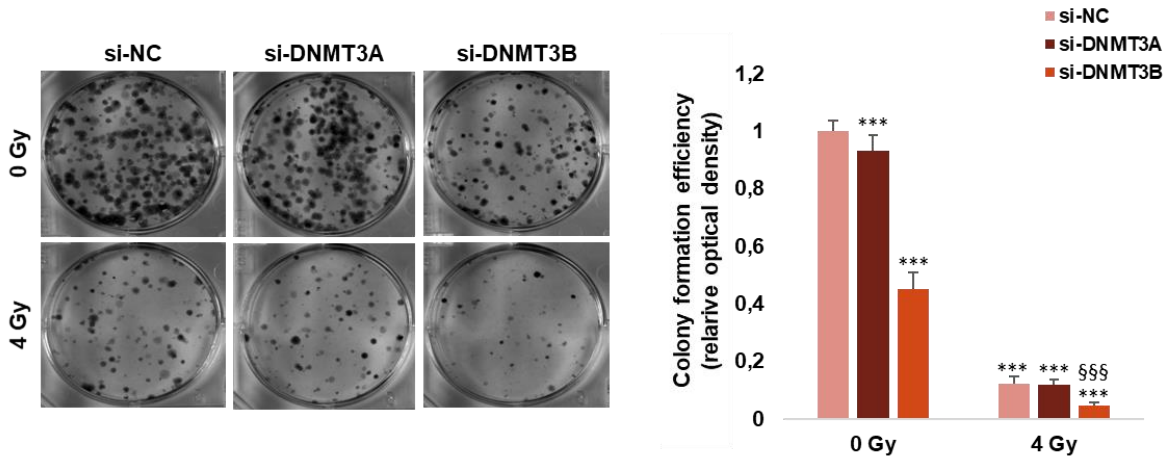

Figure 37: DNMT3B depletion impairs clonogenic ability of RD cells after irradiation. RD cells, transfected with si-DNMT3A, si-DNMT3B or si-NC for 48 h, were exposed or not to 4 Gy radiation treatment. Twenty-four h after IR, cells were seeded at low concentration for colony assays. Pictures are representative of two independent experiments, each performed in triplicate. Colony forming efficiency was calculated by crystal violet absorbance (***, $p<0.001$ *vs.* si-NC/0 Gy; §§§, $p< 0.001$ *vs.* si-NC/4 Gy).

Based on these results, we hypothesized that restoration of DNMT3B expression might increase IR-induced DNA damage. To verify this supposition, we determined whether DNMT3B knock-down affected IR-induced phosphorylation of H2AX (γ-H2AX), which is a marker of double-strand breaks (DSBs). At 24 h after irradiation a strong increase in the expression levels of γ-H2AX was observed in RD cells transfected with si-DNMT3B compared to si-DNMT3A and control cells (**Figure 38A**), suggesting that silencing of DNMT3B amplify DNA damage in RD cells. To evaluate if DNMT3B depletion was able to block the DNA repair machinery, we analysed the modulation of specific markers after IR, by using western blot. **Figure 38B** showed the decreased expression of Caveolin 1 (Cav-1), ATM (ataxia-telangiectasia mutated), DNA-PK_{cs} (DNA-dependent protein kinase, catalytic subunit), and RAD51, whose activation is linked to the non-homologous end joining (NHEJ) and the homologous recombination (HR) pathways (Maier et al., 2016), only in si-DNMT3B RD cells 24 h after irradiation, compared to both si-DNMT3A and si-NC cells. Altogether, these data suggest that DNMT3B is an upstream component of DNA damage signalling pathway and that silencing of this enzyme is a crucial step in the inhibition of DNA damage/repair, this leading to radiosensitization of ERMS cells.

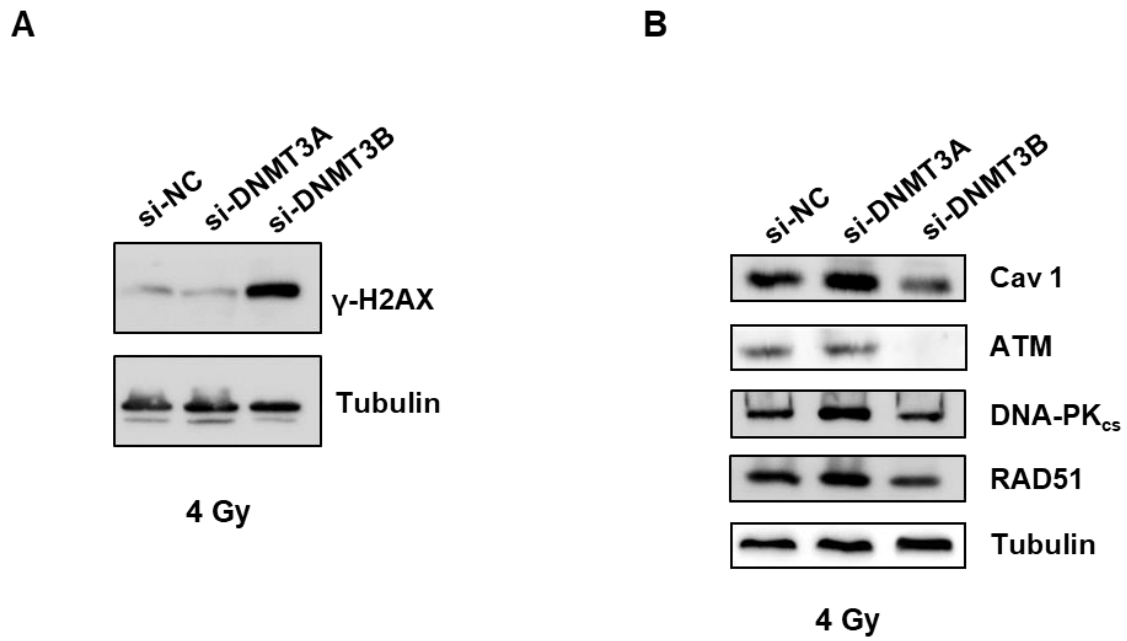

Figure 38: DNMT3B depletion impairs the DNA damage repair in RD cells. A) Western blot showing the phosphorylated H2AX levels in si-DNMT3A, si-DNMT3B and si-NC RD cells at 72 h post-transfection exposed or not to 4 Gy radiation treatment. Tubulin was used as loading control. Representative of two different assays. **B)** Immunoblotting with specific antibodies for indicated proteins of DNA repair signalling. Tubulin was used as loading control. Representative of two independent experiments.

DISCUSSION

Abnormal DNA methylation can lead to carcinogenesis, affecting cancer cell phenotype. Indeed hypermethylation, an epigenetic mechanism resulting in transcriptional silencing of tumour suppressor genes, has been frequently observed in many human cancers (Esteller, 2005; Kazanets et al., 2016; Meng et al., 2015). Rhabdomyosarcoma (RMS), the most common soft tissue sarcoma in children, representing for about 5% of malignant paediatric tumours, includes two main histological subtypes, alveolar RMS (ARMS) and embryonal RMS (ERMS), characterised by particular genetic alterations and different outcome (Parham and Barr, 2013). Aberrant methylation of CpG-islands at the promoter regions of different genes has also been observed in RMS (Mahoney et al., 2012; Sun et al., 2015).

In the current study, we found an aberrant expression of DNA methyltransferase (DNMT) 1, 3A and 3B in both ARMS and ERMS primary tumours and cell lines. In particular, our data show for the first time that DNMT3B transcripts are over-expressed in RMS tumours compared to normal skeleton muscle (NSM), suggesting that high levels of this enzyme are important molecular features of RMS. Our results indicate that the inhibition of DNMT3B expression by RNA interference impaires the *in vitro* tumour-promoting potential of ERMS cells by significantly reducing cell proliferation, migration and colony-forming ability. We observed altered levels of proteins involved in the cell cycle control, consistent with the marked cellular growth arrest at G1/S-phase transition, suggesting a key role of DNMT3B in sustaining RMS cell progression. Indeed, DNMT3B-mediated arrest correlates with the reduced expression of different cyclins (Cyclin B1, Cyclin D1 and Cyclin E2) and the block of the pRB/E2F1 pathway by inducing de-phosphorylation of RB tumour suppressor. E2F1 transcription factor plays a crucial role in the cell cycle progression (especially in the G1/S transition) and its deregulation has been reported in many human cancers (Bell and Ryan, 2004). Hypophosphorylated RB represents the active form of the protein that binds and inhibits E2F1, this preventing its nuclear translocation and blocking its ability to recruit the basic transcriptional machinery necessary for the activation of genes that are important in cell cycle progression (Dick and Rubin, 2013; Flemington et al., 1993; Helin et al., 1993). In accordance with the inhibition of cell proliferation, we observed a significant increase of the checkpoint regulators p21 and p27,

whose up-regulation might be directly related to a promoter demethylation and a concomitant re-expression upon DNMT3B depletion. Interestingly, despite the efficient growth inhibition induced by DNMT3B knock-down, flow cytometry analysis revealed that silencing of the enzyme does not affect apoptosis, as confirmed at molecular levels by cleaved PARP and Bcl-xL expression levels, but leads to the restoration of the myogenic fate in ERMS cell lines.

We found that DNMT3B down-regulation is able to activate muscle-regulatory factors (MRFs) and myomiRs in RD and TE671 cells, two human *in vitro* models of ERMS. In particular, normalization of DNMT3B expression promotes myogenesis as shown by the marked up-regulation of MYOD1, followed by Myogenin and myomiR miR-133a and miR-206 expression, as well as by changes in the cell morphology, from round shape to more elongated cellular bodies. Preliminary results indicate that DNMT3B *in vitro* down-regulation does not affect ARMS phenotype and does not sustain differentiation program. MYOD1, a master regulator of myogenesis, is expressed in proliferating myoblast and is able to activates the terminal differentiation program, by directly promoting the expression of miR-206 and many other genes involved in myogenesis (Buckingham and Rigby, 2014; Koutalianos et al., 2015). Several studies have suggested that transcriptional repression by hypermethylation of both DNA and histones at the enhancer/promoter regions of myogenic factors and cofactors is a potential mechanism to promote tumour formation and progression as well as to impair terminal differentiation in RMS (Brunk et al., 1996; Ciarapica et al., 2014; Keller and Guttridge, 2013; MacQuarrie et al., 2013). Human MYOD1 gene is located at 11p15 (Scrable et al., 1990), a chromosomal region containing the IGF2 and H19 genes regulated by parental imprinting (Nordin et al., 2014), whose expression has been found to be altered (over-expression of IGF2 and down-regulation of H19) in a subset of ERMS tumours (Casola et al., 1997). Chen and colleagues have found alterations of methylation levels in the upstream regions of the human MYOD1 gene in ERMS subtypes (Chen et al., 1998). Furthermore, RD proliferating cells show low levels of MYOD1, and has been demonstrated that an increased abundance of this transcription factor allows to switch RMS cells from an arrested phase to a differentiated state (Yang et al., 2009), this confirming that a controlled amount of MRFs is a fundamental condition for a proper skeletal muscle differentiation in ERMS cells. Therefore, the abnormal MYOD1 methylation pattern observed in RMS might be due to a generalized deregulation of the

11p15 imprinted region. In this regard, epigenetic deregulation observed in RMS might be directly due to DNMT3B over-expression, since this enzyme is responsible of *de novo* DNA methylation patterns. Interestingly, DNMT3B silencing was maintained at 144 h after siRNA-transfection and determined long-term changes in ERMS cell phenotype, as assessed by the elevated levels of MyHC protein, which is specifically related to committed muscle cells. Moreover, we supposed that DNMT3B is a downstream effector of MEK/ERK signalling pathway, since we observed the decrease of DNMT3B protein levels upon treatment with the MEK1/2 inhibitor U0126. Protein kinase cascade that leads to MAPKs activation, mediates specific responses, including proliferation, differentiation and apoptosis (Pang et al., 1995; Robinson and Cobb, 1997). As has been previously demonstrated, MEK/ERK signalling disruption affects tumour growth and reactivates myogenesis in ERMS cells (Marampon et al., 2006; Mauro et al., 2002). Thus, the concomitant MEK/ERK inhibition and DNMT3B down-regulation suggest that abrogation of the enzyme is an essential step for reverting RMS cancer phenotype towards skeletal muscle differentiation, by reducing the expression of proliferative markers and up-regulating myogenic genes. In addition, DNMT3B knock-down induced a sustained activation of p38 kinase, which has been reported to promote myogenesis and to maintain myogenic-related morphology in ERMS cells (Marampon et al., 2006; Mauro et al., 2002).
In contrast to DNMT3B, DNMT3A silencing does not reactivate myogenic differentiation in ERMS cells, but induces only a mild increase in G2 phase with a concomitant reduction in S phase of the cell cycle. Further analysis will be required to better understanding the specific role of DNMT3A in RMS development and progression, since this enzyme is overexpressed in all the analysed RMS primary tumour samples in comparison to NSM. Several studies have shown different roles for DNMT3A and DNMT3B in mammalian development: imprinted loci during gametogenesis (Kaneda et al., 2004) and major satellite repeats of the pericentromeric region are preferentially methylated by DNMT3A, whilst minor satellite repeats are methylated by DNMT3B (Chen et al., 2003). Oka et al. demonstrated that Fgf-1 is preferentially methylated by DNMT3A but not by DNMT3B (Oka et al., 2006). In addition, Linhart and colleagues found that DNMT3B but not DNMT3A is able to promotes *in vivo* tumorigenesis, by increasing the number of intestinal adenomas in mice overespressing DNMT3A or DNMT3B genes (Linhart et al., 2007).

Recently, microRNAs (miRNAs), an emerging class of epigenetic regulators which regulate gene expression at the post-transcriptional level (Esteller, 2011), have been demonstrated to function as oncogenes or tumour suppressors (Esquela-Kerscher and Slack, 2006; Medina and Slack, 2008), playing a crucial role in tumorigenesis, including RMS (Rota et al., 2011). Ectopic expression of miR-29 family members has been described in several human tumour types, such as hepatocellular carcinoma, nasopharyngeal carcinomas, breast cancer and different hematologic malignancies (Amodio et al., 2015; Cittelly et al., 2013; Sengupta et al., 2008; Xiong et al., 2009). The miR-29 family consists of miR-29a, miR-29b and miR-29c (Dostie et al., 2003; Lagos-Quintana, 2001; Lagos-Quintana et al., 2002) which share regulatory capacity. Deregulation of miR-29b has already been observed in RMS, having a role in skeletal muscle differentiation (Wang et al., 2008a). Here we found a strong down-regulation of both miR-29a and miR-29c in 14 RMS tumour samples in comparison to NSM, in agreement with the tumour suppressor activity described in other human cancers. *In silico* analysis followed by Q-PCR and western blot experiments showed that the restoration of miR-29a and miR-29c expression markedly reduced DNMT3B mRNA and protein levels in RD cells. Furthermore, miR-29a/miR-29c-transfected cells reduced cell proliferation and cell migration. We also observed changes in the cell cycle distribution with growth arrest at G1 phase, in accordance with the alterations described in si-DNMT3B RD cells. These results suggest that decreased expression of miR-29a/miR-29c in RMS plays a crucial role in DNMT3B up-regulation, this promoting its oncogenic activity. In agreement with this hypothesis, previous studies have described that miR-29 family members target DNMT transcripts in different cell systems, including lung cancer, hepatocytes and acute myeloid leukemia cells (Cicchini et al., 2015; Fabbri et al., 2007; Garzon et al., 2009; Yan et al., 2015). Epigenetic factors could also affect miRNA expression, as assessed by recent studies showing miRNA transcriptional repression by CpG island hypermethylation in cancer cells (Lehmann et al., 2008; Lujambio et al., 2007; Saito et al., 2006). Notably, some miRNAs, like miR-148a and miR-199a, target DNMT mRNAs and are themselves regulated by methylation in cancer cells, this generating feedback regulatory loops that tightly connect miRNAs and DNA methylation pathway (Chen et al., 2014; Li et al., 2014). Further analysis will be needed to elucidate whether in RMS is present this regulatory loop between miR-29a/miR-29c and DNMT3B.

Finally, our data underline the role of DNMT3B silencing in potentiating the effects of radiotherapy. Indeed, depletion of DNMT3B enhances radiosensitivity of ERMS cell lines, as demonstrated by the reduced growth rate confirmed by the alteration in cell cycle progression. In addition, clonogenic assay reveales a survival reduction of about 95% in si-DNMT3B irradiated cells in comparison to si-NC cells. Since IR induces double-strand break (DSBs) and radiosensitivity is mediated by inhibition of the NHEJ and the HR DNA repair pathways (Maier et al., 2016), we analysed the mechanism of radiosensitization in RD cells. At 24 h after irradiation with 4 Gy we observed that only DNMT3B silencing causes a marked increased in the phosphorylation levels of the H2AX histone variant (γ-H2AX), which is a marker of the DNA DSBs (Kuo and Yang, 2008), suggesting that DNMT3B enzyme is an upstream component of the DNA damage signalling pathway. Moreover, we showed that DNMT3B knock-down abrogates the IR-induced Cav-1, ATM, DNA-PK_{cs} and RAD51 expression levels. Cav-1 plays a crucial role in both HR and NHEJ DNA damage response (DDR), activating downstream molecules in the signalling cascade (Zhu et al., 2010). ATM and DNA-PK_{cs}, members of the phosphatidylinositol 3-kinase-related kinase (PIKK) family, are the primary transducers of DSB-induced signalling. DNA-PK_{cs} is itself a target of ATM, which is the master regulator of DDR through the detection of DSBs (Callén et al., 2009). DNA-PK_{cs} is essential for NHEJ (Smith and Jackson, 1999), whilst RAD51 plays a major role in HR pathway (Alshareeda et al., 2016). Altogether, our data demonstrate that inhibition of DNMT3B is a crucial mechanism to prevent DNA damage response, which in turn leads to tumour cell radiosensitivity.

Based on the present results, DNMT3B may represent a new important molecule explaining the molecular mechanisms by which ERMS cells fail to activate/complete the skeletal muscle differentiation program. Previous reports have demonstrated that epigenetic modifications, comprehending both acetylation and methylation in the 5'-flanking regulatory regions, play a crucial role in the regulation of progressional changes in transcription necessary for muscle differentiation (Hupkes et al., 2011; Laker and Ryall, 2016; Lucarelli et al., 2001). DNMT3B might act in two different way: directly by hypermethylating DNA or by cooperating with other factors able to modify chromatin, such as histone deacetylases (HDACs) and Polycomb-group (PcG) proteins (Jin et al., 2009; Purkait et al., 2016). In this regard, preliminary results obtained in our laboratory indicate that DNMT3B and the histone methyltransferase EZH2 (Enhancer of zeste

homolog 2), the catalytic subunit of the Polycomb Repressor Complex 2 (PRC2), are able to interact in both RD and TE671 ERMS cells. Bisulfite sequencing and chromatin immunoprecipitation (ChIP) assays will be carry out in our laboratory to fully characterise the possible epigenetic modifications at enhancer/promoter regions associated with myogenic markers expression in si-DNMT3B RMS cells in comparison to control mocked samples. Preliminary ChIP assay revealed an increased binding of MYOD1 to E-box 2 on the promoter of miR-206 in si-DNMT3B RD cells.

Furthermore, recent findings have shown that DNMT3 enzymes can repress transcription in a methylation-independent manner (Haney et al., 2015), since their capacity to bind with their plant homeodomain-like motif at N-terminal domain (Aasland et al., 1995) silencer complexes comprehending MBD (Methyl CpG binding) proteins or specific transcriptional repressors (Buck-Koehntop and Defossez, 2013; Hervouet et al., 2009; Oikawa et al., 2011; Palacios et al., 2010). So, the molecular mechanisms of DNMT3B-mediated transcriptional silencing at muscle-gene regulatory regions in RMS could be due to its potential repressor activity. The finding that DNMT3B knocking down induces cell cycle arrest and commits ERMS cells to myogenesis suggests that this strategy has a therapeutic potential in ERMS tumours, this outlining the importance to test the antitumour effects of this DNMT3B siRNA molecules in mouse xenograft models.

In recent years has emerged that demethylating agents or HDAC inhibitors have pro-differentiative effects in RMS cells by up-regulating the expression levels of different muscle-specific coding genes and miRNAs. In a previous work we demonstrated that 5-aza-dC DNA demethylating agents is able to up-regulate miR-378a-3p (down-regulated in RMS tumour samples), inducing apoptosis, decrease in cell migration, G2-cell cycle arrest and myogenic differentiation (Megiorni et al., 2014). Furthermore, Kim et al. previously reported that several DNMT inhibitors radiosensitize human cancer cells by suppressing DNA repair activity (Kim et al., 2012). Currently, 5-aza and 5-aza-dC DNA demethylanting agents have been approved by US FDA for the treatment of haematopoietic malignancies (Fahy et al., 2012; Flis et al., 2014; Jones et al., 2016) but, their efficacy in the treatment of human solid tumours is still controversial (Bauman et al., 2012). In addition, it is important to note that the mechanism of action of 5-aza and 5-aza-dC remains to be fully understood (Stresemann and Lyko, 2008) and that long-term exposure induces high levels of toxicity (Karahoca and Momparler, 2013). Reduced

representation bisulfite sequencing (RRBS) experiments are underway in our laboratory to characterise the genome-wide methylation profiles in si-DNMT3B *vs.* si-NC cells in order to provide a deeper insight into the RMS tumorigenesis, and to identify new potential targets for the development of more effective and less toxic epigenetic therapies. Indeed, non-nucleoside compounds, which are independent of replication for their incorporation into DNA, or other molecules with a high biochemical selectivity towards individual human DNMT enzymes might lead to promising anticancer therapies (Graça et al., 2014; Sandhu et al., 2012), and this also in RMS.

In conclusion, this study describes for the first time the over-expression of DNMT3B gene in RMS primary tumour and cell lines, suggesting that an aberrant transcriptional control mediated by this *de novo* DNMT is a key event in RMS development and progression. Our findings also outline the potential clinical application of DNMT3B inhibition in cancer treatment. DNMT3B target therapies may represent a novel clinical approach, effective not only in impairing tumour growth but also in reactivating myogenic program and increasing the sensitivity to radiotherapy, especially in ERMS subtypes.

Part of the results of this research project have been published in the international journal Oncotarget: Megiorni F, Camero S, Ceccarelli S, McDowell HP, Mannarino O, Marampon F, Pizer B, Shukla R, Pizzuti A, Marchese C, Clerico A, Dominici C. (2016) DNMT3B in vitro knocking-down is able to reverse the embryonic rhabdomyosarcoma cell phenotype through inhibition of proliferation and induction of myogenic differentiation. Oncotarget. Nov 29; 7 (48): 79342-79356.

REFERENCES

Aasland, R., Gibson, T.J., and Stewart, a. F. (1995). The PHD finger: implications for chromatin-mediated transcriptional regulation. Trends Biochem. Sci. *20*, 56–59.

Aldawsari, F.S., Aguayo-ortiz, R., Kapilashrami, K., Yoo, J., Luo, M., and Vela, C.A. (2015). Resveratrol-salicylate derivatives as selective DNMT3 inhibitors and anticancer agents. J. Enzym. Inhib. Med. Chemestry *6366*, 1–9.

Allfrey, V., Faulkner, R., and Mirsky, A. (1964). Acetylation and methylation of histones and their possible role in the regulation of RNA synthesis. Proc. Natl. Acad. Sci. *315*, 786–794.

Alshareeda, A.T., Negm, O.H., Aleskandarany, M.A., Green, A.R., Nolan, C., TigHhe, P.J., Madhusudan, S., Ellis, I.O., and Rakha, E.A. (2016). Clinical and biological significance of RAD51 expression in breast cancer: a key DNA damage response protein. Breast Cancer Res. Treat. *159*, 41–53.

Amodio, N., Rossi, M., Raimondi, L., Pitari, M.R., Botta, C., Tagliaferri, P., and Tassone, P. (2015). miR-29s: a family of epi-miRNAs with therapeutic implications in hematologic malignancies. Oncotarget *6*, 12837–12861.

Amstutz, R., Wachtel, M., Troxler, H., Kleinert, P., Ebauer, M., Haneke, T., Oehler-Janne, C., Fabbro, D., Niggli, F.K., and Schafer, B.W. (2008). Phosphorylation Regulates Transcriptional Activity of PAX3/FKHR and Reveals Novel Therapeutic Possibilities. Cancer Res. *68*, 3767–3776.

Anderson, J., Gordon, A., Pritchard-Jones, K., and Shipley, J. (1999). Genes, chromosomes, and rhabdomyosarcoma. Genes Chromosom. Cancer *26*, 275–285.

Bailey, P., Holowacz, T., and Lassar, A.B. (2001). The origin of skeletal muscle stem cells in the embryo and the adult. Curr. Opin. Cell Biol. *13*, 679–689.

Barau, J., Teissandier, A., Zamudio, N., Roy, S., Nalesso, V., Hérault, Y., Guillou, F., and Bourc'his, D. (2016). The novel DNA methyltransferase DNMT3C protects male germ cells from transposon activity. Science *2*, (In Press).

Barr, F.G. (2001). Gene fusions involving PAX and FOX family members in alveolar rhabdomyosarcoma. Oncogene *20*, 5736–5746.

Barr, F.G., Galili, N., Holick, J., Biegel, J. a, Rovera, G., and Emanuel, B.S. (1993). Rearrangement of the PAX3 paired box gene in the paediatric solid tumour alveolar rhabdomyosarcoma. Nat. Genet. *3*, 113–117.

Barr, F.G., Nauta, L.E., Davis, R.J., Schäfer, B.W., Nycum, L.M., and Biegel, J.A. (1996). In vivo amplification of the PAX3-FKHR and PAX7-FKHR fusion genes in alveolar rhabdomyosarcoma. Hum. Mol. Genet. *5*, 15–21.

Bauman, J., Verschraegen, C., Belinsky, S., Muller, C., Rutledge, T., Fekrazad, M., Ravindranathan, M., Lee, S.J., and Jones, D. (2012). A phase i study of 5-azacytidine and erlotinib in advanced solid tumor malignancies. Cancer Chemother. Pharmacol. *69*, 547–554.

Baylin, S.B., and Jones, P.A. (2014). Epigenetic determinants of cancer. Cold Spring Harb. Perspect. Biol. *8*, 1–36.

Bell, L.A., and Ryan, K.M. (2004). Life and death decisions by E2F-1. Cell Death Differ. *11*, 137–142.

Bennicelli, J.L., Edwards, R.H., and Barr, F.G. (1996). Mechanism for transcriptional gain of function resulting from chromosomal translocation in alveolar rhabdomyosarcoma. Proc. Natl. Acad. Sci. U. S. A. *93*, 5455–5459.

Bennicelli, J.L., Advani, S., Schäfer, B.W., and Barr, F.G. (1999). PAX3 and PAX7 exhibit conserved cis-acting transcription repression domains and utilize a common gain of function mechanism in alveolar rhabdomyosarcoma. Oncogene *18*, 4348–4356.

Bersani, F., Taulli, R., Accornero, P., Morotti, A., Miretti, S., Crepaldi, T., and Ponzetto, C. (2008).

Bortezomib-mediated proteasome inhibition as a potential strategy for the treatment of rhabdomyosarcoma. Eur. J. Cancer *44*, 876–884.

Biegel, J.A., Meek, R.S., Parmiter, A.H., Conard, K., and Emanuel, B.S. (1991). Chromosomal Translocation t(1;13)(p36;q14) in a Case of Rhabdomyosarcoma. Genes, Chromosom. Cancer *3*, 483–484.

Bogdanović, O., and Veenstra, G.J.C. (2009). DNA methylation and methyl-CpG binding proteins: developmental requirements and function. Chromosoma *118*, 549–565.

Bourc'his, D., Xu, G.L., Lin, C.S., Bollman, B., and Bestor, T.H. (2001). Dnmt3L and the establishment of maternal genomic imprints. Science. *294*, 2536–2539.

Brady, M.S., Gaynor, J.J., and Brennan, M.F. (1992). Radiation-associated sarcoma of bone and soft tissue. Arch. Surg. *127*, 1379–1385.

Breneman, J.C., Lyden, E., Pappo, A.S., Link, M.P., Anderson, J.R., Parham, D.M., Qualman, S.J., Wharam, M.D., Donaldson, S.S., Maurer, H.M., et al. (2003). Prognostic factors and clinical outcomes in children and adolescents with metastatic rhabdomyosarcoma--a report from the Intergroup Rhabdomyosarcoma Study IV. J. Clin. Oncol. *21*, 78–84.

Van Den Broeke, L.T., Pendleton, C.D., Mackall, C., Helman, L.J., and Berzofsky, J.A. (2006). Identification and epitope enhancement of a PAX-FKHR fusion protein breakpoint epitope in alveolar rhabdomyosarcoma cells created by a tumorigenic chromosomal translocation inducing CTL capable of lysing human tumors. Cancer Res. *66*, 1818–1823.

Brueckner, B., Stresemann, C., Kuner, R., Mund, C., Musch, T., Meister, M., Sültmann, H., and Lyko, F. (2007). The human let-7a-3 locus contains an epigenetically regulated microRNA gene with oncogenic function. Cancer Res. *67*, 1419–1423.

Brunk, B.P., Goldhamer, D.J., and Emerson, C.P. (1996). Regulated demethylation of the myoD distal enhancer during skeletal myogenesis. Dev. Biol. *177*, 490–503.

Buck-Koehntop, B.A., and Defossez, P.A. (2013). On how mammalian transcription factors recognize methylated DNA. Epigenetics *8*, 131–137.

Buckingham, M., and Rigby, P.W.J. (2014). Gene Regulatory Networks and Transcriptional Mechanisms that Control Myogenesis. Dev. Cell *28*, 225–238.

Butcher, D.T., and Rodenhiser, D.I. (2007). Epigenetic inactivation of BRCA1 is associated with aberrant expression of CTCF and DNA methyltransferase (DNMT3B) in some sporadic breast tumours. Eur. J. Cancer *43*, 210–219.

Cairns, P., Esteller, M., Herman, J.G., Sidransky, D., Schoenberg, M., Sidransky, D., Jeronimo, C., Sanchez-Cespedes, M., Chow, N.H., Grasso, M., et al. (2001). Molecular detection of prostate cancer in urine by GSTP1 hypermethylation. Clin. Cancer Res. *7*, 2727–2730.

Callén, E., Jankovic, M., Wong, N., Zha, S., Chen, H.T., Difilippantonio, S., Di Virgilio, M., Heidkamp, G., Alt, F.W., Nussenzweig, A., et al. (2009). Essential Role for DNA-PKcs in DNA Double-Strand Break Repair and Apoptosis in ATM-Deficient Lymphocytes. Mol. Cell *34*, 285–297.

Cao, L., Yu, Y., Darko, I., Currier, D., Mayeenuddin, L.H., Wan, X., Khanna, C., and Helman, L.J. (2008). Addiction to elevated insulin-like growth factor I receptor and initial modulation of the AKT pathway define the responsiveness of rhabdomyosarcoma to the targeting antibody. Cancer Res. *68*, 8039–8048.

Casanova, M., and Ferrari, A. (2011). Pharmacotherapy for pediatric soft-tissue sarcomas. Expert Opin. Pharmacother. *12*, 517–531.

Casola, S., Pedone, P. V, Cavazzana, A.O., Basso, G., Luksch, R., d'Amore, E.S., Carli, M., Bruni, C.B., and Riccio, A. (1997). Expression and parental imprinting of the H19 gene in human rhabdomyosarcoma. Oncogene *14*, 1503–1510.

Cessna, M.H., Zhou, H., Perkins, S.L., Tripp, S.R., Layfield, L., Daines, C., and Coffin, C.M. (2001). Are myogenin and myoD1 expression specific for rhabdomyosarcoma? A study of 150 cases, with emphasis on spindle cell mimics. Am. J. Surg. Pathol. *25*, 1150–1157.

Chen, T., and Li, E. (2004). Structure and function of eukaryotic DNA methyltransferases. Curr Top Dev Biol *60*, 55–89.

Chen, T., and Li, E. (2006). Establishment and maintenance of DNA methylation patterns in mammals. Curr. Top. Microbiol. Immunol. *301*, 179–201.

Chen, B., Dias, P., Jenkins, J.J., Savell, V.H., and Parham, D.M. (1998). Methylation alterations of the MyoD1 upstream region are predictive of subclassification of human rhabdomyosarcomas. Am. J. Pathol. *152*, 1071–1079.

Chen, B., Liu, X., Savell, V.H., Dilday, B.R., Johnson, M.W., Jenkins, J.J., and Parham, D.M. (1999). Increased DNA methyltransferase expression in rhabdomyosarcomas. Int. J. Cancer *83*, 10–14.

Chen, B.-F., Suen, Y.-K., Gu, S., Li, L., and Chan, W.-Y. (2014). A miR-199a/miR-214 self-regulatory network via PSMD10, TP53 and DNMT1 in testicular germ cell tumor. Sci. Rep. *4*, 6413.

Chen, T., Ueda, Y., Dodge, J.E., Wang, Z., and Li, E. (2003). Establishment and maintenance of genomic methylation patterns in mouse embryonic stem cells by Dnmt3a and Dnmt3b. Mol. Cell. Biol. *23*, 5594–5605.

Chen, T., Tsujimoto, N., and Li, E. (2004). The PWWP domain of Dnmt3a and Dnmt3b is required for directing DNA methylation to the major satellite repeats at pericentric heterochromatin. Mol Cell Biol *24*, 9048–9058.

Chen, Y., Takita, J., Mizuguchi, M., Tanaka, K., Ida, K., Koh, K., Igarashi, T., Hanada, R., Tanaka, Y., Park, M.J., et al. (2007). Mutation and expression analyses of the MET and CDKN2A in rhabdomyosarcoma with emphasis on MET overexpression. Genes Chromosom. Cancer *46*, 348–358.

Cheng, X. (1995). Structure and function of DNA methyltransferases. Annu. Rev. Biophys. Biomol. Struct. *24*, 293–318.

Cheng, X., and Blumenthal, R.M. (2008). Mammalian DNA Methyltransferases: A Structural Perspective. Structure *16*, 341–350.

Ciarapica, R., Carcarino, E., Adesso, L., De Salvo, M., Bracaglia, G., Leoncini, P.P., Dall'Agnese, A., Verginelli, F., Milano, G.M., Boldrini, R., et al. (2014). Pharmacological inhibition of EZH2 as a promising differentiation therapy in embryonal RMS. BMC Cancer *14*, 139.

Ciccarelli, C., Marampon, F., Scoglio, A., Mauro, A., Giacinti, C., De Cesaris, P., and Zani, B. (2005). p21WAF1 expression induced by MEK/ERK pathway activation or inhibition correlates with growth arrest, myogenic differentiation and onco-phenotype reversal in rhabdomyosarcoma cells. Mol. Cancer *4*, 41.

Cicchini, C., de Nonno, V., Battistelli, C., Cozzolino, A.M., De Santis Puzzonia, M., Ciafrè, S.A., Brocker, C., Gonzalez, F.J., Amicone, L., and Tripodi, M. (2015). Epigenetic control of EMT/MET dynamics: HNF4α impacts DNMT3s through miRs-29. Biochim. Biophys. Acta - Gene Regul. Mech. *1849*, 919–929.

Cittelly, D.M., Finlay-Schultz, J., Howe, E.N., Spoelstra, N.S., Axlund, S.D., Hendricks, P., Jacobsen, B.M., Sartorius, C.A., and Richer, J.K. (2013). Progestin suppression of miR-29 potentiates dedifferentiation of breast cancer cells via KLF4. Oncogene *32*, 2555–2564.

Clayer, M., Bouralexis, S., Evdokiou, a, Hay, S., Atkins, G.J., and Findlay, D.M. (2001). Enhanced apoptosis of soft tissue sarcoma cells with chemotherapy: A potential new approach using TRAIL. J. Orthop. Surg. (Hong Kong) *9*, 19–22.

Cormier, J.N., and Pollock, R.E. (2004). Soft Tissue Sarcomas. CA. Cancer J. Clin. *54*, 94–109.

Costello, J.F., Fruhwald, M.C., Smiraglia, D.J., Rush, L.J., Robertson, G.P., Gao, X., Wright, F.A., Feramisco, J.D., Peltomaki, P., Lang, J.C., et al. (2000). Aberrant CpG-island methylation has non-random and tumour-type-specific patterns. Nat Genet *24*, 132–138.

Crist, W.M., Anderson, J.R., Meza, J.L., Fryer, C., Raney, R.B., Ruymann, F.B., Breneman, J., Qualman, S.J., Wiener, E., Wharam, M., et al. (2001). Intergroup Rhabdomyosarcoma Study-IV: Results for patients with nonmetastatic disease. J. Clin. Oncol. *19*, 3091–3102.

Dagher, R., Long, L.M., Read, E.J., Leitman, S.F., Carter, C.S., Tsokos, M., Goletz, T.J., Avila, N., Berzofsky, J.A., Helman, L.J., et al. (2002). Pilot trial of tumor-specific peptide vaccination and continuous infusion interleukin-2 in patients with recurrent Ewing sarcoma and alveolar rhabdomyosarcoma: An inter-institute NIH study. Med. Pediatr. Oncol. *38*, 158–164.

Daston, G., Lamar, E., Olivier, M., and Goulding, M. (1996). Pax-3 is necessary for migration but not differentiation of limb muscle precursors in the mouse. Development *122*, 1017–1027.

Davis, R.J., and Barr, F.G. (1997). Fusion genes resulting from alternative chromosomal translocations are overexpressed by gene-specific mechanisms in alveolar rhabdomyosarcoma. Proc. Natl. Acad. Sci. U. S. A. *94*, 8047–8051.

Dawson, M.A., and Kouzarides, T. (2012). Cancer epigenetics: From mechanism to therapy. Cell *150*, 12–27.

DeVita, V.T., Hellman, S., and Rosenberg, S.A. (2005). Cancer : Principles and Practice of Oncology Collections :

Dick, F.A., and Rubin, S.M. (2013). Molecular mechanisms underlying RB protein function. Nat. Rev. Mol. Cell Biol. *14*, 297–306.

Ding, F., and Chaillet, J.R. (2002). In vivo stabilization of the Dnmt1 (cytosine-5)- methyltransferase protein. Proc. Natl. Acad. Sci. U. S. A. *99*, 14861–14866.

Dostie, J., Mourelatos, Z., Yang, M., Sharma, A., and Dreyfuss, G. (2003). Numerous microRNPs in neuronal cells containing novel microRNAs. RNA *9*, 180–186.

Douglass, E.C., Valentine, M., Etcubanas, E., Parham, D., Webber, B.L., Houghton, P.J., and Green, A.A. (1987). A specific chromosomal abnormality in rhabdomyosarcoma. Cytogenet. Genome Res. *45*, 148–155.

Douglass, E.C., Rowe, S.T., Valentine, M., Parham, D.M., Berkow, R., Paul Bowman, W., and Maurer, H.M. (1991). Variant Translocations of Chromosome 13 in Alveolar Rhabdomyosarcoma. Genes, Chromosom. Cancer *3*, 480–482.

Eads, C.A., Danenberg, K.D., Kawakami, K., Saltz, L.B., Danenberg, P. V, and Laird, P.W. (1999). CpG island hypermethylation in human colorectal tumors is not associated with DNA methyltransferase overexpression. Cancer Res. *59*, 2302–2306.

Easwaran, H.P., Schermelleh, L., Leonhardt, H., and Cardoso, M.C. (2004). Replication-independent chromatin loading of Dnmt1 during G2 and M phases. EMBO Rep. *5*, 1181–1186.

Eden, A., Gaudet, F., Waghmare, A., and Jaenisch, R. (2003). Chromosomal Instability and Tumors Promoted by DNA Hypomethylation. Science (80-.). *300*, 2003.

Epstein, J.A., Shapiro, D.N., Cheng, J., Lam, P.Y., and Maas, R.L. (1996). Pax3 modulates expression of the c-Met receptor during limb muscle development. Proc. Natl. Acad. Sci. U. S. A. *93*, 4213–4218.

Erdmann, A., Halby, L., Fahy, J., and Arimondo, P.B. (2015). Targeting DNA methylation with small molecules: What's next? J. Med. Chem. *58*, 2569–2583.

Esquela-Kerscher, A., and Slack, F.J. (2006). Oncomirs — microRNAs with a role in cancer. Nat. Rev. Cancer *6*, 259–269.

Esteller, M. (2005). Aberrant Dna Methylation As a Cancer-Inducing Mechanism. Annu. Rev. Pharmacol. Toxicol. *45*, 629–656.

Esteller, M. (2007). Cancer epigenomics: DNA methylomes and histone-modification maps. Nat. Rev. Genet. *8*, 286–298.

Esteller, M. (2008). Epigenetics in cancer. - main article. N. Engl. J. Med. *358*, 1148–1159.

Esteller, M. (2011). Non-coding RNAs in human disease. Nat Rev Genet *12*, 861–874.

Esteller, M., Corn, P.G., Urena, J.M., Gabrielson, E., Baylin, S.B., and Herman, J.G. (1998). Inactivation of glutathione S-transferase P1 gene by promoter hypermethylation in human neoplasia. Cancer Res. *58*, 4515–4518.

Esteller, M., Silva, J.M., Dominguez, G., Bonilla, F., Matias-Guiu, X., Lerma, E., Bussaglia, E., Prat, J., Harkes, I.C., Repasky, E. a, et al. (2000a). Promoter hypermethylation and BRCA1 inactivation in sporadic breast and ovarian tumors. J. Natl. Cancer Inst. *92*, 564–569.

Esteller, M., Garcia-Foncillas, J., Andion, E., Goodman, S.N., Hidalgo, O.F., Vanaclocha, V., Baylin, S.B., and Herman, J.G. (2000b). Inactivation of the DNA-repair gene MGMT and the clinical response of gliomas to alkylating agents. N. Engl. J. Med. *343*, 1350–1354.

Esteller, M., Corn, P.G., Baylin, S.B., and Herman, J.G. (2001a). A gene hypermethylation profile of human cancer. Cancer Res. *61*, 3225–3229.

Esteller, M., Fraga, M.F., Guo, M., Garcia-Foncillas, J., Hedenfalk, I., Godwin, A.K., Trojan, J., Vaurs-Barriere, C., Bignon, Y.J., Ramus, S., et al. (2001b). DNA methylation patterns in hereditary human cancers mimic sporadic tumorigenesis. Hum Mol Genet *10*, 3001–3007.

Fabbri, M., Garzon, R., Cimmino, A., Liu, Z., Zanesi, N., Callegari, E., Liu, S., Alder, H., Costinean, S., Fernandez-Cymering, C., et al. (2007). MicroRNA-29 family reverts aberrant methylation in lung cancer by targeting DNA methyltransferases 3A and 3B. Proc. Natl. Acad. Sci. *104*, 15805–15810.

Fahy, J., Jeltsch, A., and Arimondo, P.B. (2012). DNA methyltransferase inhibitors in cancer: a chemical and therapeutic patent overview and selected clinical studies. Expert Opin. Ther. Pat. *22*, 1427–1442.

Feinberg, A.P., and Vogelstein, B. (1983). Hypomethylation distinguishes genes of some human cancers from their normal counterparts. Nature *301*, 89–92.

Feinberg, A.P., Koldobskiy, M.A., and Göndör, A. (2016). Epigenetic modulators, modifiers and mediators in cancer aetiology and progression. Nat. Rev. Genet. *17*, 284–299.

Felix, C.A., Winick, N.J., Crouch, G.D., and Helman, L.J. (1992). Frequency and Diversity of p53 Mutations in Childhood Rhabdomyosarcoma. Cancer Res. *52*, 2243–2247.

Fellinger, K., Rothbauer, U., Felle, M., Längst, G., and Leonhardt, H. (2009). Dimerization of DNA methyltransferase 1 is mediated by its regulatory domain. J. Cell. Biochem. *106*, 521–528.

Fernandez, A.F., Huidobro, C., and Fraga, M.F. (2012). De novo DNA methyltransferases: Oncogenes, tumor suppressors, or both? Trends Genet. *28*, 474–479.

Ferrari, A., and Casanova, M. (2005). Current chemotherapeutic strategies for rhabdomyosarcoma. Expert Rev. Anticancer Ther. *5*, 283–294.

Flemington, E.K., Speck, S.H., and Kaelin, W.G. (1993). E2F-1-mediated transactivation is inhibited by complex formation with the retinoblastoma susceptibility gene product. Proc. Natl. Acad. Sci. U. S. A. *90*, 6914–6918.

Flis, S., Gnyszka, A., and Flis, K. (2014). DNA methyltransferase inhibitors improve the effect of chemotherapeutic agents in SW48 and HT-29 colorectal cancer cells. PLoS One *9*, e92305.

Folpe, A.L. (2002). MyoD1 and myogenin expression in human neoplasia: a review and update. Adv. Anat. Pathol. *9*, 198–203.

Fong, Y., Coit, D.G., Woodruff, J.M., and Brennan, M.F. (1993). Lymph node metastasis from soft tissue sarcoma in adults. Analysis of data from a prospective database of 1772 sarcoma patients. Ann Surg *217*, 72–77.

Fraga, M.F., Herranz, M., Espada, J., Ballestar, E., Paz, M.F., Ropero, S., Erkek, E., Bozdogan, O., Peinado, H., Niveleau, A., et al. (2004). A mouse skin multistage carcinogenesis model reflects the aberrant DNA methylation patterns of human tumors. Cancer Res. *64*, 5527–5534.

Galili, N., Davis, R.J., Fredericks, W.J., Mukhopadhyay, S., Rauscher, F.J., Emanuel, B.S., Rovera, G., and Barr, F.G. (1993). Fusion of a fork head domain gene to PAX3 in the solid tumour alveolar rhabdomyosarcoma. Nat. Genet. *5*, 230–235.

Galli, R., Paone, A., Fabbri, M., Zanesi, N., Calore, F., Cascione, L., Acunzo, M., Stoppacciaro, A., Tubaro, A., Lovat, F., et al. (2013). Toll-like receptor 3 (TLR3) activation induces microRNA-dependent reexpression of functional RARβ and tumor regression. Proc. Natl. Acad. Sci. U. S. A. *110*, 9812–9817.

Ganjavi, H., Gee, M., Narendran, A., Freedman, M.H., and Malkin, D. (2005). Adenovirus-mediated p53 gene therapy in pediatric soft-tissue sarcoma cell lines: sensitization to cisplatin and doxorubicin. Cancer Gene Ther. *12*, 397–406.

Gao, Q., Steine, E.J., Inmaculada Barrasa, M., Hockemeyer, D., Pawlak, M., Fu, D., Reddy, S., Bell, G.W., Jaenisch, R., Gaoa, Q., et al. (2011). Deletion of the de novo DNA methyltransferase Dnmt3a promotes lung tumor progression. Source Proc. Natl. Acad. Sci. United States Am. *108*, 18061–18066.

Gao, Z., Zhang, S., and Yang, G. (1998). A study of p16 gene and its protein expression in rhabdomyosarcoma. Zhonghua Bing Li Xue Za Zhi *27*, 290–293.

Gardner, K.H., and Montminy, M. (2005). Can you hear me now? Regulating transcriptional activators by

phosphorylation. Sci. STKE *301*, pe44.

Garzon, R., Liu, S., Fabbri, M., Liu, Z., Heaphy, C.E.A., Callegari, E., Schwind, S., Pang, J., Yu, J., Muthusamy, N., et al. (2009). MicroRNA-29b induces global DNA hypomethylation and tumor suppressor gene reexpression in acute myeloid leukemia by targeting directly DNMT3A and 3B and indirectly DNMT1. Blood *113*, 6411–6418.

Gastaldi, T., Bonvini, P., Sartori, F., Marrone, A., Iolascon, A., and Rosolen, A. (2006). Plakoglobin is differentially expressed in alveolar and embryonal rhabdomyosarcoma and is regulated by DNA methylation and histone acetylation. Carcinogenesis *27*, 1758–1767.

Gee, M.F.W., Tsuchida, R., Eichler-Jonsson, C., Das, B., Baruchel, S., and Malkin, D. (2005). Vascular endothelial growth factor acts in an autocrine manner in rhabdomyosarcoma cell lines and can be inhibited with all-trans-retinoic acid. Oncogene *24*, 8025–8037.

Girault, I., Tozlu, S., Lidereau, R., and Bieche, I. (2003). Expression analysis of DNA methyltransferases 1, 3A, and 3B in sporadic breast carcinomas. Clin Cancer Res *9*, 4415–4422.

Goldblum, J.R., Weiss, S.W., and Folpe, A.L. (2013). Enzinger and Weiss's Soft Tissue Tumors, 6th Edition. In Enzinger and Weiss''s Soft Tissue Tumors, pp. 784–854.

Goll, M.G., Kirpekar, F., Maggert, K.A., Yoder, J.A., Hsieh, C.-L., Zhang, X., Golic, K.G., Jacobsen, S.E., and Bestor, T.H. (2006). Methylation of tRNAAsp by the DNA methyltransferase homolog Dnmt2. Science *311*, 395–398.

Gonzalez-Zulueta, M., Bender, C.M., Yang, A.S., Nguyen, T., Beart, R.W., Van Tornout, J.M., and Jones, P.A. (1995). Methylation of the 5' CpG island of the p16/CDKN2 tumor suppressor gene in normal and transformed human tissues correlates with gene silencing. Cancer Res. *55*, 4531–4535.

Gordon, T., McManus, A., Anderson, J., Min, T., Swansbury, J., Pritchard-Jones, K., and Shipley, J. (2001). Cytogenetic abnormalities in 42 rhabdomyosarcoma: A United Kingdom Cancer Cytogenetics Group Study. Med. Pediatr. Oncol. *36*, 259–267.

Graça, I., Sousa, E.J., Costa-Pinheiro, P., Vieira, F.Q., Torres-Ferreira, J., Martins, M.G., Henrique, R., and Jerónimo, C. (2014). Anti-neoplastic properties of hydralazine in prostate cancer. Oncotarget *5*, 5950–5964.

Gravina, G.L., Marampon, F., Piccolella, M., Motta, M., Ventura, L., Pomante, R., Popov, V.M., Zani, B.M., Pestell, R.G., Tombolini, V., et al. (2011). Hormonal therapy promotes hormone-resistant phenotype by increasing DNMT activity and expression in prostate cancer models. Endocrinology *152*, 4550–4561.

Greger, V., Passarge, E., Höpping, W., Messmer, E., and Horsthemke, B. (1989). Epigenetic changes may contribute to the formation and spontaneous regression of retinoblastoma. Hum. Genet. *83*, 155–158.

Hamidi, T., Singh, A.K., and Chen, T. (2015). Genetic alterations of DNA methylation machinery in human diseases. Epigenomics *7*, 247–265.

Hanahan, D., and Weinberg, R.A. (2000). The hallmarks of cancer. Cell *100*, 57–70.

Haney, S.L., Hlady, R.A., Opavska, J., Klinkebiel, D., Pirruccello, S.J., Dutta, S., Datta, K., Simpson, M.A., Wu, L., and Opavsky, R. (2015). Methylation-independent repression of Dnmt3b contributes to oncogenic activity of Dnmt3a in mouse MYC-induced T-cell lymphomagenesis. Oncogene *34*, 5436–5446.

Hartmann, J.T., and Bauer, S. (2006). Soft tissue sarcoma. Update Cancer Ther. *1*, 385–402.

Hata, K., Okano, M., Lei, H., and Li, E. (2002). Dnmt3L cooperates with the Dnmt3 family of de novo DNA methyltransferases to establish maternal imprints in mice. Development *129*, 1983–1993.

Helin, K., Harlow, E., and Fattaey, A. (1993). Inhibition of E2F-1 transactivation by direct binding of the retinoblastoma protein. Mol. Cell. Biol. *13*, 6501–6508.

Herman, J.G., and Baylin, S.B. (2003). Gene Silencing in Cancer in Association with Promoter Hypermethylation. N. Engl. J. Med. *349*, 2042–2054.

Herman, J.G., Merlo, A., Mao, L., Lapidus, R.G., Issa, J.P., Davidson, N.E., Sidransky, D., and Baylin, S.B. (1995). Inactivation of the CDKN2/p16/MTS1 gene is frequently associated with aberrant DNA methylation in all common human cancers. Cancer Res. *55*, 4525–4530.

Herman, J.G., Graff, J.R., Myohanen, S., Nelkin, B.D., and Baylin, S.B. (1996). Methylation-specific PCR: a novel PCR assay for methylation status of CpG islands. Proc. Natl. Acad. Sci. *93*, 9821–9826.

Hervouet, E., Vallette, F.M., and Cartron, P.-F. (2009). Dnmt3/transcription factor interactions as crucial players in targeted DNA methylation. Epigenetics *4*, 487–499.

Heyn, R., Haeberlen, V., Newton, W.A., Ragab, A.H., Raney, R.B., Tefft, M., Wharam, M., Ensign, L.G., and Maurer, H.M. (1993). Second malignant neoplasms in children treated for rhabdomyosarcoma. Intergroup Rhabdomyosarcoma Study Committee. J Clin Oncol *11*, 262–270.

HORN, R.C., and ENTERLINE, H.T. (1958). Rhabdomyosarcoma: a clinicopathological study and classification of 39 cases. Cancer *11*, 181–199.

Hosoi, H., Dilling, M.B., Shikata, T., Liu, L.N., Shu, L., Ashmun, R.A., Germain, G.S., Abraham, R.T., and Houghton, P.J. (1999). Rapamycin causes poorly reversible inhibition of mTOR and induces p53-independent apoptosis in human rhabdomyosarcoma cells. Cancer Res. *59*, 886–894.

Houghton, P.J., Morton, C.L., Kolb, E.A., Gorlick, R., Lock, R., Carol, H., Reynolds, C.P., Maris, J.M., Keir, S.T., Billups, C.A., et al. (2008a). Initial testing (stage 1) of the mTOR inhibitor rapamycin by the pediatric preclinical testing program. Pediatr. Blood Cancer *50*, 799–805.

Houghton, P.J., Morton, C.L., Kolb, E.A., Lock, R., Carol, H., Reynolds, C.P., Keshelava, N., Maris, J.M., Keir, S.T., Wu, J., et al. (2008b). Initial testing (stage 1) of the proteasome inhibitor bortezomib by the pediatric preclinical testing program. Pediatr. Blood Cancer *50*, 37–45.

Hupkes, M., Jonsson, M.K.B., Scheenen, W.J., van Rotterdam, W., Sotoca, A.M., van Someren, E.P., van der Heyden, M.A.G., van Veen, T.A., van Ravestein-van Os, R.I., Bauerschmidt, S., et al. (2011). Epigenetics: DNA demethylation promotes skeletal myotube maturation. FASEB J. *25*, 3861–3872.

Izeradjene, K., Douglas, L., Delaney, A., and Houghton, J.A. (2004). Influence of casein kinase II in tumor necrosis factor-related apoptosis-inducing ligand-induced apoptosis in human rhabdomyosarcoma cells. Clin. Cancer Res. *10*, 6650–6660.

Jaboin, J., Wild, J., Hamidi, H., Khanna, C., Kim, C.J., Robey, R., Bates, S.E., and Thiele, C.J. (2002). MS-27-275, an inhibitor of histone deacetylase, has marked in vitro and in vivo antitumor activity against pediatric solid tumors. Cancer Res. *62*, 6108–6115.

Jeltsch, A. (2002). Beyond Watson and Crick: DNA Methylation and Molecular Enzymology of DNA Methyltransferases. ChemBioChem *3*, 274–293.

Jerónimo, C., Usadel, H., Henrique, R., Oliveira, J., Lopes, C., Nelson, W.G., and Sidransky, D. (2001). Quantitation of GSTP1 methylation in non-neoplastic prostatic tissue and organ-confined prostate adenocarcinoma. J. Natl. Cancer Inst. *93*, 1747–1752.

Jin, B., Yao, B., Li, J.L., Fields, C.R., Delmas, A.L., Liu, C., and Robertson, K.D. (2009). DNMT1 and DNMT3B modulate distinct polycomb-mediated histone modifications in colon cancer. Cancer Res. *69*, 7412–7421.

Jin, F., Dowdy, S.C., Xiong, Y., Eberhardt, N.L., Podratz, K.C., and Jiang, S.W. (2005). Up-regulation of DNA methyltransferase 3B expression in endometrial cancers. Gynecol. Oncol. *96*, 531–538.

Jones, P.A., and Baylin, S.B. (2007). The Epigenomics of Cancer. Cell *128*, 683–692.

Jones, P.A., Issa, J.-P.J., and Baylin, S. (2016). Targeting the cancer epigenome for therapy. Nat. Rev. Genet. *17*, 630–641.

Jurkowska, R.Z., Jurkowski, T.P., and Jeltsch, A. (2011). Structure and Function of Mammalian DNA Methyltransferases. ChemBioChem *12*, 206–222.

Kalebic, T., Blakesley, V., Slade, C., Plasschaert, S., Leroith, D., and Lee Helman, J. (1998). Expression of a kinase-deficient IGF-I-R suppresses tumorigenicity of rhabdomyosarcoma cells constitutively expressing a wild type IGF-I-R. Int. J. Cancer *76*, 223–227.

Kaneda, M., Okano, M., Hata, K., Sado, T., Tsujimoto, N., Li, E., and Sasaki, H. (2004). Essential role for de novo DNA methyltransferase Dnmt3a in paternal and maternal imprinting. Nature *429*, 900–903.

Karahoca, M., and Momparler, R.L. (2013). Pharmacokinetic and pharmacodynamic analysis of 5-aza-2'-

deoxycytidine (decitabine) in the design of its dose-schedule for cancer therapy. Clin. Epigenetics *5*, 3.

Kazanets, A., Shorstova, T., Hilmi, K., Marques, M., and Witcher, M. (2016). Epigenetic silencing of tumor suppressor genes: Paradigms, puzzles, and potential. Biochim. Biophys. Acta *1865*, 275–288.

Keller, C., and Guttridge, D.C. (2013). Mechanisms of impaired differentiation in rhabdomyosarcoma. FEBS J. *280*, 4323–4334.

Kim, H.J., Kim, J.H., Chie, E.K., Da Young, P., Kim, I.A., and Kim, I.H. (2012). DNMT (DNA methyltransferase) inhibitors radiosensitize human cancer cells by suppressing DNA repair activity. Radiat. Oncol. *7*, 39.

Kim, J.K., Samaranayake, M., and Pradhan, S. (2009). Epigenetic mechanisms in mammals. Cell. Mol. Life Sci. *66*, 596–612.

Kodet, R., Fajstavr, J., Kabelka, Z., Koutecky, J., Eckschlager, T., and Newton, W.A. (1991). Is fetal cellular rhabdomyoma an entity or a differentiated rhabdomyosarcoma? A study of patients with rhabdomyoma of the tongue and sarcoma of the tongue enrolled in the intergroup rhabdomyosarcoma studies I, II, and III. Cancer *67*, 2907–2913.

Komdeur, R., Meijer, C., Van Zweeden, M., De Jong, S., Wesseling, J., Hoekstra, H.J., and van der Graaf, W.T. (2004). Doxorubicin potentiates TRAIL cytotoxicity and apoptosis and can overcome TRAIL-resistance in rhabdomyosarcoma cells. Int. J. Oncol. *25*, 677–684.

Koufos, A., Hansen, M.F., Copeland, N.G., Jenkins, N.A., Lampkin, B.C., and Cavenee, W.K. (1985). Loss of heterozygosity in three embryonal tumors suggests a common pathogenetic mechanism. Nature *316*, 330–334.

Koutalianos, D., Koutsoulidou, A., Mastroyiannopoulos, N.P., Furling, D., and Phylactou, L.A. (2015). MyoD transcription factor induces myogenesis by inhibiting Twist-1 through miR-206. J. Cell Sci. *128*, 3631–3645.

Kuo, L.J., and Yang, L.-X. (2008). Gamma-H2AX - a novel biomarker for DNA double-strand breaks. In Vivo *22*, 305–309.

Kutko, M.C., Glick, R.D., Butler, L.M., Coffey, D.C., Rifkind, R.A., Marks, P.A., Richon, V.M., and LaQuaglia, M.P. (2003). Histone deacetylase inhibitors induce growth suppression and cell death in human rhabdomyosarcoma in vitro. Clin Cancer Res *9*, 5749–5755.

Lagos-Quintana, M. (2001). Identification of Novel Genes Coding for Small Expressed RNAs. Science. *294*, 853–858.

Lagos-Quintana, M., Rauhut, R., Yalcin, A., Meyer, J., Lendeckel, W., and Tuschl, T. (2002). Identification of tissue-specific microRNAs from mouse. Curr. Biol. *12*, 735–739.

Laird, P.W. (2003). The power and the promise of DNA methylation markers. Nat. Rev. Cancer *3*, 253–266.

Laker, R.C., and Ryall, J.G. (2016). DNA Methylation in Skeletal Muscle Stem Cell Specification, Proliferation, and Differentiation. Stem Cells Int. *2016*, 5725927.

Lamey, T.M., Koenders, A., and Ziman, M. (2004). Pax genes in myogenesis: Alternate transcripts add complexity. Histol. Histopathol. *19*, 1289–1300.

Lapidus, R.G., Nass, S.J., Butash, K.A., Parl, F.F., Weitzman, S.A., Graff, J.G., Herman, J.G., and Davidson, N.E. (1998). Mapping of ER gene CpG island methylation by methylation-specific polymerase chain reaction. Cancer Res. *58*, 2515–2519.

Laurent, L., Wong, E., Li, G., Huynh, T., Tsirigos, A., Ong, C.T., Low, H.M., Sung, K.W.K., Rigoutsos, I., Loring, J., et al. (2010). Dynamic changes in the human methylome during differentiation. Genome Res. *20*, 320–331.

Lawrence, W., Gehan, E.A., Hays, D.M., Beltangady, M., and Maurer, H.M. (1987). Prognostic significance of staging factors of the UICC staging system in childhood rhabdomyosarcoma: A report from the Intergroup Rhabdomyosarcoma Study (IRS-II). J. Clin. Oncol. *5*, 46–54.

Lee, W.H., Morton, R.A., Epstein, J.I., Brooks, J.D., Campbell, P.A., Bova, G.S., Hsieh, W.S., Isaacs, W.B., and Nelson, W.G. (1994). Cytidine methylation of regulatory sequences near the pi-class glutathione S-

transferase gene accompanies human prostatic carcinogenesis. Proc. Natl. Acad. Sci. U. S. A. *91*, 11733–11737.

Lehmann, U., Hasemeier, B., Christgen, M., Müller, M., Römermann, D., Länger, F., and Kreipe, H. (2008). Epigenetic inactivation of microRNA gene hsa-mir-9-1 in human breast cancer. J. Pathol. *214*, 17–24.

Li, E., and Zhang, Y. (2014). DNA methylation in mammals. Cold Spring Harb. Perspect. Biol. *6*.

Li, E., Bestor, T.H., and Jaenisch, R. (1992). Targeted mutation of the DNA methyltransferase gene results in embryonic lethality. Cell *69*, 915–926.

Li, H.-P., Huang, H.-Y., Lai, Y.-R., Huang, J.-X., Chang, K.-P., Hsueh, C., and Chang, Y.-S. (2014). Silencing of miRNA-148a by hypermethylation activates the integrin-mediated signaling pathway in nasopharyngeal carcinoma. Oncotarget *5*, 7610–7624.

Linhart, H.G., Lin, H., Yamada, Y., Moran, E., Steine, E.J., Gokhale, S., Lo, G., Cantu, E., Ehrich, M., He, T., et al. (2007). Dnmt3b promotes tumorigenesis in vivo by gene-specific de novo methylation and transcriptional silencing. Genes Dev. *21*, 3110–3122.

Lo, P.-K., and Sukumar, S. (2008). Epigenomics and breast cancer. Pharmacogenomics *9*, 1879–1902.

Lock, R., Carol, H., Houghton, P.J., Morton, C.L., Kolb, E.A., Gorlick, R., Reynolds, C.P., Maris, J.M., Keir, S.T., Wu, J., et al. (2008). Initial testing (stage 1) of the BH3 mimetic ABT-263 by the pediatric preclinical testing program. Pediatr. Blood Cancer *50*, 1181–1189.

Lovell, M.A., D'Cruz, C.M., and Barr, F.G. (1994). Fusion of PAX7 to FKHR by the Variant t(l;13)(p36;ql4) Translocation in Alveolar Rhabdomyosarcoma. Cancer Res. *54*, 2869–2872.

Lucarelli, M., Fuso, A., Strom, R., and Scarpa, S. (2001). The Dynamics of Myogenin Site-specific Demethylation is Strongly Correlated with its Expression and with Muscle Differentiation. J. Biol. Chem. *276*, 7500–7506.

Lujambio, A., Ropero, S., Ballestar, E., Fraga, M.F., Cerrato, C., Setién, F., Casado, S., Suarez-Gauthier, A., Sanchez-Cespedes, M., Gitt, A., et al. (2007). Genetic unmasking of an epigenetically silenced microRNA in human cancer cells. Cancer Res. *67*, 1424–1429.

Mack, G.S. (2006). Epigenetic Cancer Therapy Makes Headway. JNCI J. Natl. Cancer Inst. *98*, 1443–1444.

Mackall, C.L., Rhee, E.H., Read, E.J., Khuu, H.M., Leitman, S.F., Bernstein, D., Tesso, M., Long, L.M., Grindler, D., Merino, M., et al. (2008). A pilot study of consolidative immunotherapy in patients with high-risk pediatric sarcomas. Clin. Cancer Res. *14*, 4850.

MacQuarrie, K.L., Yao, Z., Fong, A.P., Diede, S.J., Rudzinski, E.R., Hawkins, D.S., and Tapscott, S.J. (2013). Comparison of Genome-Wide Binding of MyoD in Normal Human Myogenic Cells and Rhabdomyosarcomas Identifies Regional and Local Suppression of Promyogenic Transcription Factors. Mol. Cell. Biol. *33*, 773–784.

M Fatih Okcu, Hicks, J., and Horowitz, M. (2016). Rhabdomyosarcoma in childhood and adolescence: Epidemiology, pathology, and molecular pathogenesis. UpToDate 1–17.

Mahoney, S.E., Yao, Z., Keyes, C.C., Tapscott, S.J., and Diede, S.J. (2012). Genome-wide DNA methylation studies suggest distinct DNA methylation patterns in pediatric embryonal and alveolar rhabdomyosarcomas. Epigenetics *7*, 400–408.

Maier, P., Hartmann, L., Wenz, F., and Herskind, C. (2016). Cellular pathways in response to ionizing radiation and their targetability for tumor radiosensitization. Int. J. Mol. Sci. *17*.

Maloney, E.K., McLaughlin, J.L., Dagdigian, N.E., Garrett, L.M., Connors, K.M., Zhou, X.M., Blattler, W.A., Chittenden, T., and Singh, R. (2003). An anti-insulin-like growth factor I receptor antibody that is a potent inhibitor of cancer cell proliferation. Cancer Res *63*, 5073–5083.

Marampon, F., Ciccarelli, C., and Zani, B.M. (2006). Down-regulation of c-Myc following MEK/ERK inhibition halts the expression of malignant phenotype in rhabdomyosarcoma and in non muscle-derived human tumors. Mol. Cancer *5*, 31.

Maresca, A., Zaffagnini, M., Caporali, L., Carelli, V., and Zanna, C. (2015). DNA methyltransferase 1 mutations and mitochondrial pathology: Is mtDNA methylated? Front. Genet. *5*.

Maris, J.M., Courtright, J., Houghton, P.J., Morton, C.L., Kolb, E.A., Lock, R., Tajbakhsh, M., Reynolds, C.P., Keir, S.T., Wu, J., et al. (2008a). Initial testing (stage 1) of sunitinib by the pediatric preclinical testing program. Pediatr. Blood Cancer *51*, 42–48.

Maris, J.M., Courtright, J., Houghton, P.J., Morton, C.L., Gorlick, R., Kolb, E.A., Lock, R., Tajbakhsh, M., Reynolds, C.P., Keir, S.T., et al. (2008b). Initial testing of the VEGFR inhibitor AZD2171 by the Pediatric Preclinical Testing Program. Pediatr. Blood Cancer *50*, 581–587.

Maurer, H.M., Crist, W., Lawrence, W., Ragab, A.H., Raney, R.B., Webber, B., Wharam, M., Vietti, T.J., Beltangady, M., Gehan, E.A., et al. (1988). The intergroup rhabdomyosarcoma study-I. A final report. Cancer *61*, 209–220.

Mauro, A., Ciccarelli, C., De Cesaris, P., Scoglio, A., Bouché, M., Molinaro, M., Aquino, A., and Zani, B.M. (2002). PKCalpha-mediated ERK, JNK and p38 activation regulates the myogenic program in human rhabdomyosarcoma cells. J. Cell Sci. *115*, 3587–3599.

McDowell, H.P. (2003). Update on childhood rhabdomyosarcoma. Arch. Dis. Child. *88*, 354–357.

Medina, P.P., and Slack, F.J. (2008). microRNAs and cancer: An overview. Cell Cycle *7*, 2485–2492.

Megiorni, F., Camero, S., Ceccarelli, S., McDowell, H.P., Mannarino, O., Marampon, F., Pizer, B., Shukla, R., Pizzuti, A., Marchese, C., et al. (2016). DNMT3B in vitro knocking-down is able to reverse the embryonic rhabdomyosarcoma cell phenotype through inhibition of proliferation and induction of myogenic differentiation. Oncotarget *7*, 79342-79356.

Megiorni, F., Cialfi, S., McDowell, H.P., Felsani, A., Camero, S., Guffanti, A., Pizer, B., Clerico, A., De Grazia, A., Pizzuti, A., et al. (2014). Deep Sequencing the microRNA profile in rhabdomyosarcoma reveals down-regulation of miR-378 family members. BMC Cancer *14*, 880.

Meng, H., Meng, H., Cao, Y., Qin, J., Song, X., Zhang, Q., Shi, Y., and Cao, L. (2015). DNA methylation, its mediators and genome integrity. Int. J. Biol. Sci. *11*, 604–617.

Merlino, G., and Helman, L.J. (1999). Rhabdomyosarcoma--working out the pathways. Oncogene *18*, 5340–5348.

Merlo, a, Herman, J.G., Mao, L., Lee, D.J., Gabrielson, E., Burger, P.C., Baylin, S.B., and Sidransky, D. (1995). 5' CpG island methylation is associated with transcriptional silencing of the tumour suppressor p16/CDKN2/MTS1 in human cancers. Nat. Med. *1*, 686–692.

Meyer, W.H., and Spunt, S.L. (2004). Soft tissue sarcomas of childhood. Cancer Treat. Rev. *30*, 269–280.

Michalski, J.M., Meza, J., Breneman, J.C., Wolden, S.L., Laurie, F., Jodoin, M., Raney, B., Wharam, M.D., and Donaldson, S.S. (2004). Influence of radiation therapy parameters on outcome in children treated with radiation therapy for localized parameningeal rhabdomyosarcoma in Intergroup Rhabdomyosarcoma Study Group trials II through IV. Int. J. Radiat. Oncol. Biol. Phys. *59*, 1027–1038.

Minniti, C.P., Tsokos, M., Newton, W.A., and Helman, L.J. (1994). Specific expression of insulin-like growth factor-II in rhabdomyosarcoma tumor cells. Am. J. Clin. Pathol. *101*, 198–203.

Mohan, K.N., and Chaillet, J.R. (2013). Cell and molecular biology of DNA methyltransferase 1. Int Rev Cell Mol Biol *306*, 1–42.

Muller, H.M., Widschwendter, A., Fiegl, H., Ivarsson, L., Goebel, G., Perkmann, E., Marth, C., and Widschwendter, M. (2003). DNA methylation in serum of breast cancer patients: an independent prognostic marker. Cancer Res. *63*, 7641–7645.

Müller, C.I., Rüter, B., Koeffler, H.P., and Lübbert, M. (2006). DNA hypermethylation of myeloid cells, a novel therapeutic target in MDS and AML. Curr. Pharm. Biotechnol. *7*, 315–321.

Newton, W.A., Soule, E.H., Hamoudi, A.B., Reiman, H.M., Shimada, H., Beltangady, M., and Maurer, H. (1988). Histopathology of childhood sarcomas, Intergroup Rhabdomyosarcoma Studies I and II: clinicopathologic correlation. J. Clin. Oncol. *6*, 67–75.

Nordin, M., Bergman, D., Halje, M., Engström, W., and Ward, A. (2014). Epigenetic regulation of the Igf2/H19 gene cluster. Cell Prolif. *47*, 189–199.

O'Brien, D., Jacob, A.G., Qualman, S.J., and Chandler, D.S. (2012). Advances in pediatric

rhabdomyosarcoma characterization and disease model development. Histol. Histopathol. *27*, 13–22.

Ognjanovic, S., Linabery, A.M., Charbonneau, B., and Ross, J.A. (2009). Trends in childhood rhabdomyosarcoma incidence and survival in the United States, 1975-2005. Cancer *115*, 4218–4226.

Oikawa, Y., Omori, R., Nishii, T., Ishida, Y., Kawaichi, M., and Matsuda, E. (2011). The methyl-CpG-binding protein CIBZ suppresses myogenic differentiation by directly inhibiting myogenin expression. Cell Res. *21*, 1578–1590.

Oka, M., Rodić, N., Graddy, J., Chang, L.J., and Terada, N. (2006). CpG sites preferentially methylated by Dnmt3a in vivo. J. Biol. Chem. *281*, 9901–9908.

Okano, M., Bell, D.W., Haber, D.A., and Li, E. (1999). DNA methyltransferases Dnmt3a and Dnmt3b are essential for de novo methylation and mammalian development. Cell *99*, 247–257.

Oki, Y., Aoki, E., and Issa, J.P.J. (2007). Decitabine-Bedside to bench. Crit. Rev. Oncol. Hematol. *61*, 140–152.

Onyango, P., and Feinberg, a. P. (2011). A nucleolar protein, H19 opposite tumor suppressor (HOTS), is a tumor growth inhibitor encoded by a human imprinted H19 antisense transcript. Proc. Natl. Acad. Sci. *108*, 16759–16764.

Ooi, S.K.T., Qiu, C., Bernstein, E., Li, K., Jia, D., Yang, Z., Erdjument-Bromage, H., Tempst, P., Lin, S.-P., Allis, C.D., et al. (2007). DNMT3L connects unmethylated lysine 4 of histone H3 to de novo methylation of DNA. Nature *448*, 714–717.

Otani, J., Nankumo, T., Arita, K., Inamoto, S., Ariyoshi, M., and Shirakawa, M. (2009). Structural basis for recognition of H3K4 methylation status by the DNA methyltransferase 3A ATRX-DNMT3-DNMT3L domain. EMBO Rep *10*, 1235–1241.

Ottaviano, Y.L., Issa, J.P., Parl, F.F., Smith, H.S., Baylin, S.B., and Davidson, N.E. (1994). Methylation of the estrogen receptor gene CpG island marks loss of estrogen receptor expression in human breast cancer cells. Cancer Res. *54*, 2552–2555.

Oustanina, S., Hause, G., and Braun, T. (2004). Pax7 directs postnatal renewal and propagation of myogenic satellite cells but not their specification. Embo J *23*, 3430–3439.

Palacios, D., Summerbell, D., Rigby, P.W.J., and Boyes, J. (2010). Interplay between DNA Methylation and Transcription Factor Availability: Implications for Developmental Activation of the Mouse Myogenin Gene. Mol. Cell. Biol. *30*, 3805–3815.

Panda, S.P., Chinnaswamy, G., Vora, T., Prasad, M., Bansal, D., Kapoor, G., Radhakrishnan, V., Agarwala, S., Laskar, S., Arora, B., et al. (2017). Diagnosis and Management of Rhabdomyosarcoma in Children and Adolescents: ICMR Consensus Document. Indian J. Pediatr. *84*, 393–402.

Pang, L., Sawada, T., Decker, S.J., and Saltiel, A.R. (1995). Inhibition of MAP kinase kinase blocks the differentiation of PC-12 cells induced by nerve growth factor. J. Biol. Chem. *270*, 13585–13588.

Parham, D.M. (2001). Pathologic classification of rhabdomyosarcomas and correlations with molecular studies. Mod. Pathol. *14*, 506–514.

Parham, D.M., and Barr, F.G. (2013). Classification of Rhabdomyosarcoma and Its Molecular Basis. Adv. Anat. Pathol. *20*, 387–397.

Patra, S.K., Patra, A., Zhao, H., and Dahiya, R. (2002). DNA methyltransferase and demethylase in human prostate cancer. Mol. Carcinog. *33*, 163–171.

Paulino, A.C. (2004). Late effects of radiotherapy for pediatric extremity sarcomas. Int. J. Radiat. Oncol. Biol. Phys. *60*, 265–274.

Petak, I., Douglas, L., Tillman, D.M., Vernes, R., and Houghton, J.A. (2000). Pediatric rhabdomyosarcoma cell lines are resistant to Fas-induced apoptosis and highly sensitive to TRAIL-induced apoptosis. Clin. Cancer Res. *6*, 4119–4127.

Pradhan, M., Estève, P.O., Hang, G.C., Samaranayke, M., Kim, G. Do, and Pradhan, S. (2008). CXXC domain of human DNMT1 is essential for enzymatic activity. Biochemistry *47*, 10000–10009.

Purkait, S., Sharma, V., Kumar, A., Pathak, P., Mallick, S., Jha, P., Sharma, M.C., Suri, V., Julka, P.K., Suri, A., et al. (2016). Expression of DNA methyltransferases 1 and 3B correlates with EZH2 and this 3-marker epigenetic signature predicts outcome in glioblastomas. Exp. Mol. Pathol. *100*, 312–320.

Qiu, C., Sawada, K., Zhang, X., and Cheng, X. (2002). The PWWP domain of mammalian DNA methyltransferase Dnmt3b defines a new family of DNA-binding folds. Nat. Struct. Biol. *9*, 217–224.

Raney, R.B., Tefft, M., Maurer, H.M., Ragab, A.H., Hays, D.M., Soule, E.H., Foulkes, M.A., and Gehan, E.A. (1988). Disease patterns and survival rate in children with metastatic soft-tissue sarcoma. A report from the Intergroup Rhabdomyosarcoma Study (IRS)-I. Cancer *62*, 1257–1266.

Raney, R.B., Anderson, J.R., Barr, F.G., Donaldson, S.S., Pappo, a S., Qualman, S.J., Wiener, E.S., Maurer, H.M., and Crist, W.M. (2001). Rhabdomyosarcoma and undifferentiated sarcoma in the first two decades of life: a selective review of intergroup rhabdomyosarcoma study group experience and rationale for Intergroup Rhabdomyosarcoma Study V. J. Pediatr. Hematol. Off. J. Am. Soc. Pediatr. Hematol. *23*, 215–220.

Relaix, F., Polimeni, M., Rocancourt, D., Ponzetto, C., Schäfer, B.W., and Buckingham, M. (2003). The transcriptional activator PAX3-FKHR rescues the defects of Pax3 mutant mice but induces a myogenic gain-of-function phenotype with ligand-independent activation of Met signaling in vivo. Genes Dev. *17*, 2950–2965.

Rimel, B.J., Huettner, P., Powell, M.A., Mutch, D.G., and Goodfellow, P.J. (2009). Absence of MGMT promoter methylation in endometrial cancer. Gynecol. Oncol. *112*, 224–228.

Robinson, M.J., and Cobb, M.H. (1997). Mitogen-activated protein kinase pathways. Curr. Opin. Cell Biol. *9*, 180–186.

Rota, R., Ciarapica, R., Giordano, A., Miele, L., and Locatelli, F. (2011). MicroRNAs in rhabdomyosarcoma: pathogenetic implications and translational potentiality. Mol. Cancer *10*, 120.

Rountree, M.R., Bachman, K.E., and Baylin, S.B. (2000). DNMT1 binds HDAC2 and a new co-repressor, DMAP1, to form a complex at replication foci. Nat. Genet. *25*, 269–277.

Rubin, B.P., Nishijo, K., Chen, H.-I.H., Yi, X., Schuetze, D.P., Pal, R., Prajapati, S.I., Abraham, J., Arenkiel, B.R., Chen, Q.-R., et al. (2011). Evidence for an unanticipated relationship between undifferentiated pleomorphic sarcoma and embryonal rhabdomyosarcoma. Cancer Cell *19*, 177–191.

Ruymann, F.B., and Grovas, a C. (2000). Progress in the diagnosis and treatment of rhabdomyosarcoma and related soft tissue sarcomas. Cancer Invest. *18*, 223–241.

Saab, R., Bills, J.L., Miceli, A.P., Anderson, C.M., Khoury, J.D., Fry, D.W., Navid, F., Houghton, P.J., and Skapek, S.X. (2006). Pharmacologic inhibition of cyclin-dependent kinase 4/6 activity arrests proliferation in myoblasts and rhabdomyosarcoma-derived cells. Mol. Cancer Ther. *5*, 1299–1308.

Saito, Y., Kanai, Y., Nakagawa, T., Sakamoto, M., Saito, H., Ishi, H., and Hirohashi, S. (2003). Increased protein expression of DNA methyltransferase (DNMT) 1 is significantly correlated with the malignant potential and poor prognosis of human hepatocellular carcinomas. Int. J. Cancer *105*, 527–532.

Saito, Y., Liang, G., Egger, G., Friedman, J.M., Chuang, J.C., Coetzee, G.A., and Jones, P.A. (2006). Specific activation of microRNA-127 with downregulation of the proto-oncogene BCL6 by chromatin-modifying drugs in human cancer cells. Cancer Cell *9*, 435–443.

Sakai, T., Toguchida, J., Ohtani, N., Yandell, D.W., Rapaport, J.M., and Dryja, T.P. (1991). Allele-specific hypermethylation of the retinoblastoma tumor-suppressor gene. Am. J. Hum. Genet. *48*, 880–888.

Sandhu, R., Rivenbark, A.G., and Coleman, W.B. (2012). Enhancement of chemotherapeutic efficacy in hypermethylator breast cancer cells through targeted and pharmacologic inhibition of DNMT3b. Breast Cancer Res. Treat. *131*, 385–399.

Schaefer, M., Steringer, J.P., and Lyko, F. (2008). The Drosophila cytosine-5 methyltransferase Dnmt2 is associated with the nuclear matrix and can access DNA during mitosis. PLoS One *3*.

Schuck, A., Mattke, A.C., Schmidt, B., Kunz, D.S., Harms, D., Knietig, R., Treuner, J., and Koscielniak, E. (2004). Group II rhabdomyosarcoma and rhabdomyosarcomalike tumors: Is radiotherapy necessary? J. Clin. Oncol. *22*, 143–149.

Scrable, H., Witte, D., Shimada, H., Seemayer, T., Sheng, W.W., Soukup, S., Koufos, A., Houghton, P.,

Lampkin, B., and Cavenee, W. (1989). Molecular differential pathology of rhabdomyosarcoma. Genes, Chromosom. Cancer *1*, 23–35.

Scrable, H.J., Witte, D.P., Lampkin, B.C., and Cavenee, W.K. (1987). Chromosomal localization of the human rhabdomyosarcoma locus by mitotic recombination mapping. Nature *329*, 645–647.

Scrable, H.J., Johnson, D.K., Rinchik, E.M., and Cavenee, W.K. (1990). Rhabdomyosarcoma-associated locus and MYOD1 are syntenic but separate loci on the short arm of human chromosome 11. Proc. Natl. Acad. Sci. U. S. A. *87*, 2182–2186.

SEALE, P. (2000). Pax7 Is Required for the Specification of Myogenic Satellite Cells. Cell *102*, 777–786.

Sengupta, S., den Boon, J.A., Chen, I.-H., Newton, M.A., Stanhope, S.A., Cheng, Y.-J., Chen, C.-J., Hildesheim, A., Sugden, B., and Ahlquist, P. (2008). MicroRNA 29c is down-regulated in nasopharyngeal carcinomas, up-regulating mRNAs encoding extracellular matrix proteins. Proc. Natl. Acad. Sci. *105*, 5874–5878.

Shafiei, F., Rahnama, F., Pawella, L., Gluckman, P., and Lobie, P. (2008). DNMT3A and DNMT3B mediate autocrine hGH repression of plakoglobin gene transcription and consequent phenotypic conversion of mammary carcinoma cells. Oncogene *27*, 2602–2612.

Shetty, S., Taylor, A.C., and Harris, L.C. (2002). Selective chemosensitization of rhabdomyosarcoma cell lines following wild-type p53 adenoviral transduction. Anticancer. Drugs *13*, 881–889.

Shukla, N., Ameur, N., Yilmaz, I., Nafa, K., Lau, C.Y., Marchetti, A., Borsu, L., Barr, F.G., and Ladanyi, M. (2012). Oncogene mutation profiling of pediatric solid tumors reveals significant subsets of embryonal rhabdomyosarcoma and neuroblastoma with mutated genes in growth signaling pathways. Clin. Cancer Res. *18*, 748–757.

Skapek, S.X., Anderson, J., Barr, F.G., Bridge, J.A., Gastier-Foster, J.M., Parham, D.M., Rudzinski, E.R., Triche, T., and Hawkins, D.S. (2013). *PAX-FOXO1* fusion status drives unfavorable outcome for children with rhabdomyosarcoma: A children's oncology group report. Pediatr. Blood Cancer *60*, 1411–1417.

Smith, G.C.M., and Jackson, S.P. (1999). The DNA-dependent protein kinase. Genes Dev. *13*, 916–934.

Smith, Z.D., and Meissner, A. (2013). DNA methylation: roles in mammalian development. Nat. Rev. Genet. *14*, 204–220.

Smith, A.C., Squire, J.A., Thorner, P., Zielenska, M., Shuman, C., Grant, R., Chitayat, D., Nishikawa, J.L., and Weksberg, R. (2001). Association of alveolar rhabdomyosarcoma with the Beckwith-Wiedemann syndrome. Pediatr. Dev. Pathol. *4*, 550–558.

Stevens, M.C.G. (2005). Treatment for childhood rhabdomyosarcoma: The cost of cure. Lancet Oncol. *6*, 77–84.

Stratton, M.R., Cooper, C.S., Gusterson, B.A., and Fisher, C. (1989). Detection of Point Mutations in N-ras and K-ras Genes of Human Embryonal Rhabdomyosarcomas Using Oligonucleotide Probes and the Polymerase Chain Reaction. Cancer Res. *49*, 6324–6327.

Stresemann, C., and Lyko, F. (2008). Modes of action of the DNA methyltransferase inhibitors azacytidine and decitabine. Int. J. Cancer *123*, 8–13.

Subramaniam, D., Thombre, R., Dhar, A., and Anant, S. (2014). DNA methyltransferases: a novel target for prevention and therapy. Front. Oncol. *4*, 80.

Sultan, I., and Ferrari, A. (2010). Selecting multimodal therapy for rhabdomyosarcoma. Expert Rev. Anticancer Ther. *10*, 1285–1301.

Sun, W., Chatterjee, B., Wang, Y., Stevenson, H.S., Edelman, D.C., Meltzer, P.S., and Barr, F.G. (2015). Distinct methylation profiles characterize fusion-positive and fusion-negative rhabdomyosarcoma. Mod. Pathol. *28*, 1214–1224.

Taniguchi, E., Nishijo, K., McCleish, A.T., Michalek, J.E., Grayson, M.H., Infante, A.J., Abboud, H.E., Legallo, R.D., Qualman, S.J., Rubin, B.P., et al. (2008). PDGFR-A is a therapeutic target in alveolar rhabdomyosarcoma. Oncogene *27*, 6550–6560.

Taulli, R., Scuoppo, C., Bersani, F., Accornero, P., Forni, P.E., Miretti, S., Grinza, A., Allegra, P., Schmitt-

Ney, M., Crepaldi, T., et al. (2006). Validation of Met as a therapeutic target in alveolar and embryonal rhabdomyosarcoma. Cancer Res. *66*, 4742–4749.

Tiffin, N., Williams, R.D., Shipley, J., and Pritchard-Jones, K. (2003). PAX7 expression in embryonal rhabdomyosarcoma suggests an origin in muscle satellite cells. Br. J. Cancer *89*, 327–332.

Tomek, S., Koestler, W., Horak, P., Grunt, T., Brodowicz, T., Pribill, I., Halaschek, J., Haller, G., Wiltschke, C., Zielinski, C.C., et al. (2003). Trail-induced apoptosis and interaction with cytotoxic agents in soft tissue sarcoma cell lines. Eur. J. Cancer *39*, 1318–1329.

Trahair, T., Andrews, L., and Cohn, R.J. (2007). Recognition of Li Fraumeni syndrome at diagnosis of a locally advanced extremity rhabdomyosarcoma. Pediatr. Blood Cancer *48*, 345–348.

Tsokos, M., and Helman, L.J. (1994). In Vivo Treatment with Antibody against IGF-1 Receptor Suppresses Growth of Human Rhabdomyosarcoma and Down-Regulates p34cdc. Cancer Res. *54*, 5531–5534.

Wachtel, M., and Schäfer, B.W. (2010). Targets for cancer therapy in childhood sarcomas. Cancer Treat. Rev. *36*, 318–327.

Waddington, C.H. (1942). The epigenotype. Endeavour 18–20.

Waddington, C.H. (1968). Towards a Theoretical Biology. Nature *218*, 525–527.

Wan, X., Shen, N., Mendoza, A., Khanna, C., and Helman, L.J. (2006). CCI-779 inhibits rhabdomyosarcoma xenograft growth by an antiangiogenic mechanism linked to the targeting of mTOR/Hif-1alpha/VEGF signaling. Neoplasia *8*, 394–401.

Wang, H., Garzon, R., Sun, H., Ladner, K.J., Singh, R., Dahlman, J., Cheng, A., Hall, B.M., Qualman, S.J., Chandler, D.S., et al. (2008a). NF-κB-YY1-miR-29 Regulatory Circuitry in Skeletal Myogenesis and Rhabdomyosarcoma. Cancer Cell *14*, 369–381.

Wang, Q., Fang, W.H., Krupinski, J., Kumar, S., Slevin, M., and Kumar, P. (2008b). Pax genes in embryogenesis and oncogenesis: Genes... J. Cell. Mol. Med. *12*, 2281–2294.

Wang-Wuu, S., Soukup, S., Ballard, E., Gotwals, B., and Lampkin, B. (1988). Chromosomal Analysis of Sixteen Human Rhabdomyosarcomas. Cancer Res. *48*, 983–987.

Weksberg, R., Shuman, C., and Beckwith, J.B. (2010). Beckwith-Wiedemann syndrome. Eur. J. Hum. Genet. *18*, 8–14.

Widschwendter, M., Siegmund, K.D., Müller, H.M., Fiegl, H., Marth, C., Müller-Holzner, E., Jones, P.A., and Laird, P.W. (2004). Association of breast cancer DNA methylation profiles with hormone receptor status and response to tamoxifen. Cancer Res. *64*, 3807–3813.

Wu, H., Chen, Y., Liang, J., Shi, B., Wu, G., Zhang, Y., Wang, D., Li, R., Yi, X., Zhang, H., et al. (2005). Hypomethylation-linked activation of PAX2 mediates tamoxifen-stimulated endometrial carcinogenesis. Nature *438*, 981–987.

Wu, C.t. and Morris, J.R. (2001). Genes, genetics, and epigenetics: a correspondence. Science *293*, 1103–1105.

Xia, S.J., Pressey, J.G., and Barr, F.G. (2002). Molecular pathogenesis of rhabdomyosarcoma. Cancer Biol. Ther. *1*, 97–104.

Xiong, Y., Fang, J.-H., Yun, J.-P., Yang, J., Zhang, Y., Jia, W.-H., and Zhuang, S.-M. (2009). Effects of MicroRNA-29 on apoptosis, tumorigenicity, and prognosis of hepatocellular carcinoma. Hepatology *51*, 836-845.

Yan, M.-D., Yao, C.-J., Chow, J.-M., Chang, C.-L., Hwang, P.-A., Chuang, S.-E., Whang-Peng, J., and Lai, G.-M. (2015). Fucoidan Elevates MicroRNA-29b to Regulate DNMT3B-MTSS1 Axis and Inhibit EMT in Human Hepatocellular Carcinoma Cells. Mar. Drugs *13*, 6099–6116.

Yang, P., Grufferman, S., Khoury, M.J., Schwartz, A.G., Kowalski, J., Ruymann, F.B., and Maurer, H.M. (1995). Association of childhood rhabdomyosarcoma with neurofibromatosis type i and birth defects. Genet. Epidemiol. *12*, 467–474.

Yang, Z., MacQuarrie, K.L., Analau, E., Tyler, A.E., Dilworth, F.J., Cao, Y., Diede, S.J., and Tapscott, S.J.

(2009). MyoD and E-protein heterodimers switch rhabdomyosarcoma cells from an arrested myoblast phase to a differentiated state. Genes Dev. *23*, 694–707.

Zahm, S.H., and Fraumeni, J.F. (1997). The epidemiology of soft tissue sarcoma. Semin. Oncol. *24*, 504–514.

Zhang, W., and Xu, J. (2017). DNA methyltransferases and their roles in tumorigenesis. Biomark. Res. *5*, 1.

Zhao, Z., Wu, Q., Cheng, J., Qiu, X., Zhang, J., and Fan, H. (2010). Depletion of DNMT3A suppressed cell proliferation and restored PTEN in hepatocellular carcinoma cell. J. Biomed. Biotechnol. *2010*.

Zhu, H., Yue, J., Pan, Z., Wu, H., Cheng, Y., Lu, H., Ren, X., Yao, M., Shen, Z., and Yang, J.-M. (2010). Involvement of Caveolin-1 in repair of DNA damage through both homologous recombination and non-homologous end joining. PLoS One *5*, e12055.